



UNIVERSIDADE DE BRASÍLIA - UnB
INSTITUTO DE GEOCIÊNCIAS - IG
CURSO DE PÓS-GRADUAÇÃO EM GEOLOGIA

Caraterização petrográfica, geoquímica e isotópica do sienito de Uruana e suas implicações sobre a gênese do magmatismo sin-tectônico da Faixa Brasília.

Dissertação de Mestrado nº 378.

Orientador: Prof. Dr. Massimo Matteini

Sergio Andres Reyes Sandoval

Brasília, DF, 29 Julho de 2016.

**UNIVERSIDADE DE BRASÍLIA - UnB
INSTITUTO DE GEOCIÊNCIAS - IG
CURSO DE PÓS-GRADUAÇÃO EM GEOLOGIA**

Caracterização petrográfica, geoquímica e isotópica do sienito de Uruana e suas implicações sobre a gênese do magmatismo sin-tectônico da Faixa Brasília.

Área de concentração: Mineralogia e Petrologia

Sergio Andres Reyes Sandoval

Orientador:

Prof. Dr. Massimo Matteini

Coorientador:

Banca Examinadora:

Prof. Dr. Massimo Matteini - (UnB)

Prof. Dr. José Affonso Brod - (UnB)

Prof. Dr. Sérgio Castro Valente (UFRJ)

Brasília, DF, 29 Julho de 2016.

FICHA CATALOGRÁFICA

Reyes, Sergio Andres, Sandoval

Caracterização petrográfica, geoquímica e isotópica do sienito de Uruana e suas implicações
Sobre a gênese do magmatismo sin-tectônico da Faixa Brasília, 2016.

Nº de páginas: 96

Área de concentração: Mineralogia e Petrologia

Orientador: Prof. Dr. Massimo Matteini.

AGRADECIMENTOS

- Aos professores e funcionários dos laboratórios (Edna, fransica, Raymundo, Rafael) do Instituto de Geociências da Universidade de Brasília pelos ensinamentos e comprometimento sem os quais não seria possível a construção desta dissertação. Em especial, ao Prof. Massimo Matteini por ter me dado uma oportunidade única para abrir mais meus horizontes.
- Ao meu grande Orientador e amigo celestial, DEUS, pela paz e força proporcionada para a culminação do meu mestrado.
- A minha mãe minha “LUCILDA” por ser a melhor orientadora da minha vida, pelo apoio e animo incondicional para continuar no meu caminho.
- Aos amigos, colegas e companheiros os mais sinceros agradecimentos pelos conselhos e conhecimentos adquiridos.
- Aos meus grandes amigos Daniel Oliveira, Mauricio Merino, Sergio Pertuz (chelli), Luiz, Clayton, Dudu (B2), Giselle, Lili, Talita e Marcinho pela força, paciência e colaboração na minha formatura de mestrado. Levo no meu coração aqueles momentos compartilhados e sorrisos vividos junto com milhões copos de cachaça e xícaras de café.

*“Comece fazendo o que é necessário,
Depois o que é possível, e de repente
Você estará fazendo o impossível”*

São Francisco de Assis

SUMÁRIO

1.1	APRESENTAÇÃO E OBJETIVOS	1
1.2	LOCALIZAÇÃO.....	1
1.3	ESCOPO DA DISSERTAÇÃO.....	2
2.	PETROGRAPHY, GEOCHEMISTRY AND ISOTOPIC FEATURES OF THE URUANA SYENITE AND IMPLICATIONS FOR THE GENESIS OF SYN-TECTONIC MAGMATISM IN THE BRASÍLIA BELT.....	3
2.1	INTRODUCTION.....	4
2.2	REGIONAL GEOLOGY	5
2.3	MATERIAL AND METHODS.....	8
2.3.1	<i>Sampling and petrography</i>	8
2.3.2	<i>Mineral Chemistry</i>	8
2.3.3	<i>Lithogeochemistry</i>	8
2.3.4	<i>Sm-Nd isotopes</i>	9
2.3.5	<i>Shrimp U-Pb</i>	9
2.4	RESULTS.....	10
2.4.1	<i>Field relationships and petrography</i>	10
2.4.2	<i>Mineral chemistry</i>	15
2.4.2.1	Clinopyroxene	15
2.4.2.2	Amphibole.....	16
2.4.2.3	Mica	20
2.4.3	<i>Whole-rock geochemistry</i>	21
2.4.4	<i>Shrimp zircon U-Pb dating</i>	31
2.4.5	<i>Sm-Nd isotopes</i>	33
2.5	DISCUSSION	34
2.5.1	<i>Potassium and ultrapotassic affinity.</i>	34
2.5.2	<i>Geochemical comparisons</i>	35
2.5.3	<i>Relationship between lamproite, minette and syenite magmas</i>	37
2.5.4	<i>Petrogenetic considerations</i>	38
2.5.5	<i>Petrogenesis of the Uruana syenite rocks</i>	39
2.6	CONCLUSIONS	41
2.7	ACKNOWLEDGEMENTS.....	42
2.8	REFERENCES	42
3.	CONCLUSÕES.....	48
4.	ANEXOS.....	50

ÍNDICE DE FIGURAS

Figura 1: Mapa de localização e acesso da área estudada.....	2
Figure 2. Geologic Sketch map showing the main tectonic features and components of the Brasília Belt.....	7
Figure 3. (A) Simplified geological map of the Itapuranga-Uruana area (sheet SD.22-Z-C-VI), adapted from Oliveira (1997). (B) Composite color images (CMY and KPERC) of aerial gamma-ray spectrometric data of the study area. The limits of the different intrusive bodies are highlighted (Data from CPRM database).....	11
Figure 4. Main geological features of the Uruana sienite lithotypes. (A) Coarse grained quartz sienitic rocks of the main body (B) Typical porphyritic texture of the Quartz syenite (C, D) Typical ellipsoidal disk-shaped Microgranular Enclaves (Mes) hosted in the quartz syenite. The presence of K-Feldspar xenocrysts from the quartz syenite are evidences of magma mixing (mingling). (E) Syn-magmatic intermediate to felsic dike. (F) Syn-magmatic tabular intrusion of ultramafic composition sub-parallel to the mylonitic foliation.....	13
Figure 5. Photomicrographs (plane-polarized light) of the rocks Uruana syenite (A-B) Quartz syenites, (C-D), Microgranular enclaves, (E-G), Ultramafic dike (H-J). Alkali feldspar syenite (A) subhedral to euhedral phenocrysts of perthitic K-feldspar dispersed in a faneritic matrix composed by k-feldspar, amphibole, biotite and minor quartz and plagioclase. (B) Microphenocrysts of hornblende, showing common biotite inclusions. (C) K-feldspar xenocrysts of the Mes that were encompassed from the hosting Quartz syenite. (D) Typical paragenese of the Mes, represented by K-feldspar, biotite, clinopyroxene, plagioclase and quartz crystals. (E) micro-phenocrysts of clinopyroxenes and minor amphibole immersed in a groundmass of biotite and k-feldspar. (F) Clinopyroxenes with reaction rim of actinolite and characteristic zircon macrocrystal. (G) Contact between ultramafic dike and quartz syenitic host attain to Xenocrists of K-feldspar from the host syenite assimilated by the ultramafic dike. (H) Clinopyroxenes and minor amphibole immersed in a groundmass of biotite and k-feldspar. (I) Phenocrysts of k-feldspar and clinopyroxene immersed in a micro-faneritic matrix of k-feldspar, biotite, plagioclase and quartz. (J) Actinolite reaction rim of clinopyroxenes.....	15
Figure 6. Wollastonite-(Wo), (En)-Enstatite (Fs)-Ferrosilite classification diagram (Morimoto et al., 1988) for clinopyroxene from the different lithology of Uruana syenite	15
Figure 7. Classification diagrams for amphiboles (Leake et al., 1997) .A) $(Na + K)_A \geq 0,50$.B) $(Na + K)_A < 0,50$	17
Figure 8. Classification diagram compositions for mica (Rieder et al., 1998).....	20
Figure 9. A). Q'-F'-ANOR normative classification diagram for plutonic rock (after Streckeisen, Lemaitre 1979). B) Total alkali vs silica (TAS) classification of plutonic rocks (Cox et al., 1989).....	22
Figure 10. Major elements and trace elements representative Harker diagrams for the Uruana syenite rocks.....	29
Figure 11. A) Multi-variation primitive mantle-normalized (A) and Chondrite-normalized REE diagram for the different lithotypes of the Uruana syenite compared with the compositional range of the Quartz syenites, normalization values are from Sun and McDonough (1989).	30
Figure 12. Wetherill Concordia diagram for zircons from sample Uru-09.....	31

Figure 13. Nd isotope compositions of rocks from Uruana syenite.....	33
Figure 14. Discrimination diagrams (wt%) of Foley et al. (1987) applied to different groups of Ultrapotassic rock of the Uruana syenite.....	35
Figure 15. Spider diagram normalized to Ocean Island Basalt (OIB) Data from Sun and McDonough (1989), for the studied Uruana rock, compared with compositional range of: A) Lamproites from SE Spain and Mediterranean, B) Minettes from the Piquiri syenite massif, C) Mantle-derived Medium-K Calc-Alkaline Basalts at AzumaVolcano, D) High-K Mafic Plinian Eruptions of Volcán de Colima, E) The syenitic rocks of the Piquiri massif syenite. D) Rare earth element patterns normalized to C1-chondritic values for the Uruana rocks.	37
Figure 16 Selected trace element and major element oxide ratios vs Zr as an index of magma mixing (Prelevic et al., 2003).	38
Figure 17. The following geological scheme is presented to show the evolution of rocks of the Uruana syenite summarizing the main stages. (1) 670-600 Ma, metasomatism of the continental lithospheric mantle produced by the dehydration of the oceanic slab of the Goiás magmatic arc (2) 630 Ma, thickening of the continental crust produced by the continental collision increasing the density of the lower crust. (3) 614 Ma, the continuous increase of thickening and the eclogitization of lower crust produced of the evolution of collision, creates a gravitational instability and eventually a lithospheric delamination which allowed the rise of the asthenospheric mantle inducing for one side increase isotherms that they would cause the melting of MCLM and lower crustal, for the other side a melting by adiabatic depressurization of the same asthenospheric mantle. (4) the melting of the MCLM generated potassic syenitic magmas that by field relationships and natural textures of mingling these would be the first to arise and stay in the crust, where subsequently these melts would be intruded by ultrapotassics magmas of transitional and lamproitic signature, at the same time the product of the partial melting of lithospheric mantle would generate another magmatic pulse surrounding of this body that would give origin to the alkali feldspar syenite stocks with geochemical signatures of minette. The fusion of different portions of the lithospheric asthenosferic mantle and variations in mineralogy and chemistry of the lithospheric source would generated different magmatic melts and ultrapotasic rocks.	40

ÍNDICE DE TABELAS

Table 1. Representative analyses of Cpx	16
Table 2. Representative analyses of Amphiboles.....	18
Table 3. Representative analyses of micas	21
Table 4. Chemical analyses and CIPW data of rocks of the Uruana syenite.	23
Table 5. SHRIMP U-Th-Pb isotopic data for the Uruana syenite.....	32
Table 6. Sm-Nd isotopic data for rock for the Uruana syenite. The $\epsilon_{\text{Nd}}(T)$ values were calculated considering the U-Pb crystallization age of 614 Ma (see section 2.4.4).	33
Table 7. Geochemical characteristics of the Uruana syenite rocks, which are considered as ultrapotassic rocks, according to the criteria established by Foley (1987).....	35
Tabela 8. Química mineral dos anfibólios estudados	50
Tabela 9. Química mineral dos clinopiroxênios estudados.....	68
Tabela 10. Química mineral das flogopitas estudadas.	72

RESUMO

A Faixa Brasília é um grande cinturão Neoproterozóico que se localiza na parte central do Brasil e é constituído pelas seguintes unidades morfotectônicas (I) uma espessa sequência de rochas sedimentares e metassedimentares Neoproterozoicas, (II) O bloco arqueando Goiás (IV) complexo granulítico Anápolis-Itauçu, e (IV) Arco magmático Neoproterozóico de Goiás. A parte central e sul da Faixa Brasília se caracteriza pela presença de um extenso magmatismo sin- a pós-colisional. O sienito Uruana é um complexo intrusivo composto principalmente por um corpo quartzo sienítico elipsoidal que mede 20x7 quilômetros e está alongado na direção E-W, um corpo alongado na direção NW-SE e alguns stocks subordinados de composição álcaldi-feldspato sieníticas que afloram a norte do corpo principal e têm até 1 quilômetro de diâmetro, Todos os litotipos do sienito de Uruana apresentam deformação proto-milonítica a milonítica e uma paragênese metamórfica de xisto verde, Esses intrusivos preservam algumas texturas e minerais primários. Os quartzo sienitos representam a principal litologia do corpo principal e se caracterizam por ter uma textura porfirítica definida por fenocristais centimétricos de microclínio envolvidos por matriz fanerítica composta principalmente por edenita, flogopita, k-feldspato quartzo e plagioclásio. Os quartzo sienitos se caracterizam pela presença de enclaves microgranulares (EM) que têm composições que desde granodiorítica até quartzo sienítica e são representados por uma paragênese mineralógica de microclínio, edenita, pargasita, flogopita e em menores quantidades de diopsídio plagioclásio e quartzo. A parte norte do corpo principal é interceptada por diques sin-magmáticos de composições que variam desde ultramáficas a intermediárias. Os diques ultramáficos são principalmente constituídos por flogopita, diopsídio e menores conteúdos de álcaldi feldspato. Os diques intermediários apresentam uma paragênese mineral similar ao quartzo sienito hospedeiro que é representada minerais essências de álcaldi feldspato, anfibólito, flogopita e menores quantidades de quartzo e plagioclásio. Os stocks subordinados são principalmente constituídos por álcaldi-feldspato sienitos. Mostram textura porfirítica definida por fenocristais de tamanhos centimétricos de microclínio e micro-fenocristais de diopsídio e augita imersos em matriz microfanerítica de k-feldspato, biotita e em menor conteúdo de quartzo e plagioclásio. O sienito de Uruana se caracteriza geoquimicamente por ter ampla variação em SiO₂ (45.08 -67.12%) alto conteúdo de K₂O (2.25 -8.62 %), altas razões de K₂O/Na₂O (1.42-4.46), altos enriquecimentos em LILE (Ba=270-5897 ppm; Sr=294-2185 ppm) e em terras raras leves (LREE). Características geoquímicas indicam que as rochas do sienito de Uruana têm afinidade potássica a ultrapotásica. Os quartzo sienitos têm assinatura potássica, os diques ultramáficos têm assinatura lamproítica, enquanto os álcaldi-feldspato sienito têm assinatura minettica e os diques e MMes são rochas ultrapotássicas transicionais. Os quartzo sienitos e os EM tem valores de ϵ_{Nd} que variam entre 9.06 -+0.22. Características geoquímicas e isotópicas do Sienito Uruana sugerem que os magmas geradores destas rochas, foram derivados da fusão parcial do manto litosférico heterogêneo metassomatizado com pequenos aportes do manto astenosférico. Idades de U-Pb em zircão indicam que o sienito de Uruana se cristalizou em 614.7±3.1 Ma, essa idade é contemporânea ou pouco mais jovem com o do pico metamórfico da orogenia Brasiliana na porção central da Faixa Brasília, sugerindo que a fusão parcial do manto continental litosférico metassomatizado e o manto astenosférico ocorreu num contexto sin a pós colisional associado a delaminação litosférica. Este processo permitiu a ascensão do manto astenosférico que causou a fusão parcial de pequenas porções do manto astenosférico, por

descompressão adiabática e ao mesmo tempo gerou uma anomalia térmica que deu origem a uma fusão extensiva do manto continental heterogêneo metassomatizado

Palavras-chave: Sienito de Uruana, Magmatismo Sin-tectônico, Magmatismo Ultrapotássico, Faixa Brasília

ABSTRACT

The Brasília Belt is a large Neoproterozoic orogenic belt in central Brazil consisting of different morphotectonic units: (i) Neoproterozoic supracrustal sequences (ii) the Goiás Archean block (iii) the Anápolis-Itauçu granulite complex and iv) the Neoproterozoic Goiás Magmatic Arc. An extensive syn-to post-collisional magmatism is present in the central and southern parts of the Brasilia belt. The Uruana syenite represents a complex intrusive composed by a main ellipsoidal body of quartz syenites with dimension of approximately 20x7 km to the west, an elongated body to the east and some peripheral stocks of alkali feldspar granites of approximately 1 km in diameter located to the NW of the main body, all intrusives body show a green schist metamorphic paragenesis and a proto-mytonitic to mylonitic deformation, preserving primary magmatic textures. Porphyritic quartz syenites represents the most abundant lithology of the main ellipsoidal body. Their texture is characterized by cm-size phenocrysts of microcline in a faneritic matrix composed of edenite, biotite, microcline, and minor quartz diopside, augite and plagioclase. The quartz syenite is characterized by the presence of microgranular enclaves (Mes) with granodioritic to quartz syenitic composition and is represented by microcline, edenite, pargasite, phlogopite, and minor diopside plagioclase and quartz. Syn-magmatic dykes, of ultramafic to intermediate composition cropout in the northern sector of the main body. The ultramafic dykes are mainly constituted of phlogopite, diopside and minor k-feldspar, whereas intermediate dikes have paragenesis similar to the quartz syenitic host. The peripheral stocks are represented by porphyritic alkali feldspar syenite with cm-size microcline phenocrysts and clinopyroxene microphenocryst in a microfaneritic matrix of k-feldspar, phlogopite, and minor quartz and plagioclase. The geochemical composition of the Uruana syenite rocks show wide variation in SiO₂ (45.08 to 67.12 wt. %), high K₂O content (2.25 to 8.62 wt. %), high K₂O/Na₂O ratios (1.42 to 4.46), display strong enrichment in LILE (e.g., Ba=270-5897 ppm; Sr=294-2185 ppm) and rare earth elements (LREE). The Uruana syenite rocks have potassic to ultrapotassic affinit i) ultramafic dykes show lamproitic signature, ii) felsic dike and the Mes have transitional ultrapotassic characteristics iii) Alkali feldspar syenite present minette-type signature and iv) syenite have potassic signature. The quartz syenite and the Mes show variable Nd isotopic compositions with ϵ_{Nd} values varying from -9.06 to +0.22. Geochemical and isotopic characteristics suggest that the different lithotypes of the Uruana syenite represent magmas derived by partial melting of a heterogeneous Metasomatized Continental Lithospheric Mantle (MCLM) and in minor part of the asthenospheric mantle. The crystallization age of the Uruana syenite of 614.7 ± 3.1 Ma similar to the age of the metamorphic peak in the central part of the Brasilia belt suggesting that the partial melting processes could be related to lithospheric delamination. This mechanism permitted the ascent of hot asthenospheric mantle that underwent to small scale partial melting by adiabatic decompression and at the same time generated a thermal anomaly that generated a more extensive partial melting of the MCLM.

Keywords: Uruana syenite, Syn-tectonic magmatism, Geochemistry, ultrapotassic rock, Brasilia Belt

1.1 Apresentação e objetivos

A Faixa Brasília (FB) é um grande cinturão Neoproterozoico formado pela convergência entre os paleocontinentes Amazonas, São Francisco e Paranapanema, que é constituída pelas seguintes unidades morfotectônicas: (I) espessas sequências de rochas sedimentares e metassedimentares que se depositaram na porção oeste do cráton São Francisco e são agrupadas em sete unidades principais compostas pelos grupos Paranoá, Canastra, Ibiá, Araxá, Vazante, Serra da Mesa e Bambuí (Valeriano et al., 2008 and Sial et al., 2009), (II) maciço de Goiás que é interpretado como um bloco alóctone que inclui os terrenos arqueanos da área Goiás-Crixás, (III) núcleo metamórfico do orógeno conhecido como complexo granulítico Anapolis-Itauçu que apresenta similaridades com uma associação de rochas nomeadas como Uruaçu expostas ao norte do complexo Ánapolis Itau(Pimentel et al., 2000) e (IV) arco magmático juvenil Neoproterozóico de Goiás composto por uma ampla associação de rochas plutônicas e vulcânicas (Pimentel and Fuck, 1992). Dados isotópicos e geoquímicos sugerem que os magmas parentais do Arco Magmático de Goiás foram gerados em zonas de subducção intraoceânicas (Pimentel, 1991; 1997), associados a um sistema de multiarcos com cristalização de magmas primitivos toleíticos a cálcio-alcalinos em dois intervalos de tempo de 930-860 Ma e 670–610 Ma, junto com magmas jovens progressivamente mais evoluídos (Pimentel and Fuck, 1992; Pimentel et al., 1999, 2000; Junges et al., 2002, 2003; Laux et al., 2005; Fuck et al., 2006)

A FB também é caracterizada pela presença de importante granitogênese de caráter sin- e pós-colisional. Recentes mapeamentos nas porções central e sul da Faixa Brasília têm demonstrado a existência de numerosos corpos plutônicos Neoproterozóicos sin e pós tectônicos que intrudem rochas supracrustais do grupo Araxá e os lineamentos dos pirineus. Esses corpos de composição granítica e sienítica de dimensões variáveis se caracterizam pelo desenvolvimento de texturas miloníticas, especialmente ao longo das suas margens que em alguns casos apresentam formas alongadas (Pimentel et al, 1999; Marini et al, 1981; Fuck, 1994; Dardenne, 2000). Um desses corpos, o sienito de Uruana, é o objeto de estudo do presente trabalho de mestrado.

Aqui serão apresentados dados de afloramentos, petrografia, mineralogia, química mineral, bem como a caracterização litogegeoquímica e geocronológica dos corpos sieníticos, com o objetivo de compreender o contexto geodinâmico no âmbito da Faixa Brasília. A proposta deste trabalho, portanto, é contribuir para a produção de novos dados geológicos, geoquímicos e geocronológicos, e de forma geral, no acréscimo do conhecimento dos processos de evolução crustal da porção central da Faixa Brasília. Além da possibilidade de abrir novos caminhos, para melhorar o conhecimento do magmatismo sin-tectônico na porção central da Faixa Brasília.

1.2 Localização

A área de estudo na presente dissertação tem 320 km² e localiza-se na porção centro-oeste do Estado de Goiás entre as cidades de Uruana e Itapuranga (Figura 1). O acesso a partir de Brasília se dá principalmente pela BR-070, até a cidade de Uruana. Na região existem estradas vicinais de acesso a fazendas que tornam fácil o acesso à unidade intrusiva investigada.

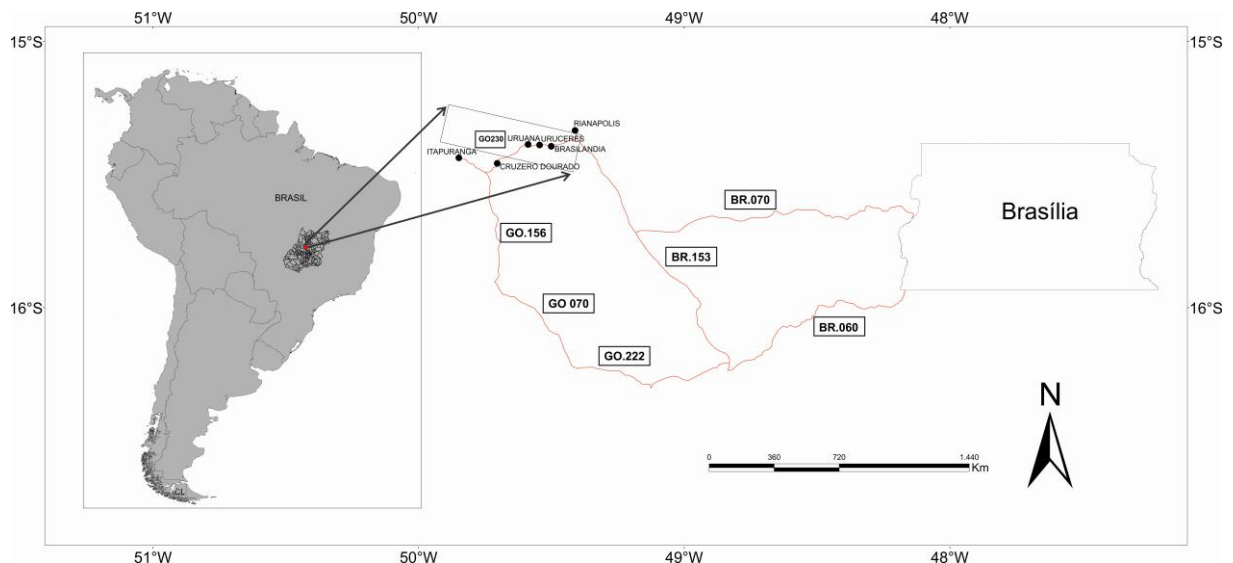


Figura 1: Mapa de localização e acesso da área estudada.

1.3 Escopo da Dissertação

Esta dissertação apresenta-se estruturada na forma de artigo a ser submetido para publicação em periódico científico especializado sobre o tema. O artigo é intitulado “*Petrography, geochemistry and isotopic features of the Uruana syenite and implications for the genesis of syn-tectonic magmatism in the Brasília Belt*”, elaborado entre 2014 e 2016.

O objetivo principal do artigo é apresentar a caracterização petrográfica, petrológica, litogeoquímica e geocronológica do corpo sienítico da suíte Itapuranga, porção central da Faixa Brasília. Serão abordados aspectos tais como a natureza do magma parental e a evolução crustal das rochas sieníticas, bem como seu significado petrogenético na geologia da Faixa Brasília.

O artigo (“segundo capítulo”) é precedido por um capítulo de apresentação, no qual estão contidas informações gerais sobre a dissertação: Apresentação e Objetivos, Localização, e este Subcapítulo, “Escopo da Dissertação”.

O Capítulo de Conclusões apresenta de forma sintetizada os resultados da pesquisa previamente discutidos no artigo.

2. PETROGRAPHY, GEOCHEMISTRY AND ISOTOPIC FEATURES OF THE URUANA SYENITE AND IMPLICATIONS FOR THE GENESIS OF SYN-TECTONIC MAGMATISM IN THE BRASÍLIA BELT.

Sergio A. REYES¹, Massimo. MATTEINI¹. Elton L. DANTAS¹ & Márcio M. PIMENTEL¹.

¹Instituto de Geociências, Universidade de Brasília, Campus D. Ribeiro, 70910-900 Brasília-DF, Brasil.

Corresponding author: Sergio A. REYES (geosergioreyes@gmail.com)/ Massimo. MATTEINI (massimo@.unb.br)/ Márcio M.PIMENTEL¹([márcio@unb.br](mailto:marcio@unb.br))/ Elton L. DANTAS (elton@unb.br).

Abstract

Keywords: syn-tectonic magmatism, geochemistry, ultrapotassic rock, Brasilia Belt

The Brasília Belt is a large Neoproterozoic orogenic belt in central Brazil consisting of different morphotectonic units: (i) Neoproterozoic supracrustal sequences (ii) Goiás Archean block (iii) the Anápolis-Itauçu granulite complex and iv) the Neoproterozoic Goiás Magmatic Arc. An extensive syn-to post-collisional magmatism is present in the central and southern parts of the Brasilia belt. The Uruana syenite represents a complex intrusive composed by a main ellipsoidal body of quartz syenites with dimension of approximately 20x7 km elongated to the west, an elongated body to the east and some peripheral stocks of alkali feldspar granites of approximately 1 km in diameter located to the NW of the main body, all intrusive bodies show a greenschist metamorphic paragenesis and a protomylonitic to mylonitic deformation, preserving primary magmatic textures. Porphyritic quartz syenites represent the most abundant lithology of the main ellipsoidal body their texture is characterized by cm-size phenocrysts of microclinic k-feldspar in a faneritic matrix composed of edenite, biotite, microcline, and minor quartz diopside, augite and plagioclase. The quartz syenite is characterized by the presence of microgranular enclaves (Mes) with granodioritic to quartz syenitic composition and is represented by microcline, edenite, pargasite, phlogopite, and minor diopside plagioclase and quartz. Syn-magmatic dykes of ultramafic to intermediate composition cropout in the northern sector of the main body. The ultramafic dikes are mainly constituted by phlogopite, diopside and minor k-feldspar, whereas intermediate dikes have parageneses similar to the quartz syenitic host. The peripheral stocks are represented by porphyritic alkali feldspar syenite with cm-size microclinic K-feldspar phenocrysts and clinopyroxene microphenocrysts in a microfaneritic matrix of k-feldspar, phlogopite, and minor quartz and plagioclase. The geochemical composition of the Uruana syenite rocks show wide variation in SiO₂ (45.08 to 67.12 wt. %), high K₂O content (2.25 to 8.62 wt. %), high K₂O/Na₂O ratios (1.42 to 4.46), and strong enrichment in LILE (e.g., Ba=270-5897 ppm; Sr=294-2185 ppm) and rare earth elements (LREE). The Uruana syenite rocks have potassic to ultrapotassic affinity i) ultramafic dykes shows lamproitic signature, ii) felsic dike and the Mes show transitional ultrapotassic characteristics iii) Alkali feldspar

syenite present minette-type signature and iv) quartz syenites have potassic signature. The quartz syenite and the Mes show variable Nd isotopic compositions with ϵ_{Nd} values varying from -9.06 to $+0.22$. Geochemical and isotopic characteristics suggest that the different lithotypes of the Uruana syenite represent magmas derived by partial melting of a heterogeneous MCLM and in minor part of the asthenospheric mantle.

The crystallization age of the Uruana syenite is 614.7 ± 3.1 Ma similar to the age of the metamorphic peak in the central part of the Brasilia belt, suggesting that the partial melting processes could be related to lithospheric delamination. This mechanism permitted the ascent of hot asthenospheric mantle that underwent small scale partial melting by adiabatic decompression and at the same time generated a thermal anomaly that generated a more extensive partial melting of the MCLM.

2.1 Introduction

The Brasília Belt is a large and well-preserved Neoproterozoic orogenic belt in central Brazil formed by the convergence between the Amazon, São Francisco-Congo and Paranapanema paleocontinents. It consists of different morphotectonic units: (i) a thick sequence of metasedimentary and sedimentary rocks deposited and deformed along the western margin of the São Francisco-Congo Craton, (ii) the Goiás Massif, interpreted as an allochthonous sialic block consisting mainly Archean granite-greenstone and orthogneiss TTG grounds, Meso-Neoproterozoic ultramafic complexes of Barro Alto, Niquelândia, Cana Brava and associated volcano-sedimentary sequences, (iii) the metamorphic core of the orogen, known as the Anápolis-Itauçu granulite complex; very similar rock associations are exposed in the so called Uruaçu Complex, to the north of the Anápolis-Itauçu complex (Pimentel et al., 2000), and (iv) a large exposure of Neoproterozoic juvenile volcanic/plutonic associations, the Goiás Magmatic Arc that includes primitive tholeiitic to calc–alkaline magmatism in two age intervals, 930–860 and 670–610 Ma, with younger magmas being progressively more evolved (Pimentel and Fuck, 1992; Pimentel et al., 1999, 2000; Junges et al., 2002, 2003; Laux et al., 2005; Fuck et al., 2006).

SHRIMP U-Pb data in zircon and Sm-Nd data in garnet (Piuzana, 2003) indicate that the peak of high-grade metamorphism in the Anápolis–Itauçu Complex occurred between ca. 650–640 Ma.

The Brasília Belt is characterized by the presence of important granitogenesis of syn and post-collisional character (Pimentel et al, 1999; Marini et al, 1981; Fuck, 1994; Dardenne, 2000). Recent field, isotopic and geochronologic data in the central and southern portions of the Brasilia belt have demonstrated the existence of numerous Neoproterozoic syn-, and post-tectonic plutons that intrude supracrustals rock of the Araxá Groups and the Pireneus lineament. These bodies of granitic and syenite composition of various dimensions are characterized by the development of milonitic textures especially along their margins, in some cases they form narrow elongated bodies

One of these bodies, the Uruana syenite, is the main object of this study in this paper. Here will be present field, petrographic, mineralogical, mineral chemistry data, the lithogeochronological characterization and of the syenitic bodies, in order to understand the geodynamic context within the Brasilia Belt.

2.2 Regional Geology

The Tocantins Province (TP) represents a large N-S orogen direction developed in the Neoproterozoic Pan-African/Brasiliano cycle (Almeida et al., 1981) and was formed by the convergence and collision of three major continental blocks: Amazonian Craton (northwest), San Francisco-Congo Craton (east) and Paranapanema Craton (south), presently covered by Phanerozoic rocks of the Paraná Basin. The TP consists of Paraguay and Araguaia Belts, which thrusts with vergence to the east in the east margin of the Amazonian Craton and the Brasilia Belt follow and thrust with vergence to east-southeast in the western margin of San Francisco Craton (Pimentel et al, 2000; Dardenne et al, 2000).

The Brasilia Belt is located in the center-east portion of the Tocantins Province along a N-S trend of 1200 kilometers of since the southern part of Minas Gerais states until the north of Tocantins state. The Brasilia Belt comprises a set of terrains, crustal chips and thrusted metasediments above the west part of São Francisco craton and shows tectonic vergence in the direction of the cratonic area (Figure 2).

The eastern portion of the Brasilia Belt consists of thick sedimentary sequences that are grouped into seven main stratigraphic units: the Paranoá, Canastra, Ibiá, Araxá, Vazante, Serra da Mesa and Bambuí groups (Valeriano et al., 2008 and Sial et al., 2009), which were deposited on the western portion São Francisco craton. These sequences shows tectonic deformation and the metamorphic grade progressively more intense towards to the west. In the Craton area occurs a transition of non-metamorphosed sediments in the cratonic area to of amphibolite facies rocks and even granulites in the Brasilia Belt western portion (Campos Neto & Caby, 2000; Dardenne, 2000; Seer et al., 2000, 2001; Piuzana et al., 2003).

The Brasilia Belt covers, in the central portion, an older unit known as The Goias massif, which includes mostly Archean granite-greenstone and orthogneiss TTG terrains, The Meso-Neoproterozoic ultramafic complexes of Barro Alto, Niquelândia, Cana Brava and the associated volcano-sedimentary sequences. The eastern portion of the massif is marked by a gravity anomaly associated to suture zones, that later would be interpreted as allochthonous terrains amalgamated to the Brasilia Belt during the Neoproterozoic era (Brito Neves & Cordani, 1991; Pimentel et al., 2000b; Piuzana et al., 2003b).

The Neoproterozoic Goias magmatic arc (GMA) is located in the western portion of the Brasilia Belt and comprises ca. 930–860 Ma old calc-alkaline orthogneiss and remnants of volcano-sedimentary sequences, younger orthogneiss and supracrustals of continental arc affinity (670–610 Ma), as well as a number of post-orogenic granite intrusions. Most of these rocks present juvenile character with a strong mantle input, as indicated by the positive eNd (T) values and TDM model ages mostly between 0.9 and 1.2 Ga (Pimentel and Fuck, 1992).

The main metamorphic episode occurred between ca. 650–640 Ma. and is interpreted as the result of final ocean closure during the Brasiliano event (Pimentel et al., 1997, Junges et al., 2002, 2003, Piuzana et al., 2003).

In southern portion of the Brasilia Belt, between the GMA and The Araxá Group occurs the Anápolis-Itauçu Complex, formed by orthogranulites and deformed granites that emerge along intensely metamorphosed zones, elongated in NW-SE direction. Isotopic Nd data shows equivalences between

felsic granulites and intrusive granites of this complex and The Araxá Group metasediments (T_{DM} = 1.1–1.3 e 1.9–2.3), which suggests that some Anápolis-Itauçu Complex granulites could represent high grade metasedimentary rocks of The Araxá Group (Fischel et al., 1998; 1999; Pimentel et al., 1999; 2001; Seer, 1999; Piuzana et al., 2003).

One of the most conspicuous structural features of the Brasília Belt is the approximately EW lineaments that occur in its central and southern parts, some of which have been interpreted as lateral ramps related to the important eastward mass transport in the southern part of the belt (Strieder and Suita 1999, Araújo Filho 2000). The Pireneus lineament is the most obvious of these structures, and extends for over 200 km roughly in the EW direction, marking the so-called Pireneus Syntaxis (Araújo Filho 2000).

Lineaments with EW direction characterize the Anápolis-Itauçu Complex, and along them are two intrusive bodies, the Itapuranga alkali granite and the Uruana syenite representative of the Itapuranga suite (Souza et al, 1993, Lacerda Filho & Oliveira 1995, Oliveira 1997). SHRIMP and conventional U-Pb data of these intrusions (Pimentel, 2003) indicate that they are roughly coeval and have crystallized at 624 ± 10 Ma and 618 ± 4 Ma, respectively. They are contemporaneous or younger than the metamorphic peak of the Brasiliano event in the central portion of the Brasilia Belt. Their accommodation along the Pirineus lineament suggests that the intrusions are syn-tectonic bodies with regard to these structures, having crystallized in transtension zones along the faults (Pimentel, 2003).

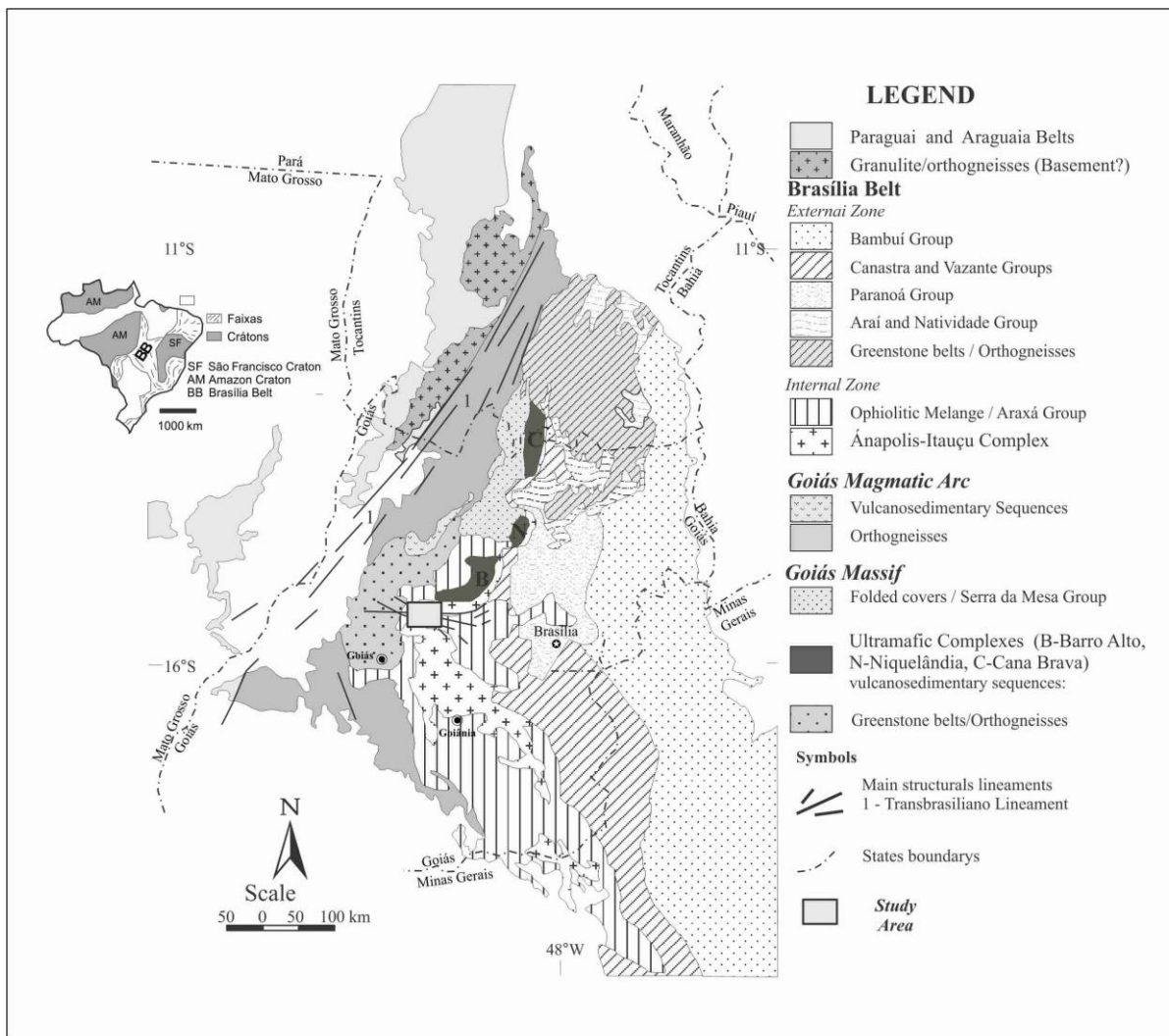


Figure 2. Geologic Sketch map showing the main tectonic features and components of the Brasília Belt.

The Itapuranga suite was initially correlated as belonging to the Basal Complex (Almeida, 1967) and the Araxá group (Barbosa., et al 1967), which would later be mapped by Pena et al. (1975), in the Goiania II project (sheet SD.22-Z-C) as granite core Rubiataba-Itapuranga, forming part of the main lithologies Basal Complex. According to the author above, this granitic core is composed of biotite granite, biotite-hornblende granite with gradations for gneisses and migmatites, limited by an extensive filonitic belt.

Sá (1987), in the metallogenetic maps Project and Mineral Resource Forecast, near the towns of Itapuranga and Uruana, denominated the set of plutonic bodies formed by metagranites and metasyenites with subvolcanic facies of "Intermediate and Acid Plutonic Rocks" and placed in the Lower Proterozoic, by this author. Oliveira (1997) proposed the term "Itapuranga Suite" (Itapuranga alkali granite and Uruana syenite) to join subalkaline potassic rocks (shoshonitic) calcium-alkaline (Souza et al., 1993), mainly composed of metaquartz syenites, alkali feldspar granites with gradations para-metaquartz monzonite, metaquartz diorites, granodiorite and tonalites, which feature various deformational protomylonites stages, mylonite to ultramylonites. This Suite is also characterized by the presence of microgranular enclaves (Mes) and ultramafic dykes with sizes varying from centimeters to decimeters.

The Itapuranga and Uruana bodies are exposed just to the north of the Anápolis-Itauçu high-grade complex and are intrusive into deformed granites of the Paleoproterozoic Jurubatua suite age, supracrustal rocks of the possibly Paleoproterozoic-Neoproterozoic Rio do Peixe volcano-sedimentary sequence and into metasediments of the Araxá Group and Serra Dourada Sequence. In general, the contacts between the intrusions and the country-rocks are marked by mylonitic zones and crosscutting.

The Jurubatuba suite includes, the jurubatuba granite (Piuzana, 2002) deformed gneisses and migmatites. The Rio do Peixe volcano-sedimentary sequence is formed by amphibolite, calc-silicate rocks, and micaschist with garnet and staurolite. The felsic metavolcanic rocks are less abundant (Oliveira 1997). The Araxá Group is formed dominantly by micaschists, quartzites and carbonate-bearing schists, the most abundant rock types are garnet-feldspar-biotite-muscovite schist, kyanite-garnet-biotite- muscovite schist, garnet quartzite and chlorite-muscovite schist. Garnet crystals are commonly involved by biotite and muscovite, forming a protomylonitic foliation (Lacerda Filho & Oliveira, 1995), and the Serra Dourada Sequence, of possible paleoproterozoic age, comprises quartz schist and quartzite (Oliveira, 1997) (Figure 3A).

2.3 . Material and Methods

2.3.1 Sampling and petrography

Fieldwork was carried out to identify and characterize the main lithological facies of the Uruana syenite. A group of forty rocks were sampled between syenite, enclaves (Mes) and sin magmatic dikes with relevant features and Cross-Cutting relationships. Thirty samples were selected for petrographic studies, we used light Zeiss Image A2m and Olympus BX-60 Transmitted Light Polarizing Microscopes with coupled axiocamICc3 and Q-Imaging 5.0 RTV cameras respectively.

2.3.2 Mineral Chemistry

The composition of minerals was obtained using a Cameca SX-50 electron microprobe at the Electron Microprobe Laboratory of the University of Brasilia (Brazil). Wavelength-Dispersive (WDS) analyses were performed at an accelerating voltage of 15 kV and a beam current of 25 nA with a spot size of 1 µm. Acquisition time was 100 s. Each element was standardized using either synthetic or natural minerals.

2.3.3 Lithogeochemistry

Twenty-six samples for geochemical analyses were selected. Weathered rocks and veined surfaces were cut off. The rocks were crushed and milled in a vídea mill up to a very fine powder. Major and trace elements were analyzed by ICP-OES and by ICP-MS at the ACME Laboratories in Canada.

2.3.4 Sm-Nd isotopes

The bulk rock Sm–Nd isotopic analyses were carried out at the Geochronology Laboratory of the University of Brasília. Sample dissolution was done in Teflon Savillex vials or in Parr-type Teflon bombs. Sm and Nd extraction from whole-rock powders and garnet concentrates followed the technique of Richard et al. (1976), in which the separation of the REE as a group using cation-exchange columns precedes reversed-phase chromatography for the separation of Sm and Nd using columns loaded with HDEHP (Di-2-ethylhexylphosphoric acid) supported on Teflon powder. We have also used the RESpec and Ln-Spec resins for REE and Sm–Nd separation. A mixed ^{149}Sm – ^{150}Nd spike was used. Sm and Nd samples were loaded onto Re filaments of a double filament assembly. Sm and Nd isotopic analyses were carried out using a Finnigan MAT-262 mass spectrometer. Uncertainties on Sm/Nd and $^{143}\text{Nd}/^{144}\text{Nd}$ ratios are considered to be better than $\pm 0.05\%$ (1σ) and $\pm 0.003\%$ (1σ), respectively, based on repeated analyses of international rock standards BCR-1 and BHVO-1. The $^{143}\text{Nd}/^{144}\text{Nd}$ ratios were normalized to a $^{146}\text{Nd}/^{144}\text{Nd}$ ratio of 0.7219. The Nd procedure blanks were smaller than 100 pg.

2.3.5 Shrimp U-Pb

Zircon concentrates were extracted from ca. 10 kg rock samples, using conventional gravimetric (DENSITEST®) and magnetic (Frantz isodynamic separator) techniques at the Geochronology Laboratory of the University of Brasília. Final purification was achieved by hand picking using a binocular microscope. The preparation of epoxy mounts and the high resolution secondary ion mass spectrometer coupled with an Ion Microprobe (Ile/MC) Analysis SHRIMP were made at the Geochronology Laboratory of the Universidade de São Paulo (USP).

Zircon grains were mounted in epoxy resin and polished with diamond compound (1 – 7 μm) to reveal grain centers, for the cleaning procedures in a clean room the mounting was wash with detergent, three times with Petroleum Spirit and three times with ultrapure hot water (MILIQ, 50–60 °C) and subsequently was drying at 50 – 60°C for 2 hours. Scanning electron microscope cathodoluminescence imagery was used to investigate the internal structures of the zircon crystals prior to analysis. The images were acquired before gold coating of 2 – 3 μm .

Cathodoluminescence (CL) images were obtained by FEI Quanta 250 Scanning Electron Microscope (SEM) and XMAX CL detector (Oxford Instruments) SEM analytical conditions were high voltage = 15 kV, work distance = 16.9 mm, detector = PMD, filament emission = 100 μA , and magnification range = 95 to 250x after CL acquisition, the gold was removed and the mount was recleaned the thickness (~3 μm) of the final gold coating was reached after a two-minutes exposuae and an electrical conductivity resistance of approximately 15 – 17 Ω (between the border and the center of mount).

Analyses on the SHRIMP Ile were carried out under, the following primary beam analytical conditions: Kohler aperture = 120 μm , spot size = 30 μm , and O₂ beam density = around 2.5 – 7 nA and Secondary beam analytical conditions: source slit = 80 μm ; mass resolutions for $^{196}(\text{Zr}2\text{O})$, ^{206}Pb , ^{207}Pb , ^{208}Pb , ^{238}U , $^{248}(\text{ThO})$ and $^{254}(\text{UO})$ ranging between 5,000 and 5,500 (1%), and residues < 0.025.

Data were collected and reduced as described by Williams (1998) Stacey and Kramer (1975), Temora 2 was used as $^{206}\text{Pb}/^{238}\text{U}$ age reference (416.78 Ma, Black et al., 2004), and SL13 (238 ppm)

was used as U composition reference. (Ludwig, 2003) software and the uncertainties of the ratios are of 1σ and 2σ . Concordia diagrams were made using ISOPLOT 4.15 software

2.4 Results

2.4.1 Field relationships and petrography

The Uruana syenite represents a complex intrusive body. The gamma-spectrometric data especially the potassium radioelement image (KPERC) and ternary CMY (K/Th/U) composition image, allowed to clearly delimit different intrusive bodies in the study area: i) an ellipsoidal main body with ca. 20x7 km elongate in E-W direction ii) some minor peripheral sub-circular stocks of approximately 1 km in diameter localized to the NW of the main body; iii) an approximately NW-SE elongated body to the east (Figure 3B). All intrusive rocks show protomylonitic to mylonitic deformation being the main body and peripheral stocks less deformed, preserving some primary magmatic textures. All intrusive bodies present metamorphic greenschist facies parageneses constituted by actinolite+epidote+oligoclase+titanite. Only the main body and peripheral stocks are the objects of this study.

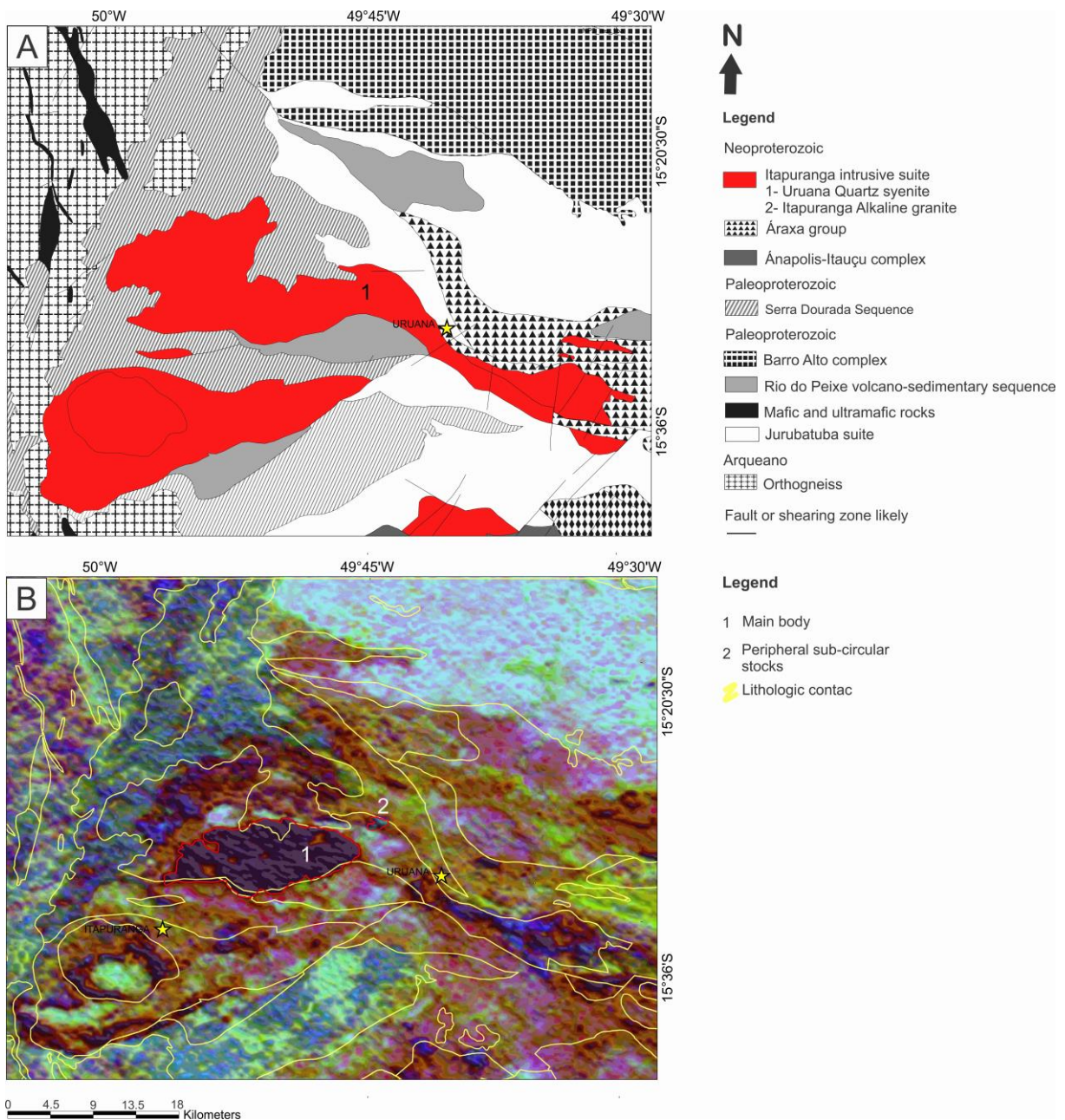


Figure 3. (A) Simplified geological map of the Itapuranga-Uruana area (sheet SD.22-Z-C-VI), adapted from Oliveira (1997). (B) Composite color images (CMY and KPERC) of aerial gamma-ray spectrometric data of the study area. The limits of the different intrusive bodies are highlighted (Data from CPRM database).

The main body is a homogeneous quartz syenite (Figure 4A), composition showing an ubiquitous porphyritic texture constituted by phenocrysts of subhedric to euhedral perthitic microcline dispersed in a faneritic matrix composed of k-feldspar, biotite and minor quartz and plagioclase (Figure 4B; 5A; 5B). Sometimes hornblende microphenocrysts are present, showing common biotite inclusions. Titanite, epidote, apatite and zircon represent accessory minerals.

The quartz syenite main body is characterized by the presence of abundant microgranular enclaves (Mes). They are light to dark gray in color, generally show a characteristic ellipsoidal diskshapes (Figure 4C), and vary in size from few centimeters to approximately two meters. Sometimes the Mes show porphiritic texture with cm-size K-feldspars that represent original phenocrysts of the host syenite being inglobate during the mingling process (Figure 4D; 5C). Enclaves with amphibole and

clinopyroxene phenocryst are also present. The paragenesis of the Mes is represented by K-feldspar, amphibole, biotite and minor clinopyroxene, also plagioclase and quartz (Figure 5D). The relative abundance of mafic minerals, biotite and amphibole, vary with the Mes composition. Titanite, epidote, apatite and zircon represent accessory minerals.

Have been identified Syn-magmatic dikes In some outcrops in the northern portion of the mafic body. The Syn-magmatic dikes are not planar tabular intrusion, showing plastic geometry and vary in thickness from centimetric to decimetric. At outcrop scale they generally present sharp contact with the host syenite and may be locally concordant or discordant to the main mylonitic foliation.

Two types of these syn-magmatic dikes have been identified: i) intermediate to felsic dike with fine to medium grain size, up to 30 cm in thickness with plastic contact with the host syenite (Figure 4E). The paragenesis is very similar to the host quartz syenite with abundant k-feldspar, amphibole, biotite and minor quartz and plagioclase. Titanite, epidote, apatite and zircon represent accessory minerals. ii) Ultramafic dike with fine to medium grain size, up to 30 cm in thickness. These preserves a typical tabular geometry and locally it dismembered in discrete portions as discrete microgranular mafic enclaves (Figure 4F). The paragenesis of the ultramafic dikes is mainly constituted by micro-phenocrysts of clinopyroxenes and minor amphibole immersed in a groundmass of biotite and K-feldspar (Figure 5E), clinopyroxenes show reaction rims of amphibole (Figure 6F). Xenocrysts of K-feldspar from the host syenite are present (Figure 5H). Accessory minerals are represented by zircon macrocryst, up to 1 mm in size, titanite, epidote, apatite and oxides.

The peripheral stocks are constituted by alkali feldspar syenite and are characterized by subvolcanic texture defined by microcline phenocrysts and minor clinopyroxene with amphibole rims (Figure 5H; 5J). These crystals are immersed in a micro-faneritic matrix of k-feldspar, biotite, plagioclase and quartz (Figure 5I). Accessory minerals are titanite, epidote, apatite, zircon and oxides.

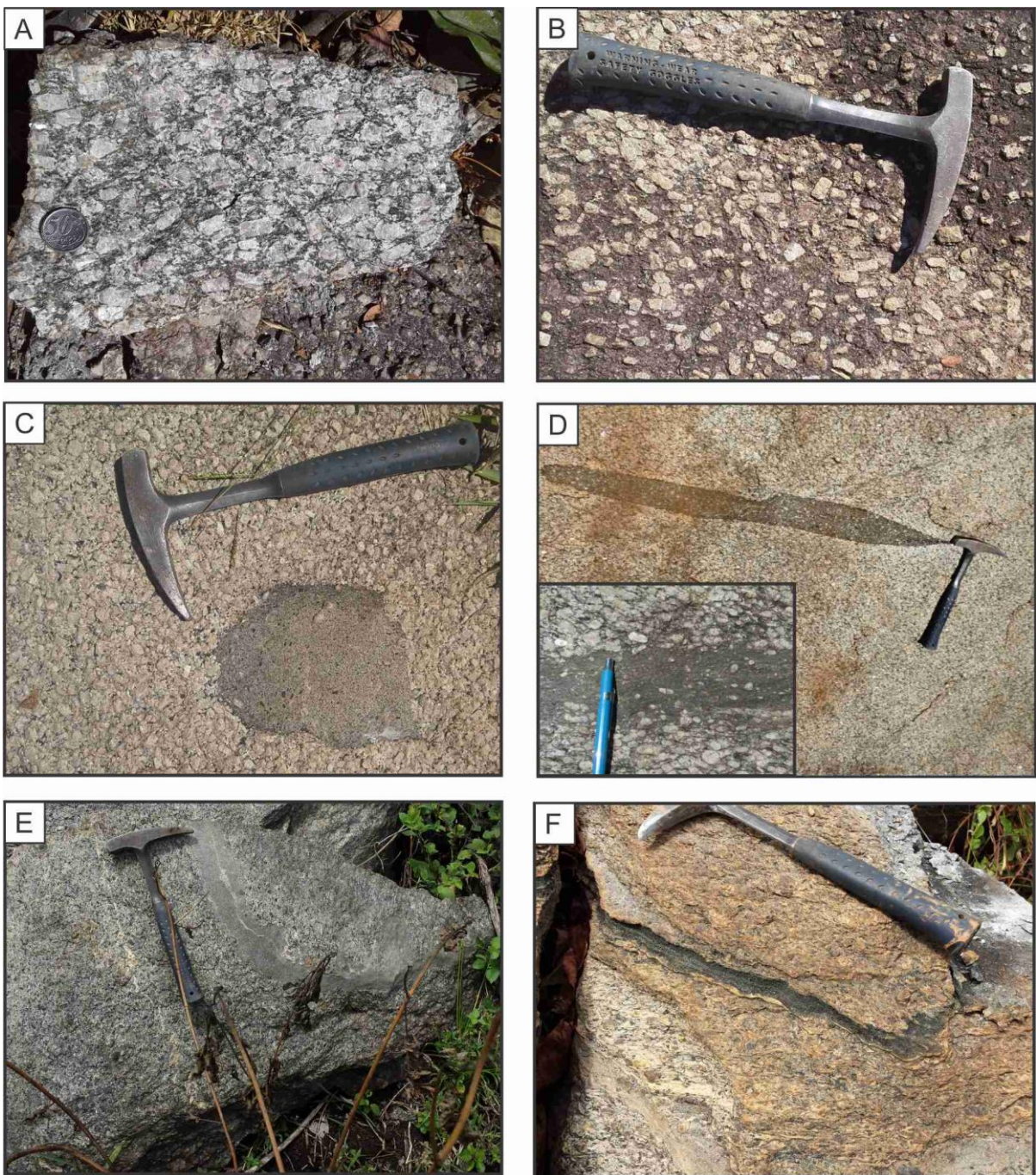


Figure 4. Main geological features of the Uruana sienite lithotypes. (A) Coarse grained quartz sienitic rocks of the main body (B) Typical porphyritic texture of the Quartz syenite (C, D) Typical ellipsoidal disk-shaped Microgranular Enclaves (Mes) hosted in the quartz syenite. The presence of K-Feldspar xenocrysts from the quartz syenite are evidences of magma mixing (mingling). (E) Syn-magmatic intermediate to felsic dike. (F) Syn-magmatic tabular intrusion of ultramafic composition sub-parallel to the mylonitic foliation.

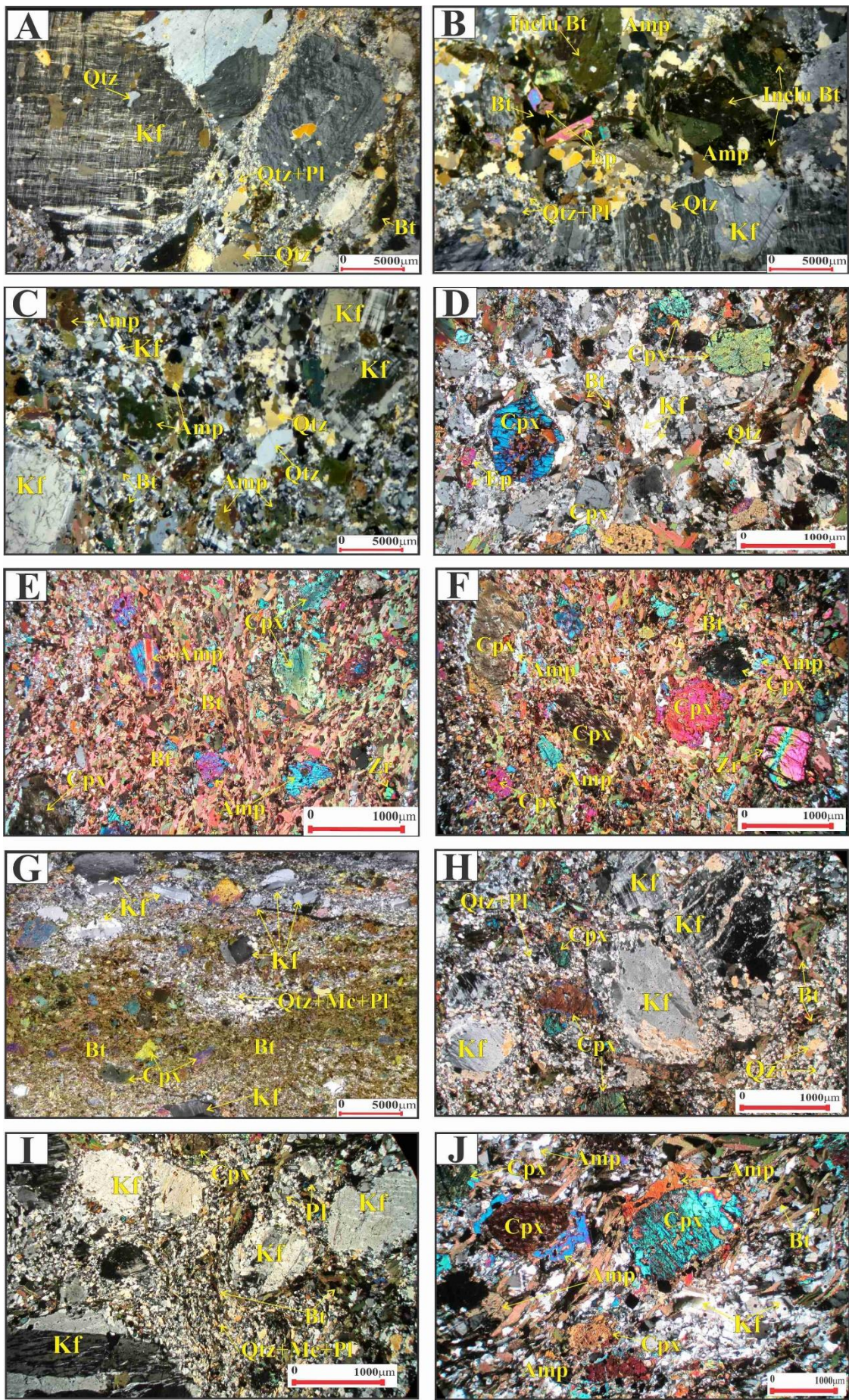


Figure 5. Photomicrographs (plane-polarized light) of the rocks Uruana syenite (A-B) Quartz syenites, (C-D), Microgranular enclaves, (E-G), Ultramafic dike (H-J). Alkali feldspar syenite (A) subhedral to euhedral phenocrysts of perthitic K-feldspar dispersed in a faneritic matrix composed by k-feldspar, amphibole, biotite and minor quartz and plagioclase. (B) Microphenocrysts of hornblende, showing common biotite inclusions. (C) K-feldspar xenocrysts of the Mes that were encompassed from the hosting Quartz syenite. (D) Typical paragenesis of the Mes, represented by K-feldspar, biotite, clinopyroxene, plagioclase and quartz crystals. (E) micro-phenocrysts of clinopyroxenes and minor amphibole immersed in a groundmass of biotite and k-feldspar. (F) Clinopyroxenes with reaction rim of actinolite and characteristic zircon macrocrystal. (G) Contact between ultramafic dike and quartz syenitic host attain to Xenocrysts of K-feldspar from the host syenite assimilated by the ultramafic dike. (H) Clinopyroxenes and minor amphibole immersed in a groundmass of biotite and k-feldspar. (I) Phenocrysts of k-feldspar and clinopyroxene immersed in a micro-faneritic matrix of k-feldspar, biotite, plagioclase and quartz. (J) Actinolite reaction rim of clinopyroxenes.

2.4.2 Mineral chemistry

Mineral chemistry studies were carried out for clinopyroxene, amphibole, and micas in samples representatives of different lithologies of the Uruana syenite.

2.4.2.1 Clinopyroxene

The analysis of clinopyroxene crystals are show in Table 1. All the analyzed crystals belong to the calcic series with diopside to augite composition (Figure 6). The diopside grains are characterized by compositions in the range of Wo 46.1–49, En 35.6 -42.1 and Fs 8.8-17.7, whereas the augite grains have contents compositions of Wo 32.3-44.8, En 29.7-47.7 and Fs 14.4-31.1.

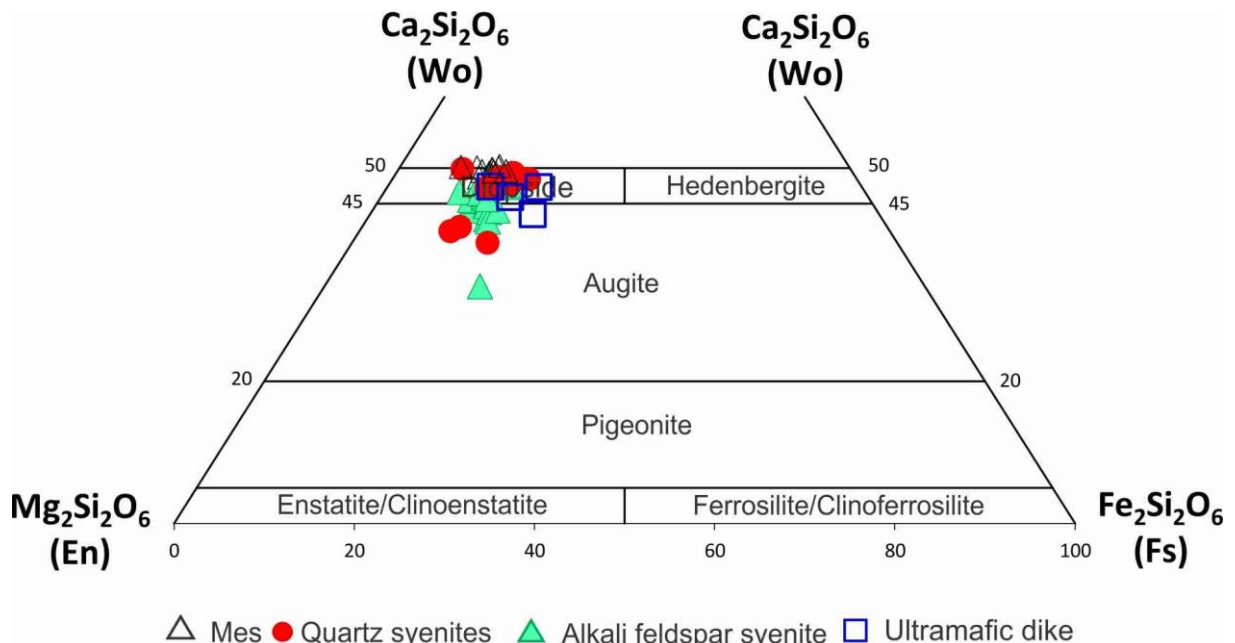


Figure 6. Wollastonite-(Wo), (En)-Enstatite (Fs)-Ferrosilite classification diagram (Morimoto et al., 1988) for clinopyroxene from the different lithology of Uruana syenite

Table 1. Representative analyses of Cpx

Rock	Quartz syenite		Syn magmatic ultramafic dike		microgranular enclaves		Alkaline feldspar syenite	
Sample	<u>Uru-25</u>		<u>Uru-27</u>		<u>Uru-36</u>		<u>Uru-45</u>	
	CPX Crystals		CPX Crystals		CPX Crystals		CPX Crystals	
SiO ₂	54,47	54,03	53,52	53,25	53,43	53,92	53,44	53,14
TiO ₂	0,14	0,09	0,36	0,25	0,10	0,00	0,39	0,57
Al ₂ O ₃	1,08	1,84	0,87	1,06	1,94	1,37	1,17	1,06
FeO	9,28	10,64	10,24	11,79	9,94	9,73	9,16	9,41
MnO	0,27	0,38	0,35	0,19	0,41	0,37	0,43	0,36
MgO	12,74	14,13	12,20	11,29	11,75	12,00	13,37	13,33
CaO	20,08	16,57	19,22	18,13	21,14	21,46	19,17	19,51
Na ₂ O	2,27	2,70	2,44	2,81	1,93	1,76	2,10	1,80
Total	100,33	100,36	99,21	98,77	100,63	100,61	99,23	99,18
Ti	0,0039	0,0023	0,0102	0,0070	0,0028	0,0000	0,0110	0,0160
Al	0,0468	0,0527	0,0357	0,0468	0,0568	0,0513	0,0367	0,0287
Fe ³⁺	0,0998	0,1603	0,1229	0,1405	0,1035	0,0832	0,1069	0,0873
Fe ²⁺	0,1777	0,1383	0,1866	0,2145	0,2002	0,2144	0,1637	0,1889
Mg	0,6681	0,6464	0,6446	0,5893	0,6366	0,6512	0,6817	0,6792
Sum M1	1,00	1,00	1,00	1,00	1,00	1,00	1,00	1,00
Fe ²⁺	0,0081	0,0262	0,0099	0,0157	0,0031	0,0031	0,0141	0,0172
Mn	0,0084	0,0116	0,0110	0,0060	0,0127	0,0116	0,0134	0,0113
Mg	0,0304	0,1227	0,0342	0,0432	0,0098	0,0094	0,0585	0,0619
Ca	0,7913	0,6484	0,7686	0,7300	0,8361	0,8495	0,7629	0,7796
Na	0,1618	0,1911	0,1762	0,2050	0,1384	0,1263	0,1510	0,1299
Sum M2	1,00	1,00	1,00	1,00	1,00	1,00	1,00	1,00
Si	2,0037	1,9733	1,9973	2,0018	1,9724	1,9918	1,9855	1,9820
Al	0,0000	0,0267	0,0027	0,0000	0,0276	0,0082	0,0145	0,0180
Sum T	2,00	2,00	2,00	2,00	2,00	2,00	2,00	2,00
Wo	44,57	37,22	43,50	42,12	46,73	46,92	42,67	42,98
En	39,34	44,14	38,42	36,49	36,13	36,48	41,41	40,85
Fs	16,09	18,64	18,08	21,39	17,15	16,60	15,92	16,17

2.4.2.2 Amphibole

Representative analysis of amphibole crystals are presented in Table 2. The analyses were carried out on amphibole crystals in the Quartz syenites, Mes, Alkali feldspar syenite and ultramafic dike. Amphiboles growing at the rim of clinopyroxenes were also analysed. According to the classification proposed by Leake et al.(1997), the amphiboles belong to the calcic group showing compositions varying from edenite, to pargasite (Figure 7A). The amphiboles that grow to the rim of the clynopyroxenes have actinolite compositions (Figure 7B).

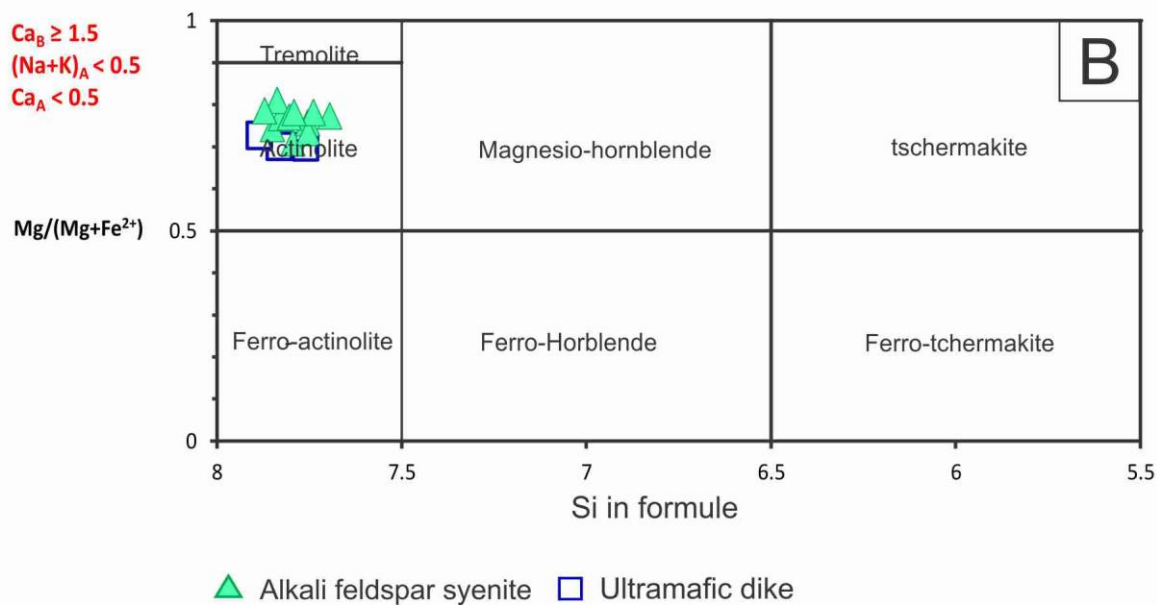
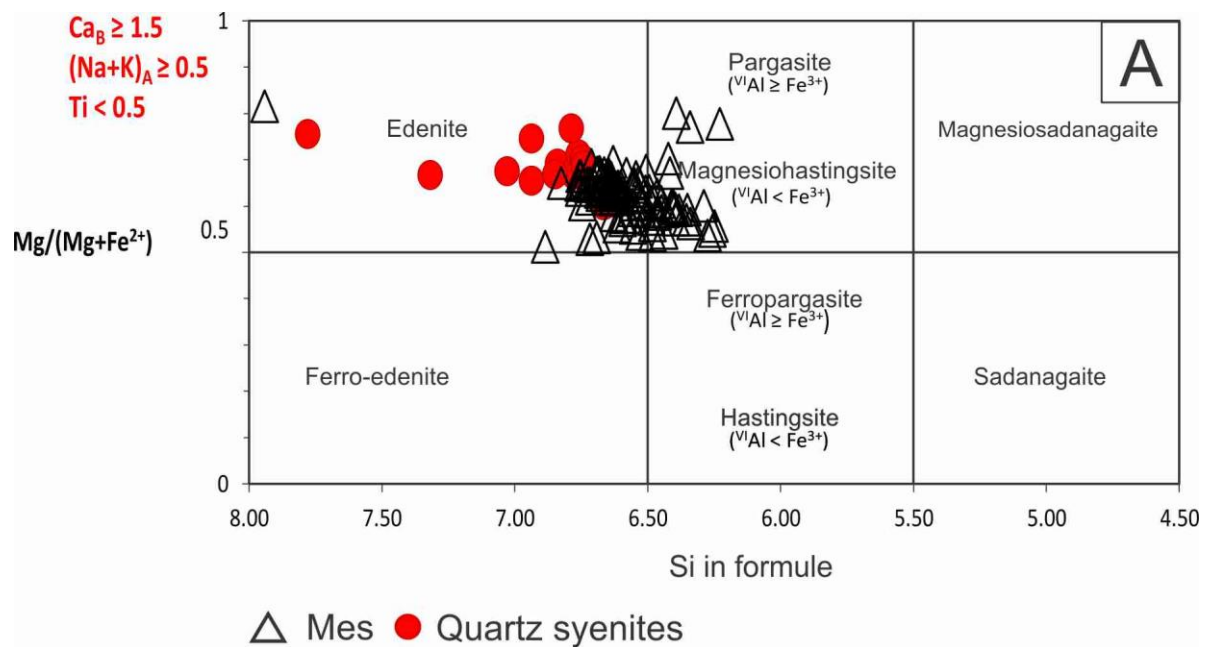


Figure 7. Classification diagrams for amphiboles (Leake et al., 1997) .A) $(\text{Na} + \text{K})_A \geq 0,50$.B) $(\text{Na} + \text{K})_A < 0,50$.

Table 2. Representative analyses of Amphiboles.

Rock Sample	Microgranular enclave		Syn magmatic ultramafic dike		Quartz Syenite		Alkaline feldspar syenite	
	Uru-09		Uru-27		Uru-37		Uru-45	
	Crystal	Crystal	Crystal	Crystal	Crystal	Rim		
SiO ₂	46,24	45,53	53,17	53,34	44,59	44,82	54,79	54,03
TiO ₂	1,25	1,47	0,00	0,02	1,31	1,60	0,00	0,02
Al ₂ O ₃	8,38	8,95	1,39	0,98	8,43	8,65	1,40	1,82
FeO	15,49	15,94	13,05	13,10	16,49	16,51	12,46	11,74
MnO	0,45	0,27	0,35	0,46	0,38	0,17	0,25	0,29
MgO	12,19	12,11	15,89	15,51	11,58	11,50	16,31	17,31
CaO	10,48	10,90	11,11	11,02	10,99	10,98	11,04	11,37
Na ₂ O	2,02	2,27	1,32	1,28	2,21	2,25	1,03	0,87
K ₂ O	1,20	1,24	0,35	0,23	1,18	1,21	0,23	0,19
F	0,00	0,00	0,39	0,41	0,63	0,53	0,00	0,00
Cl	0,06	0,09	0,02	0,01	0,13	0,08	0,00	0,01
V ₂ O ₃	0,00	0,04	0,00	0,00	0,07	0,10	0,04	0,00
ZnO	0,00	0,04	0,00	0,00	0,02	0,00	0,01	0,07
SrO	0,00	0,00	0,00	0,00	0,01	0,07	0,00	0,00
O=F,Cl	0,01	0,02	0,17	0,17	0,29	0,24	0,00	0,00
TOTAL	97,73	98,84	96,93	96,20	97,72	98,21	97,55	97,73
Si	6,8330	6,6990	7,7704	7,8445	6,2625	6,6734	7,8421	7,7216
Al	1,1670	1,3010	0,2296	0,1555	1,7375	1,3266	0,1579	0,2784
SUM T	8,00	8,00	8,00	8,00	8,00	8,00	8,00	8,00
Al	0,2917	0,2502	0,0098	0,0137	0,5806	0,2294	0,0781	0,0277
Ti	0,1390	0,1631	0,0000	0,0017	0,1288	0,1353	0,0000	0,0026
Fe ³⁺	0,3020	0,2562	0,0563	0,0785	0,4880	0,2676	0,1932	0,1583
V	0,0000	0,0051	0,0000	0,0000	0,0079	0,0124	0,0047	0,0000
Mg	2,6858	2,6550	3,4625	3,4002	2,4250	2,5517	3,4794	3,6886
Zn	0,0000	0,0045	0,0000	0,0000	0,0018	0,0000	0,0012	0,0070

Table 2. Representative analyses of Amphiboles (Continued).

Fe2+	1,5815	1,6660	1,4633	1,5019	1,3680	1,8036	1,2435	1,1148
SUM C	5,0000	5,0000	5,0000	5,0000	5,0000	5,0000	5,0000	5,0000
Mn	0,0563	0,0339	0,0433	0,0569	0,0363	0,0436	0,0298	0,0345
Fe2+	0,0302	0,0393	0,0758	0,0311	0,1046	0,0329	0,0544	0,1298
Ca	1,6593	1,7180	1,7393	1,7359	1,6540	1,7514	1,6924	1,7402
Sr	0,0000	0,0000	0,0000	0,0000	0,0005	0,0059	0,0000	0,0000
Na	0,2542	0,2088	0,1416	0,1761	0,2046	0,1662	0,2234	0,0955
SUM B	2,0000	2,0000	2,0000	2,0000	2,0000	2,0000	2,0000	2,0000
Na	0,3231	0,4398	0,2316	0,1898	0,3961	0,4830	0,0635	0,1464
K	0,2264	0,2323	0,0654	0,0422	0,2119	0,2298	0,0418	0,0354
SUM A	0,5495	0,6721	0,2970	0,2320	0,6080	0,7128	0,1053	0,1817
Si	6,7879	6,6615	7,7609	7,8311	6,1954	6,6343	7,8090	7,6949
NaB	0,3517	0,2916	0,1598	0,2014	0,3632	0,2530	0,2857	0,1470
CaB	1,6483	1,7084	1,7372	1,7330	1,6363	1,7411	1,6853	1,7342
Ti	0,1380	0,1622	0,0000	0,0017	0,1274	0,1345	0,0000	0,0026
(Ca+Na)B	2,0000	2,0000	1,8970	1,9344	1,9995	1,9942	1,9710	1,8812
(Na+K)A	0,4467	0,5844	0,2783	0,2059	0,7134	0,6197	0,0416	0,1293
Mg/(Mg+Mn2+)	0,9795	0,9874	0,7002	0,7004	0,4406	0,6209	0,7593	0,7727

2.4.2.3 Mica

Analysis of Representative mica crystals from the Uruana Syenite rocks are shown in Table 3. Analyses on crystals of biotites and on biotites representing microinclusions in amphibole were done. Compositions are characterized by Mg# ranging between 0.79 and 0.54 with most of the analyzed crystals plotting in the phlogopite field (Figure 8).

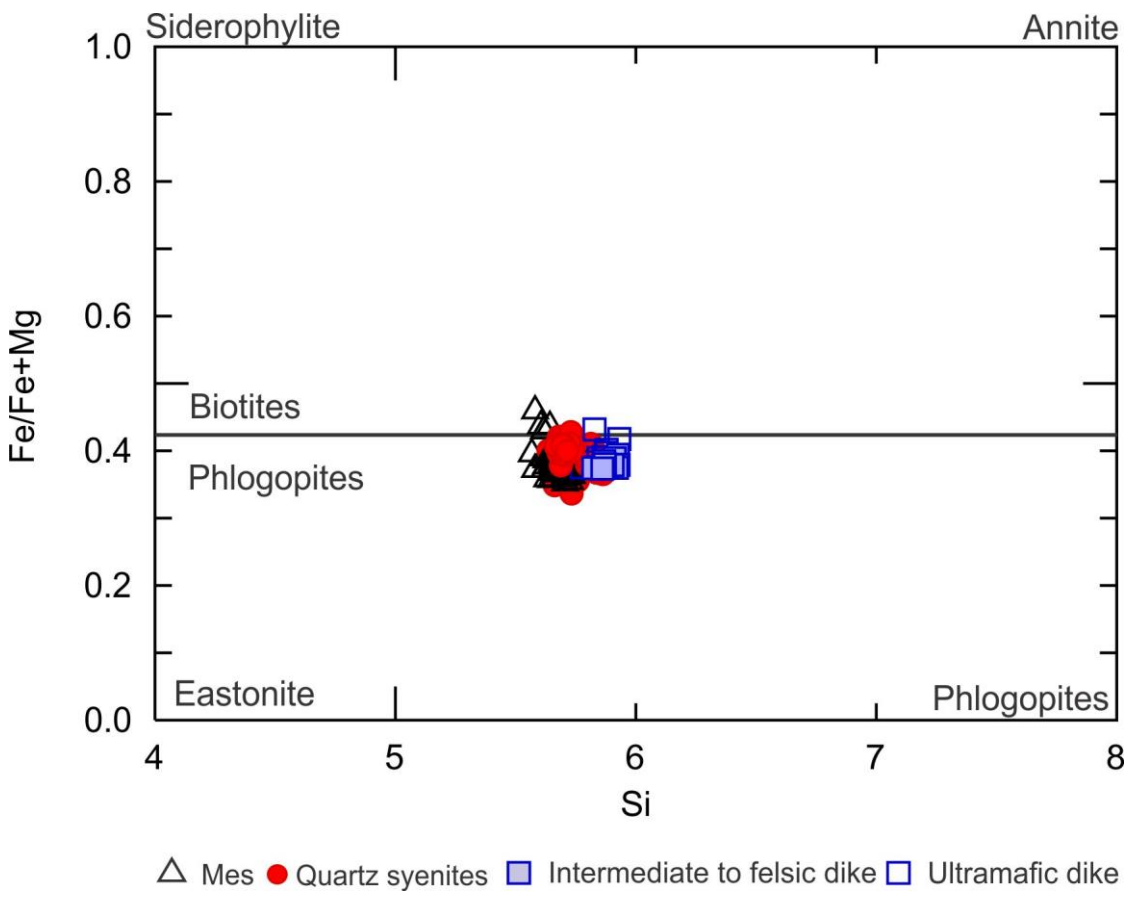


Figure 8. Classification diagram compositions for mica (Rieder et al., 1998).

Table 3. Representative analyses of micas

Rock	Quartz syenite		Microgranular enclaves		Syn magmatic felsic dike		Syn magmatic ultramafic dike	
Sample	Uru-06		Uru-09		Uru-26		Uru-27	
SiO ₂	37,83	38,21	38,97	38,77	39,17	38,63	38,63	38,61
TiO ₂	1,71	1,39	1,11	1,30	0,84	0,89	1,26	1,28
Al ₂ O ₃	13,71	13,86	14,90	14,39	11,15	10,98	14,21	14,07
FeO	17,54	17,71	16,00	15,95	17,30	16,76	17,36	17,29
MnO	0,39	0,27	0,30	0,19	0,20	0,33	0,33	0,15
MgO	13,55	13,80	14,47	15,17	15,57	15,76	14,38	14,56
CaO	0,03	0,00	0,01	0,00	0,06	0,00	0,05	0,04
Na ₂ O	0,09	0,03	0,11	0,09	0,07	0,16	0,07	0,09
K ₂ O	9,58	9,71	9,69	9,75	9,64	9,35	9,37	9,57
SrO	0,00	0,00	0,01	0,01	0,00	0,00	0,08	0,00
ZnO	0,00	0,00	0,08	0,12	0,00	0,00	0,10	0,12
Cl	0,14	0,12	0,09	0,09	0,18	0,18	0,18	0,15
Li ₂ O*	1,31	1,41	1,63	1,58	1,69	1,53	1,54	1,53
H ₂ O*	3,52	3,50	4,09	4,08	3,06	3,91	4,04	4,04
O=F,Cl	0,42	0,46	0,02	0,02	0,83	0,04	0,04	0,03
Total	100,01	100,47	101,45	101,46	99,97	100,34	101,55	101,46
Si	5,6804	5,6918	5,6853	5,6635	5,8686	5,8610	5,6731	5,6741
Al ^{IV}	2,3196	2,3082	2,3147	2,3365	1,9690	1,9629	2,3269	2,3259
Al ^{VI}	0,1065	0,1257	0,2477	0,1407	0,0000	0,0000	0,1330	0,1113
Ti	0,1934	0,1554	0,1213	0,1426	0,0948	0,1020	0,1391	0,1409
Fe	2,2022	2,2068	1,9524	1,9482	2,1682	2,1265	2,1323	2,1252
Mn	0,0491	0,0334	0,0372	0,0230	0,0258	0,0422	0,0412	0,0189
Mg	3,0322	3,0638	3,1464	3,3031	3,4770	3,5638	3,1471	3,1888
Zn	0,0000	0,0000	0,0088	0,0132	0,0000	0,0000	0,0107	0,0132
Li*	0,7889	0,8467	0,9583	0,9260	1,0180	0,9366	0,9072	0,9035
Ca	0,0050	0,0000	0,0016	0,0000	0,0090	0,0005	0,0071	0,0068
Na	0,0262	0,0092	0,0297	0,0255	0,0189	0,0468	0,0185	0,0245
K	1,8341	1,8455	1,8038	1,8169	1,8427	1,8099	1,7550	1,7944
Al total	2,4261	2,4340	2,5623	2,4773	1,9690	1,9629	2,4598	2,4372
Fe/Fe+Mg	0,4207	0,4187	0,3829	0,3710	0,3841	0,3737	0,4039	0,3999

2.4.3 Whole-rock geochemistry

Major and trace element analyses were carried out on twenty-six selected samples (see table 4). The samples encompasses a wide range of compositions from quartz diorite, granodiorite, syenite, quartz syenite, quartz-Alkali feldspar syenite and alkali feldspar syenite (Figure 9A) with SiO₂ content varying from 45.08 to 67.12 wt.%.

The syn-magmatic dikes, range in SiO_2 from 45.08-61.96 wt.%, Microgranular enclaves (Mes), 50.46-66.45 wt.%, alkali feldspar syenite 52.13-56.81 wt.% and Quartz syenitic rocks 59.4-67.12 wt.% respectively (Figure 9B). Most samples are metaluminous although some are peraluminous with alumina saturation index of A/CNK ($\text{Al}_2\text{O}_3/(\text{CaO}+\text{Na}_2\text{O}+\text{K}_2\text{O})_{\text{mol}}$) ranging from 0.92-1.54.

The rocks of the syenite Uruana have high K_2O (2.25 to 8.62 wt.%) contents (Figure 10) and $\text{K}_2\text{O}/\text{Na}_2\text{O}$ ratios from 1.42 to 4.46.

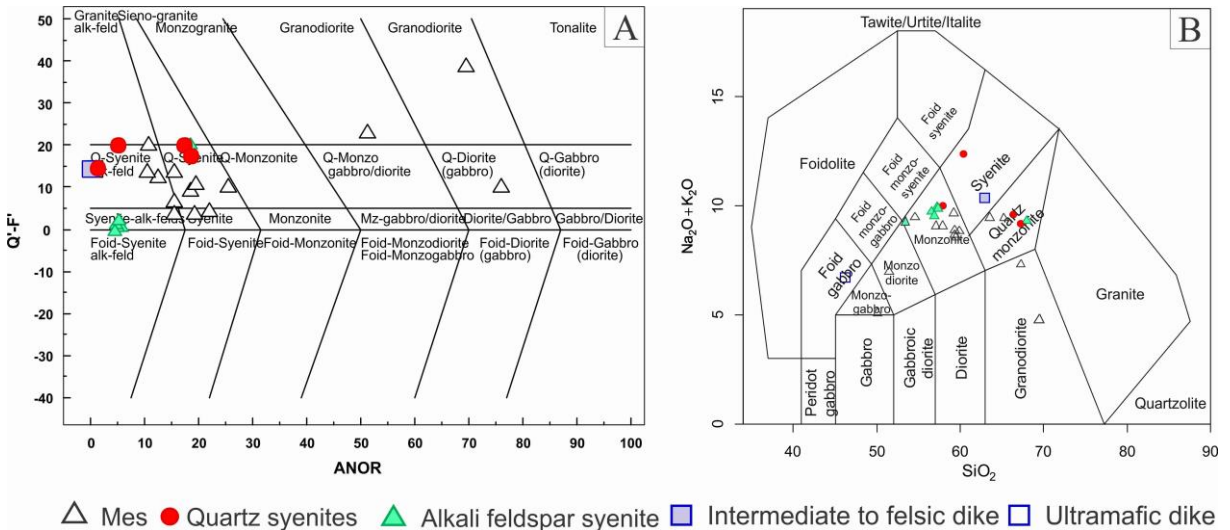


Figure 9. A). Q'-F'-ANOR normative classification diagram for plutonic rock (after Streckeisen, Lemaitre 1979). B) Total alkali vs silica (TAS) classification of plutonic rocks (Cox et al., 1989).

The Harker diagrams show a general decrease in MgO (11.1 to 1.61 wt.%), CaO (9.3 to 1.1 wt.%), MnO and TiO₂ (2.75 to 0.47 wt.%) and increase of, Al_2O_3 (16.33 to 7.36 wt.%) and Na_2O (4.96 to 1.25) with increasing SiO_2 . K_2O does not show any clear trend. The samples have high Ba and Sr contents defining a scattered trend with the alkali feldspar syenitic rocks defining a different group (Figure 10).

Table 4. Chemical analyses and CIPW data of rocks of the Uruana syenite.

Sample	Major oxides (wt%)											
	Uru-06	Uru-09	Uru-10	Uru-16	Uru-18-A	Uru-19	Uru-19-A	Uru-21	Uru-22	Uru-23	Uru-25	Uru-26
Lat	S15° 29' 43.19"	S15°28' 43.86"	S15°28' 40.41"	S15°29' 33.08"	S15°29' 30.14"	S15°29' 20.21"	S15°28' 20.21"	S15°28' 27.56"	S15°28' 27.56"	S15°27' 53.71"	S15°26' 54.75"	S15°26' 54.75"
Long	W49° 46' 56.04"	W49° 46' 24.69"	W49° 46' 18.41"	W49°48' 42.48"	W49°50' 1.54"	W49°47' 42.72"	W49°47' 42.72"	W49°49' 4.86"	W49°49' 4.86"	W49°48' 54.16"	W49°49' 1.11"	W49°49' 1.11"
Rock type	QS	Mes	Mes	Mes	Mes	QS	Mes	Mes	Mes	Mes	QS	SFD
SiO ₂	65,68	58,2	64,57	56,07	58,51	67,12	58,45	67,62	66,45	57,06	59,4	61,96
Al ₂ O ₃	15,30	14,50	15,08	13,58	13,66	14,74	12,48	13,01	16,33	14,98	15,46	12,25
Fe ₂ O _{3t}	3,16	6,02	5,82	7,15	6,41	2,89	6,62	6,21	3,73	6,61	4,71	4,97
MnO	0,06	0,11	0,06	0,15	0,10	0,05	0,16	0,11	0,06	0,13	0,06	0,08
MgO	1,82	4,18	2,12	5,61	5,48	1,61	5,94	2	1,36	4,35	2,7	3,84
CaO	2,62	4,26	1,10	5,22	4,36	2,46	3,64	3,15	2,99	4,93	2,39	3,25
Na ₂ O	3,63	2,57	3,37	2,41	2,79	3,78	1,79	3,57	4,96	3,25	3,55	1,92
K ₂ O	5,87	6,91	5,95	6,48	5,74	5,4	6,83	1,11	2,25	5,68	8,62	8,27
P ₂ O ₅	0,31	0,6	0,19	0,66	0,68	0,24	0,71	0,13	0,14	0,53	0,53	0,77
TiO ₂	0,57	0,89	0,72	0,92	0,94	0,47	0,96	0,61	0,54	1,11	1,01	1,18
Cr ₂ O ₃	0,007	0,016	0,01	0,02	0,03	0,010	0,038	0,016	0,004	0,01	0,014	0,021
LOI	0,5	1,2	0,7	1,1	0,7	0,8	1,8	2,2	0,9	0,8	0,9	0,7
Total	99,53	99,46	99,69	99,37	99,40	99,57	99,42	99,736	99,71	99,44	99,34	99,21
<i>an</i>	19,94	24,83	12,23	24,70	23,74	17,71	26,68	31,56	23,81	24,58	2,42	2,17
<i>Q</i>	14,28	3,75	14,95	0,59	5,00	17,08	6,97	30,42	19,48	1,92	0,00	10,40
<i>or</i>	35,03	41,71	35,83	39,10	34,42	32,34	41,68	6,88	13,44	34,05	51,44	50,14
<i>ab</i>	32,93	23,58	30,84	22,10	25,43	34,40	16,60	33,61	45,02	29,61	32,20	17,69
<i>an</i>	8,20	7,79	4,30	7,25	7,92	7,40	6,04	15,50	14,07	9,65	0,80	-
<i>ne</i>	-	-	-	-	-	-	-	-	-	-	-	-
<i>C</i>	-	-	1,73	-	-	-	-	0,59	0,70	-	-	-
<i>di</i>	2,31	7,84	-	11,84	7,63	2,70	6,26	-	-	9,33	6,15	8,79
<i>hy</i>	3,92	10,24	8,57	13,83	14,24	3,15	16,88	9,52	4,08	9,97	3,54	6,48

Table 4. Chemical analyses and CIPW data of rocks of the Uruana syenite (continued)

<i>wo</i>	-	-	-	-	-	-	-	-	-	-	-	-
<i>ol</i>	-	-	-	-	-	-	-	-	-	-	0,69	-
<i>ac</i>	-	-	-	-	-	-	-	-	-	-	-	-
<i>mt</i>	1,24	2,55	2,37	2,58	2,59	1,06	2,66	2,31	2,16	2,77	2,64	2,55
<i>il</i>	0,80	1,27	1,02	1,31	1,33	0,66	1,38	0,89	0,76	1,57	1,42	1,69
<i>hem</i>	0,63	-	-	-	-	0,68	-	-	-	-	-	0,21
<i>ap</i>	0,65	1,28	0,40	1,41	1,44	0,51	1,53	0,28	0,30	1,12	1,12	1,65
Trace elements (ppm)												
Sc	6	12	14	16	15	5	13	14	9	16	6	9
Co	9	20	15	27	25	9	24	14	8	22	14	17
Ni	28	70	43	85	143	31	158	49	10	58	43	87
Zn	44	63	78	67	75	44	111	51	48	56	56	65
Rb	231	281	306	327	284	242	460	75	147	242	396	395
Sr	1171	1019	320	881	1045	954	592	528	520	1049	979	1025
Y	19	31	23	32	26	19	35	30	23	32	21	29
Zr	217	313	222	280	263	211	594	172	171	266	715	999
Nb	18	25	15	24	17	18	29	11	10	34	46	62
Ba	2087	2004	701	1874	2053	1567	1634	390	598	1632	2560	2903
Hf	6	8	6	7	7	5	16	4	5	7	15	27
Ta	2	2	1	1	1	2	1	1	1	3	2	4
Pb	11,5	7,5	2,1	11,6	4,8	13,6	19,5	4,2	2,8	5,1	42,6	17,3
Th	23,7	24,1	9,0	36,8	20,0	48,2	78,6	6,8	10,0	23,5	15,9	83,9
U	4,2	3,9	1,5	6,9	3,1	7,5	30,1	1,1	4,2	5,3	3,4	10,4

Table 4. Chemical analyses and CIPW data of rocks of the Uruana syenite (Continued).

	Rare earth elements (ppm)											
La	65,00	117,20	45,30	129,50	74,70	76,70	138,60	32,50	32,20	88,50	117,50	204,30
Ce	133,40	221,30	81,50	199,70	133,00	117,20	287,50	51,10	67,50	251,10	230,70	416,90
Pr	16,15	31,02	8,91	27,58	18,11	15,97	34,21	6,51	6,44	30,66	24,98	48,03
Nd	61,30	116,10	34,00	105,10	68,90	55,20	129,50	25,50	24,00	123,20	87,80	180,50
Sm	10,47	19,72	6,98	17,56	13,92	10,28	23,21	5,65	4,45	20,56	14,07	27,38
Eu	2,29	4,08	1,50	3,78	3,10	2,11	3,53	1,23	1,08	4,22	2,77	5,16
Gd	7,45	13,31	5,93	13,10	10,55	7,25	15,03	5,77	4,55	14,00	8,93	15,97
Tb	0,83	1,50	0,89	1,49	1,33	0,82	1,75	0,93	0,63	1,60	1,07	1,69
Dy	3,80	7,01	4,71	6,69	6,05	3,87	7,50	5,31	3,71	7,13	4,61	7,37
Ho	0,63	1,12	0,98	1,10	1,03	0,59	1,24	1,25	0,78	1,09	0,80	1,03
Er	1,51	2,55	2,62	2,59	2,51	1,57	3,13	3,28	2,32	2,83	1,70	2,38
Tm	0,21	0,36	0,39	0,38	0,33	0,23	0,45	0,49	0,34	0,42	0,27	0,36
Yb	1,44	2,31	2,36	2,39	2,18	1,24	2,83	3,38	2,16	2,34	1,59	2,15
Lu	0,19	0,30	0,34	0,32	0,31	0,21	0,42	0,47	0,37	0,36	0,22	0,33
Σ REE	304,67	537,88	196,41	511,28	336,02	293,24	648,90	143,37	150,53	548,01	497,01	913,55

Rock type: QS =Quartz syenite, Mes = microgranular enclaves , SFD = Syn magmatic felsic dike , SUD = Syn magmatic ultramafic dike.

Table 4. Chemical analyses and CIPW data of rocks of the Uruana syenite (Continued).

Sample	Major oxides (wt%)												
	Uru-27	Uru-31	Uru-36	Uru-37	Uru-37-A	Uru-40	Uru-41	Uru-42	URU 44	URU 44-B	URU 45	URU 46	URU 47
Lat	S15°26' 54.7476"	S15°27' 24.7428"	S15°27' 40.7700"	S15°27' 40.7700"	S15°27' 40.7700"	S15°27' 40.7700"	S15°27' 40.7700"	S15°27' 40.7700"	S15°27' 17.79"	S15°27' 17.79"	S15°27' 17.79"	S15°27' 17.79"	S15°27' 17.79"
Long	W49°49' 1.1100"	W49° 49' 56.5212"	W49°49' 54.6960"	W49°49' 54.6960"	W49°49' 54.6960"	W49°51' 22.5180"	W49°51' 22.5180"	W49°51' 22.5180"	W49°44' 8.63"	W49°44' 8.63"	W49°44' 8.63"	W49°44' 8.63"	W49°44' 8.63"
Rock type	SUD	Mes	Mes	QS	Mes	Mes	Mes	Mes	AFS	AFS	AFS	AFS	AFS
SiO ₂	45,1	62,1	53,5	66,2	50,5	58,2	49,2	58,6	56,3	55,2	56,1	52,1	55,8
P ₂ O ₅	1,6	0,5	0,7	0,3	1,2	0,7	0,2	1,2	0,9	1,1	0,9	1,3	1,1
Al ₂ O ₃	7,4	14,2	13,1	14,4	11,0	14,7	14,6	14,2	12,9	12,5	12,6	11,5	12,1
Fe ₂ O _{3t}	13,7	4,5	7,6	3,3	12,3	6,5	12,3	6,5	6,5	6,6	6,4	7,7	6,8
MnO	0,2	0,1	0,2	0,1	0,2	0,1	0,3	0,1	0,1	0,1	0,1	0,2	0,1
MgO	11,1	3,2	7,1	2,1	9,6	4,0	6,6	4,0	5,5	5,8	5,6	7,1	5,8
CaO	9,3	3,3	5,5	2,7	4,9	4,4	9,5	4,4	5,5	6,0	5,7	7,6	6,2
Na ₂ O	1,7	3,3	2,3	3,6	1,3	3,2	4,0	3,0	2,5	2,5	2,3	1,8	2,0
K ₂ O	4,9	6,0	7,0	5,4	5,6	5,2	1,0	5,8	7,3	7,0	7,4	7,2	7,3
TiO ₂	2,8	0,7	1,1	0,5	1,6	1,0	0,7	1,0	0,8	0,8	0,8	1,1	0,8
Cr ₂ O ₃	0,1	0,0	0,0	0,0	0,1	0,0	0,0	0,0	0,0	0,0	0,0	0,0	0,0
LOI	1,4	1,6	1,3	1,0	1,4	1,6	1,4	1,5	0,6	1,5	1,0	1,2	0,9
Total	99,1	99,4	99,4	99,6	99,6	99,5	99,7	100,3	99,0	99,0	98,9	98,8	99,0
<i>an</i>	-	18,34	20,52	17,30	41,39	27,14	39,39	23,66	10,64	9,09	9,78	14,62	11,75
Q	-	10,27	0,00	16,21	0,00	6,14	0,00	6,45	0,00	0,00	0,00	0,00	0,00
or	30,05	36,12	41,80	32,47	34,17	31,57	6,10	34,73	43,72	42,24	44,42	43,62	44,19
ab	1,63	29,88	19,16	33,20	11,63	29,10	29,86	27,44	22,67	22,94	21,22	12,04	18,68
ne	6,12	-	1,23	0,00	0,00	0,00	4,02	0,00	0,00	0,00	0,00	2,86	0,00
C	-	-	0,00	0,00	0,00	0,00	0,00	0,00	0,00	0,00	0,00	0,00	0,00
di	29,60	5,55	14,61	3,92	7,32	5,64	22,01	4,72	15,40	16,93	16,40	22,33	17,67
hy	-	7,18	0,00	3,90	23,06	11,26	0,00	11,59	6,59	4,05	7,99	0,00	9,87

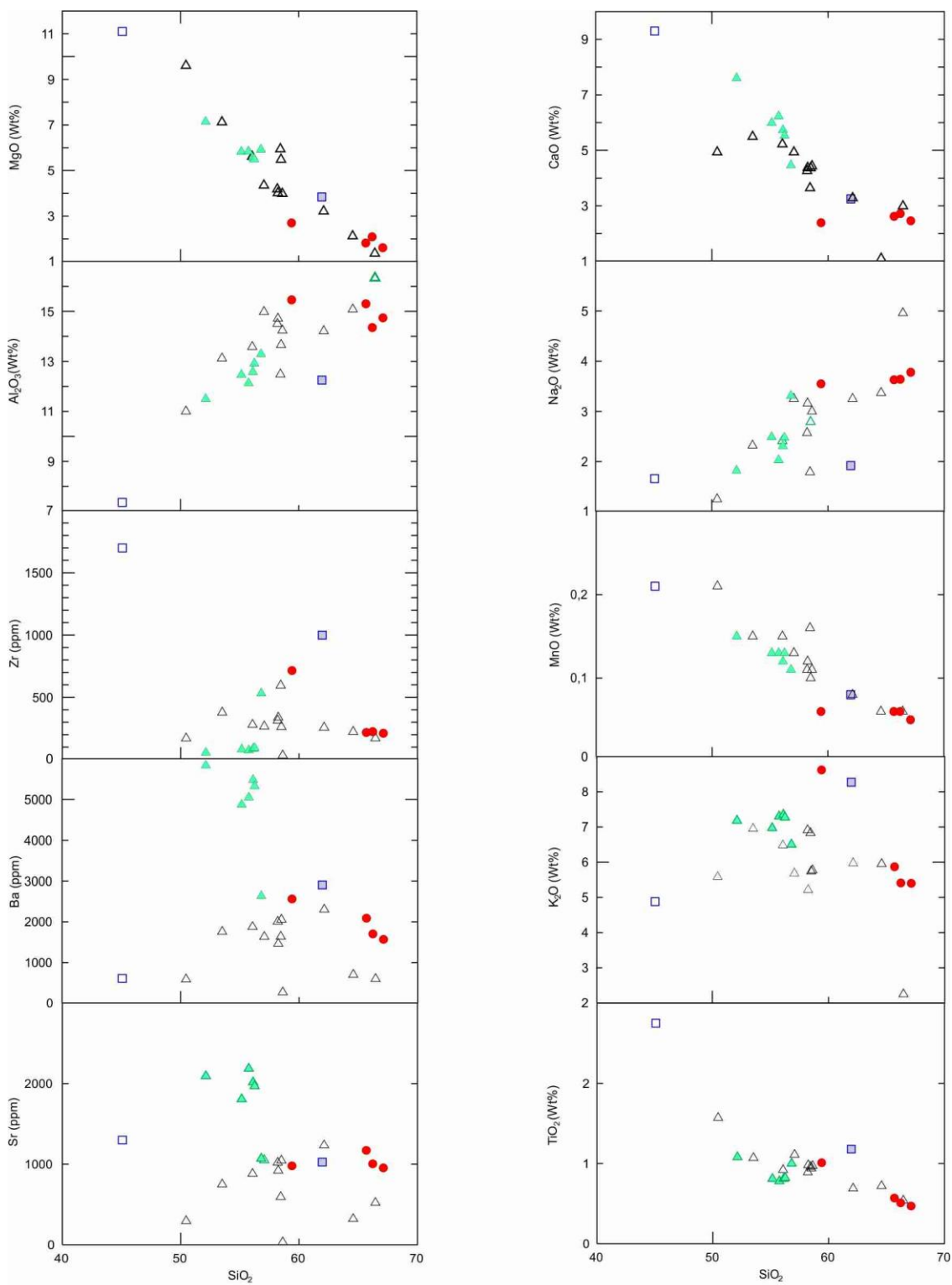
Table 4. Chemical analyses and CIPW data of rocks of the Uruana syenite (Continued).

<i>wo</i>	-	-	0,00	0,00	0,00	0,00	0,00	0,00	0,00	0,00	0,00	0,00	0,00
<i>ol</i>	18,57	-	12,56	0,00	7,45	0,00	14,89	0,00	3,38	5,67	2,03	9,94	1,27
<i>ac</i>	2,97	-	0,00	0,00	0,00	0,00	0,00	0,00	0,00	0,00	0,00	0,00	0,00
<i>mt</i>	3,52	2,34	2,74	1,83	3,33	2,66	2,34	2,63	2,47	2,48	2,47	2,77	2,44
<i>il</i>	3,99	0,98	1,52	0,72	2,27	1,40	0,98	1,38	1,16	1,16	1,15	1,55	1,11
<i>hem</i>	-	-	0,00	0,20	0,00	0,00	0,00	0,00	0,00	0,00	0,00	0,00	0,00
<i>ap</i>	3,55	0,96	1,45	0,59	2,56	1,39	0,39	2,56	1,92	2,25	2,01	2,82	2,27
Trace elements (ppm)													
Sc	31	10	18	7	19	15	45	15	17	17	16	17	16
Co	46	17	30	10	49	21	43	22	25	26	25	26	25
Ni	125	74	168	38	258	49	27	46	84	74	77	74	77
Zn	159	57	71	44	217	82	32	77	43	48	30	48	30
Rb	638	302	576	252	767	244	22	914	262	262	245	262	245
Sr	1299	1234	749	1004	295	919	538	31	1968	1807	2017	1807	2017
Y	63	20	54	17	13	31	16	281	30	33	33	33	33
Zr	1699	257	378	224	170	337	42	33	93	82	87	82	87
Nb	97	15	22	18	15	35	4	67	20	18	18	18	18
Ba	609	2299	1755	1704	588	1461	178	270	5328	4875	5481	4875	5481
Hf	35	7	9	6	5	9	1	7	3	3	3	3	3
Ta	4	1	1	1	1	3	0	2	1	1	1	1	1
Pb	13,8	14,7	14,8	16,7	3,6	7,6	8,4	7,4	5,5	4,5	5,0	4,5	5,0
Th	36,9	21,0	42,8	39,8	24,0	29,5	3,7	23,5	6,3	7,5	7,3	7,5	7,3
U	8,2	4,7	11,9	8,3	4,5	4,9	1,1	5,8	2,1	1,7	1,7	1,7	1,7

Table 4. Chemical analyses of rocks and CIPW data of the Uruana syenite (Continued).

	Rare earth elements (ppm)												
La	333,10	73,90	153,40	82,50	48,80	77,50	17,60	79,40	111,90	132,10	124,80	132,10	124,80
Ce	625,50	118,00	264,10	124,90	94,00	207,90	23,10	190,70	228,20	262,70	256,90	262,70	256,90
Pr	70,41	15,39	36,95	15,84	9,86	25,21	3,06	25,58	26,66	30,36	29,22	30,36	29,22
Nd	248,10	62,90	139,00	57,10	36,90	103,10	12,20	102,50	103,70	118,30	113,20	118,30	113,20
Sm	41,11	11,06	27,38	8,92	6,36	18,02	2,56	17,84	18,12	20,05	19,10	20,05	19,10
Eu	7,40	2,42	5,83	2,00	1,12	3,55	0,89	3,57	3,75	4,06	3,92	4,06	3,92
Gd	28,11	8,25	20,25	6,87	5,08	12,97	2,86	12,05	12,53	14,23	13,40	14,23	13,40
Tb	3,32	0,96	2,56	0,72	0,59	1,55	0,46	1,50	1,51	1,71	1,60	1,71	1,60
Dy	14,89	4,45	11,99	3,35	2,75	7,09	2,62	6,98	6,93	7,33	7,48	7,33	7,48
Ho	2,15	0,68	2,03	0,62	0,44	1,09	0,63	1,15	1,10	1,14	1,18	1,14	1,18
Er	5,60	1,89	5,43	1,60	1,18	2,86	1,73	2,95	2,45	2,82	2,89	2,82	2,89
Tm	0,75	0,27	0,76	0,20	0,19	0,42	0,26	0,43	0,34	0,37	0,37	0,37	0,37
Yb	4,77	1,60	4,57	1,38	1,04	2,57	1,55	2,53	2,15	2,31	2,18	2,31	2,18
Lu	0,65	0,23	0,66	0,19	0,17	0,36	0,24	0,38	0,27	0,33	0,32	0,33	0,32
ΣREE	1385,86	302,00	674,91	306,19	208,48	464,19	69,76	447,56	519,61	597,81	576,56	597,81	576,56

Rock type: Qs =Quartz syenite, Mes =microgranular enclaves , AFS= Alkaline feldspar syenite, SFD = Syn magmatic felsic dike , SUD = Syn magmatic ultramafic dike.



△ Mes ● Quartz syenites ▲ Alkali feldspar syenite ■ Intermediate to felsic dike □ Ultramafic dike

Figure 10. Major elements and trace elements representative Harker diagrams for the Uruana syenite rocks.

The analyzed samples are strongly enriched in large ion lithophile elements (LILE) (e.g., Ba=270-5897 ppm; Sr=294-2185 ppm) (Figure 12A), show moderate to high HFSE contents (e.g., Zr=32.6-1699 ppm; Nb=42-95.6; Y=13.2-280; La=17.6-333.1) and evident negative Nb, Ta, P, Zr and Ti anomalies.

Syn magmatic dikes are strongly enriched in LILE ($\text{Rb} = 395.3\text{--}638 \text{ ppm}$; $\text{Ba} = 609\text{--}2903 \text{ ppm}$; $\text{Sr} = 1025.2\text{--}1298.9 \text{ ppm}$), HFSE ($\text{Nb} = 62.2\text{--}96.5 \text{ ppm}$; $\text{Zr} = 999.2\text{--}1699 \text{ ppm}$; $\text{Y} = 29\text{--}63.2 \text{ ppm}$) and REE with minor Ta, Nb and Ti negative anomalies, compared to enclaves and quartz syenite rocks, they display moderate concentrations in these elements (Figure 11A).

Total REE concentrations range from 376 to 798 ppm (Table 4). Chondrite-normalized trace element patterns (Figure 11B) with LREE values from 600 to approximately 10000 time greater than the chondrite values. All samples are characterized by a slight negative Eu anomaly ($\text{Eu/Eu}^* = 0.57\text{--}0.79$) and $(\text{La/Yb})_N$ ratio varying from 10.12 to 65.55

Quartz syenite samples show ΣREE values between 293.24 and 497.01 ppm, LREE slight enrichment ($\text{La}_N/\text{Yb}_N = 30.6\text{--}50.2$) and slight Eu anomaly ($\text{Eu/Eu}^* = 0.75\text{--}0.79$). The MEs exhibit similar or less LREE enrichment compared to compositional range of the quartz syenites, while Alkali feldspar syenite and syn-magmatic dikes display higher enrich compared to the range compositional of the host rock.

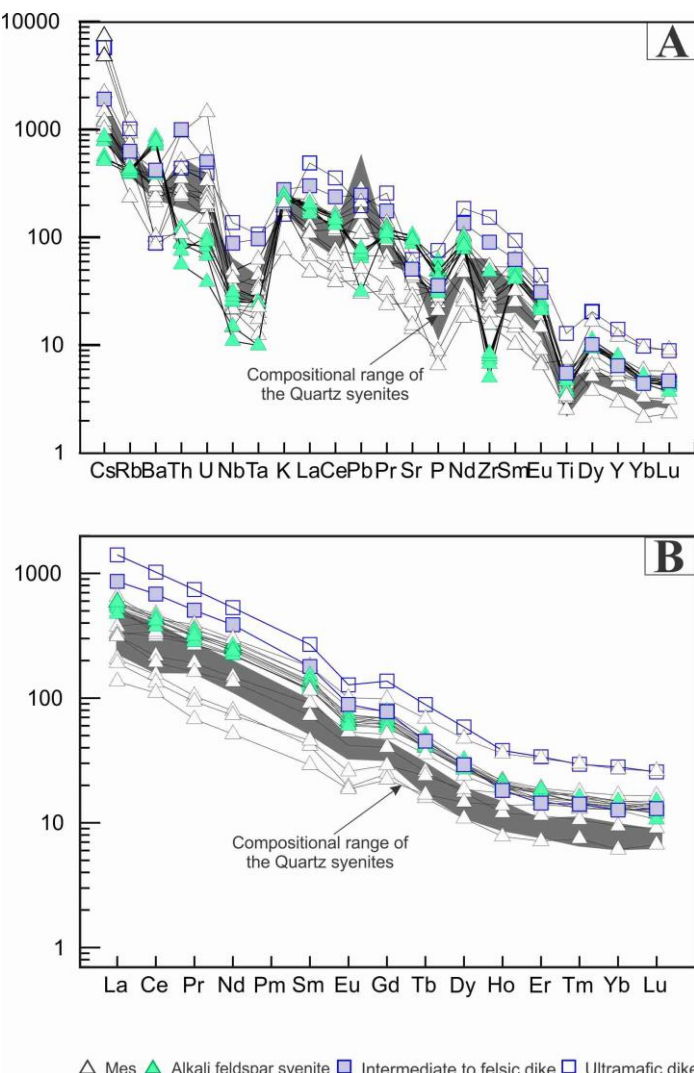


Figure 11. A) Multi-variation primitive mantle-normalized (A) and Chondrite-normalized REE diagram for the different lithotypes of the Uruana syenite compared with the compositional range of the Quartz syenites, normalization values are from Sun and McDonough (1989).

2.4.4 Shrimp zircon U–Pb dating

Zircon from a microgranular enclave (sample Uru-09) were dated using SHRIMP U–Pb method. Results are summarized in Table 09 and shown in the Concordia diagram (Figure 12)

The analysed zircon grains are light pink to colourless, prismatic, euhedral approximately 100 µm in size with developed magmatic oscillatory zoning. Most U–Pb analyses plot in a group on the Concordia line defining a Concordia age of 614.7 ± 3.1 Ma (MSWD= 1.19) which is considered the best estimation of the crystallization age of the magma. Some inherited zircons with Neo- to Paleoproterozoic ages are present.

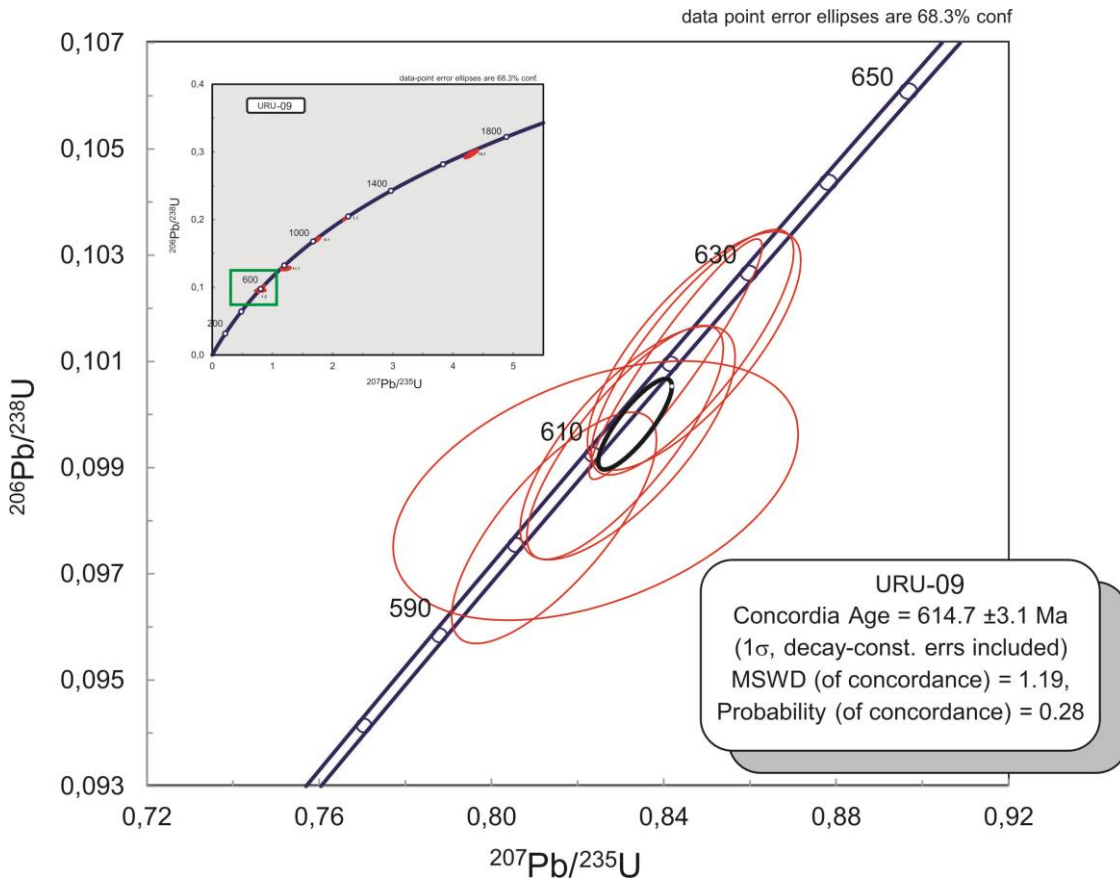


Figure 12. Wetherill Concordia diagram for zircons from sample Uru-09.

Table 5. SHRIMP U-Th-Pb isotopic data for the Uruana syenite.

Spot Name	% ²⁰⁶ Pbc	ppm U	ppm Th	²³² Th / ²³⁸ U	ppm Rad ²⁰⁶ Pb	(1) ²⁰⁶ Pb* / ²³⁸ U*	1σ err	(1) ²⁰⁷ Pb* / ²⁰⁶ Pb*	1σ err	% Discor-dant	(1) ²⁰⁷ Pb* / ²⁰⁶ Pb*	% err	(1) ²⁰⁷ Pb* / ²³⁵ U	% err	²⁰⁶ Pb* / ²³⁸ U	%err
URU-1.1	0.01	296.52	252.01	0.88	51.60	1188.79	16.20	1190.20	13.19	0.12	0.08	0.65	2.23	1.64	0.20	1.49
URU-2.1	0.17	853.00	369.51	0.45	73.02	611.27	8.52	624.70	23.18	2.20	0.06	0.76	0.83	1.81	0.10	1.46
URU-4.1	0.17	702.85	335.12	0.49	61.21	621.38	8.67	628.83	27.15	1.20	0.06	1.05	0.85	1.93	0.10	1.46
URU-6.1	0.25	263.79	109.00	0.43	38.75	1015.08	14.13	1051.80	24.80	3.62	0.08	0.77	1.75	1.94	0.17	1.50
URU-7.1	0.45	120.06	74.12	0.64	10.21	605.86	9.45	626.66	73.31	3.43	0.06	1.66	0.82	3.77	0.10	1.64
URU-8.1	0.33	889.56	450.40	0.52	76.27	611.17	8.51	626.43	29.06	2.50	0.06	0.80	0.83	1.99	0.10	1.46
URU-9.1	0.33	840.14	403.45	0.50	70.87	601.78	8.44	616.64	27.18	2.47	0.06	0.61	0.81	1.93	0.10	1.47
URU-10.1	-0.01	285.19	197.60	0.72	24.79	621.28	8.93	628.42	22.45	1.15	0.06	1.04	0.85	1.83	0.10	1.51
URU-12.1	-0.02	1072.97	772.87	0.74	93.13	620.52	8.75	621.18	11.58	0.11	0.06	0.54	0.84	1.57	0.10	1.48
URU-15.1	0.31	173.23	86.38	0.52	44.37	1676.53	22.50	1716.33	17.59	2.37	0.11	0.61	4.30	1.80	0.30	1.52

Errors are 1σ; Pbc and Pb* indicate the common and radiogenic portions, respectively. (1) Common Pb corrected using measured ²⁰⁴Pb. Error in Standard calibration is 2.85 % (2σ)

2.4.5 Sm-Nd isotopes

Eleven representative Samples between quartz syenite and Mes of the Uruana syenite were selected for whole-rock Nd isotope analysis. The initial ϵ_{Nd} values were recalculated using the U-Pb crystallization age of 614 Ma, range between -9.06 and 0.22 (Figure 13). TDM model ages vary between 1.17 and 1.72 Ga (Table 6). The Sample Uru-42 shows the highest value of $\epsilon_{\text{Nd}}(t)$ (+0.22), and the sample Uru-18A show the lowest value of $\epsilon_{\text{Nd}}(t)$ (-9.06).

Table 6. Sm-Nd isotopic data for rock for the Uruana syenite. The $\epsilon_{\text{Nd}}(T)$ values were calculated considering the U-Pb crystallization age of 614 Ma (see section 2.4.4).

Sample	Rock	Sm (ppm)	Nd (ppm)	$^{147}\text{Sm}/^{144}\text{Nd}$	$(^{143}\text{Nd}/^{144}\text{Nd})_t$	2σ	$\epsilon_{\text{Nd}}(t)$	$T_{\text{DM}}(\text{Ga})$
URU-06	Quartz syenite	11.53	66.208	0.1053	0.511650	0.000005	-3.84	1.361
URU-37	Quartz syenite	11.162	71.95	0.0938	0.511632	0.000006	-4.18	1.312
URU-42	Mes	20.464	115.565	0.1071	0.511635	0.000006	-4.13	1.395
URU-31	Mes	13.568	74.568	0.1101	0.511613	0.000007	-4.56	1.448
URU-36	Mes	18.302	104.148	0.1063	0.511662	0.000005	-3.60	1.350
URU-18A	Mes	6.989	40.689	0.1039	0.511383	0.000033	-9.06	1.721
URU-40	Mes	9.259	51.292	0.1092	0.511648	0.000015	-3.89	1.392
URU-22	Mes	4.946	25.687	0.1165	0.511702	0.000005	-2.82	1.364
URU-41	Mes	2.842	13.639	0.1260	0.511858	0.000009	0.22	1.178
URU-16	Mes	8.584	51.999	0.0999	0.511684	0.000026	-3.17	1.280
URU-37A	Mes	7.572	48.922	0.0936	0.511672	0.000005	-3.40	1.261

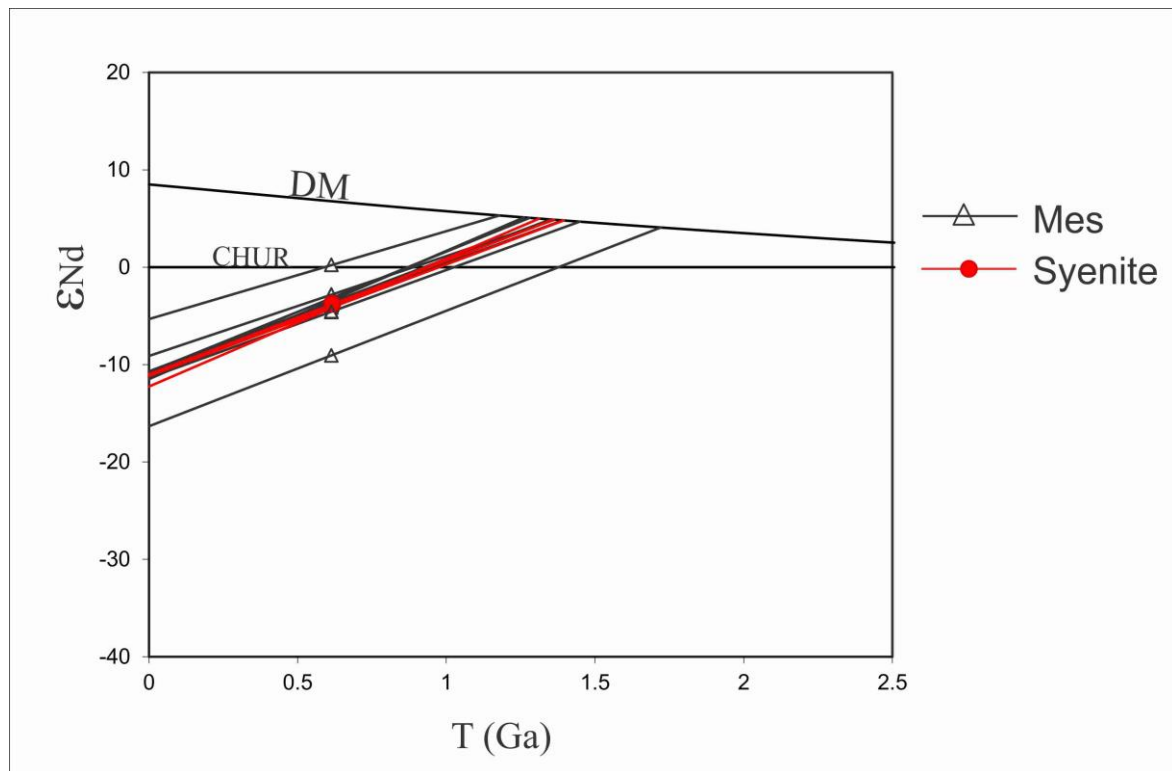


Figure 13. Nd isotope compositions of rocks from Uruana syenite

2.5 Discussion

Field, petrographic and geochemical data permitted to define the Uruana Syenite as a complex intrusive composed by a main Qz-syenitic ellipsoidal body (20x7 km in size) and by minor (~1 km in diameter) peripheral subcircular alkali qz-syenite stocks. All intrusives show a greenschist metamorphic paragenesis and a proto-mylonitic to mylonitic deformation, preserving primary magmatic textures.

Four main lithotypes have been recognized: I) Qz-syenite represents the most abundant lithology of the main ellipsoidal body. Porphyritic texture is characterized by cm-size phenocrysts of microcline and microphenocrysts of hornblende a faneritic matrix composed by edenite, phlogopite, k-feldspar, quartz and minor plagioclase. II) microgranular enclaves with granodioritic to quartz syenitic composition that are hosted in the quartz syenite of the main ellipsoidal body and are represent by microcline, edenite, pargasite, phlogopite, and minor diopside; III) syn-magmatic dykes, of ultramafic to intermediate composition that cropout in the northern sector of the main body.

Fine to medium-grained ultramafic dikes, with thickness up to 10 cm, are composed of phlogopite, diopside, and minor amphiboles. The fine-grained intermediate dikes have paragenesis similar to the quartz-syenitic host; IV) alkali feldspar syenite representing the main lithology of the. The peripheral stocks show a porphyritic texture with phenocrysts of cm-size microclin K-feldspar, micro-phenocryst of diopside and augite immersed in a microfaneritic matrix of k-feldspar, biotite, and minor quartz and plagioclase.

2.5.1 Potassium and ultrapotassic affinity.

Quartz syenites are metaluminous and have moderate K_2O/Na_2O ratios (1.4 to 1.6) these rocks are classified as potassic rock according to the criteria established by Peccerillo (1992). The sample Uru-25 have $K_2O/Na_2O > 2$, is considered as ultrapotassic rock contrasting with the other Quartz syenites samples.

The Mes and the syn-magmatic dykes are metaluminous, showing high MgO (1.36 to 11.1) and K₂O content (5.21 to 8.6%) and high K_2O/Na_2O ratios (2.2 to 4.4) typical of ultrapotassic rocks (see table 7). In the Al_2O_3 vs CaO and SiO_2 vs K_2O/Al_2O_3 diagram for classification of ultrapotassic rocks proposed by Foley (1987), alkali feldspar syenite, Mes and the felsic to intermediary dyke plot in the field of the transitional group IV whereas the ultramafic syn-magmatic dike plot in the lamproite field (Figure 14).

Table 7. Geochemical characteristics of the Uruana syenite rocks, which are considered as ultrapotassic rocks, according to the criteria established by Foley (1987).

Lithotype	Chemistry (wt%)			
	MgO	K ₂ O	K ₂ O/Na ₂ O	
Quartz-syenites	1.82-5.92	5.41-8.62	1.96-2.42	
Mes	1.36-9.60	1.01-6.95	1.64-3.81	
Sin-magmatic dikes	Intermediary to felsic dike	3.84	8.27	4.3
	Ultramafic dike	11.1	4.88	2.93
Quartz alkali feldspar syenites	1.61-7.14	5.40-7.35	1.42-3.95	

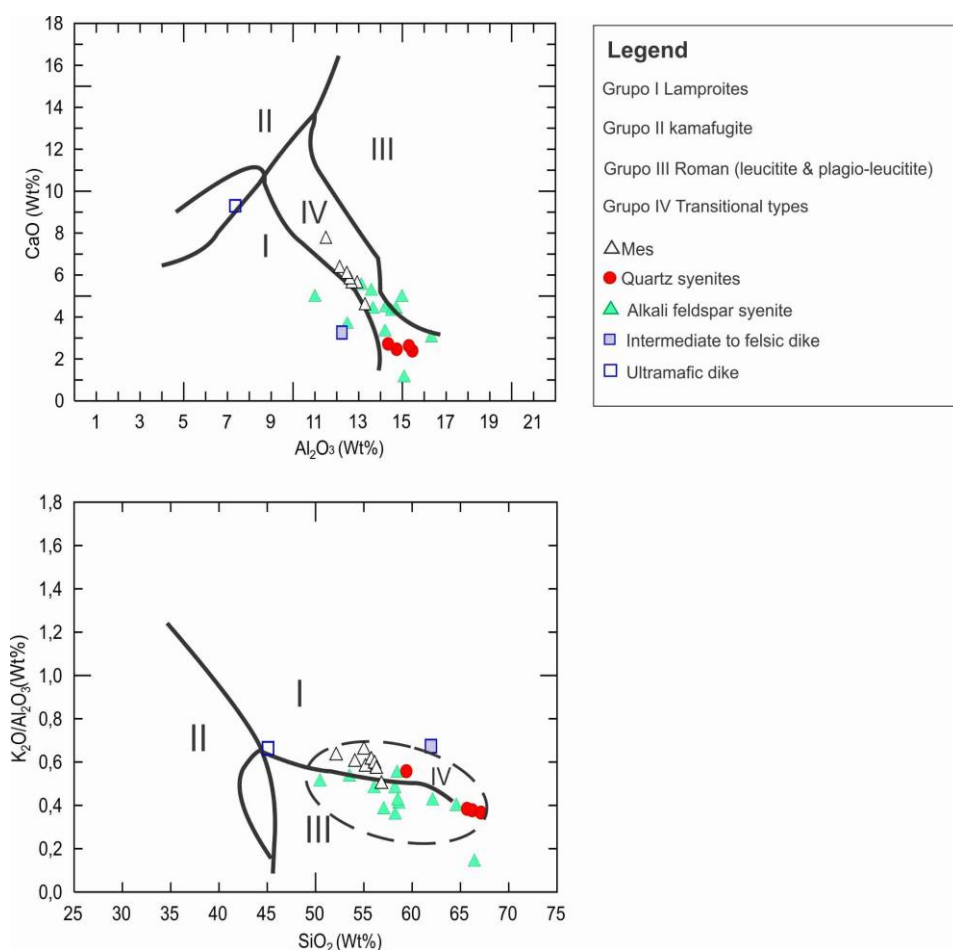


Figure 14. Discrimination diagrams (wt%) of Foley et al. (1987) applied to different groups of Ultapotassic rock of the Uruana syenite.

2.5.2 Geochemical comparisons

Trace element and REE contents permitted to define five groups of rocks with similar geochemical characteristics (Figure 15). For comparison, a compositional field of representative the

ultrapotassic rocks and calc-alkaline basalts from literature have been plotted together with each group in the OIB-normalized spider diagrams.

The syn-magmatic ultramafic and felsic dikes, together with two Mes (samples Uru 19 and Uru 36) have composition very similar to the lamproites from Spain and Mediterranean area (Figure 15A) (Conticelli et al., 2009; Duggen et al., 2005; Prelević et al., 2008; Turner et al., 1999; Pérez-Valera et al., 2013).

Samples from the peripheral stocks (Figure 15B) show geochemical characteristics typical of minettes (very high contents of Ba, Sr and negative anomaly of Ta-Nb) and a strong similarity with the field of the minette from Piquiri massif of south Brazil (Plá Cid et al., 2004; Nardi et al., 2007, 2008).

Two group of Mes are less enriched in trace element and REE than rocks with lamproitic and minette affinities. These groups have been compared with low-K and high-K calc-alkaline basalts (Takahashi et al., 2013, Crummy et al., 2014) respectively (Figure 15C and 15D). Both groups show a similar behavior when compared with the respective compositional field, except that they present a general stronger enrichment in LILE and LREE.

The quartz syenite of the main body (Figure 15E) shows a pattern very similar to that of the syenites from the Piriqui massif in central Brazil (Nardi et al., 2007)

For comparison, the five different groups have been plotted in the chondrite-normalized REE diagram to show the less enriched character of the Mes group defined (Figure 15F).

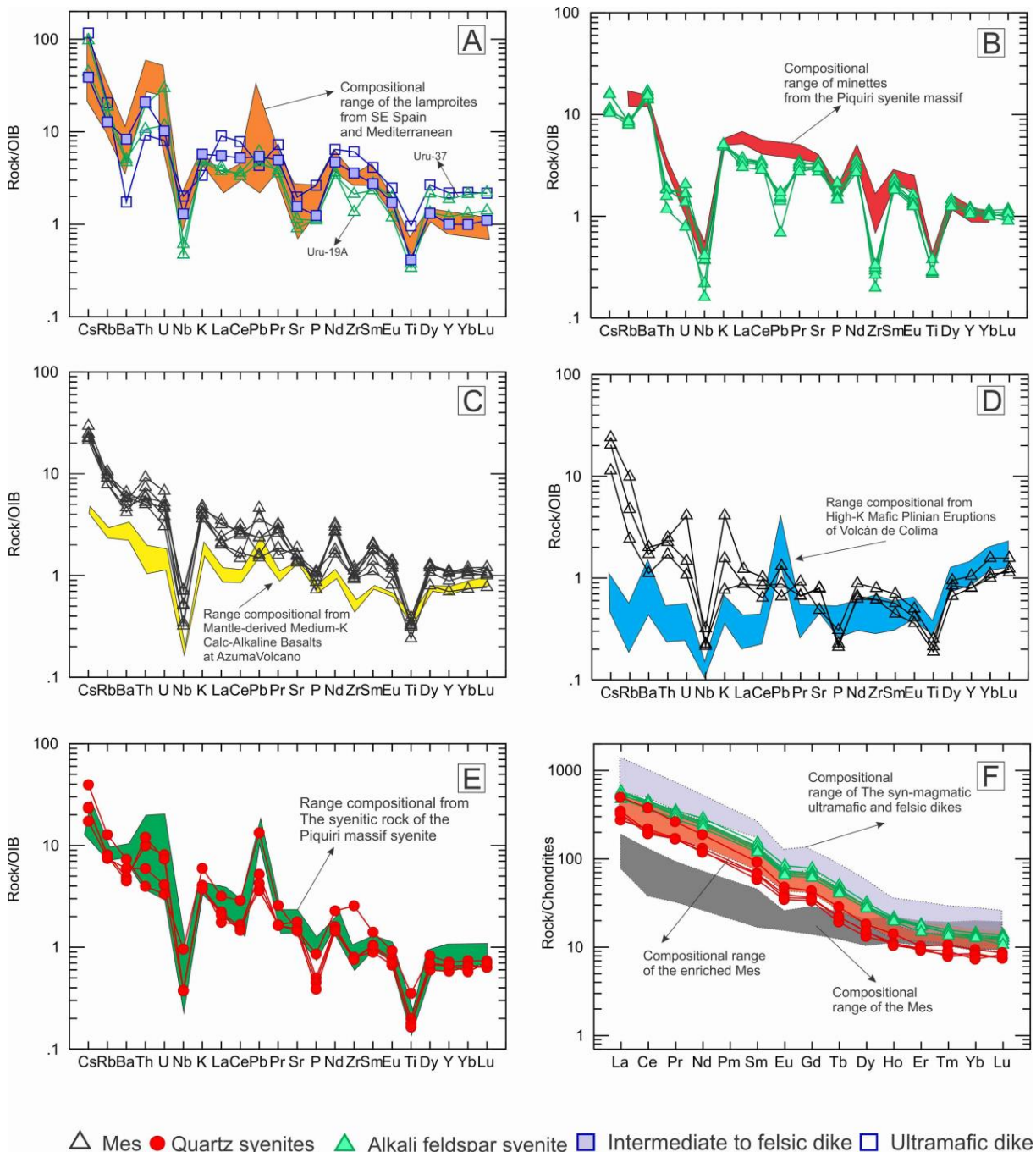


Figure 15. Spider diagram normalized to Ocean Island Basalt (OIB) Data from Sun and McDonough (1989), for the studied Uruana rock, compared with compositional range of: A) Lamproites from SE Spain and Mediterranean, B) Minettes from the Piquiri syenite massif, C) Mantle-derived Medium-K Calc-Alkaline Basalts at AzumaVolcano, D) High-K Mafic Plinian Eruptions of Volcán de Colima, E) The syenitic rocks of the Piquiri massif syenite. D) Rare earth element patterns normalized to C1-chondritic values for the Uruana rocks.

2.5.3 Relationship between lamproite, minette and syenite magmas

Rock (1987) suggested a petrogenetic relationship between minette and potassic syenitic magma, and proposed on the basis the geochemical evidences that calc-alkaline lamprophyres could be generated by mixing between lamproitic and anatexic magmas. Other authors (Prelevic, 2003) suggested the same model of hybridization of lamproitic melts by traquitic melts could generate magmas

with minette signature in a pos-collisional tectonic setting. Nb/Zr ratios vary from about 0.2 in the rocks of the peripheral stocks with minettic signature to about 0.09 in the Quartz syenites, whilst Ba/Zr, SiO₂/Zr and Al₂O₃/Zr ratios are higher in the minettes (Figure 16).

The behaviour of these elements and ratios is not consistent with the mixing mode proposed by the authors mentioned above, and the diagrams shown pointed to a derivation of the Uruana syenite rocks were by partial melting of an heterogeneous metasomatic lithospheric continental mantle (MLCM) or, alternatively, by different degree of partial melting of the same MLCM source.

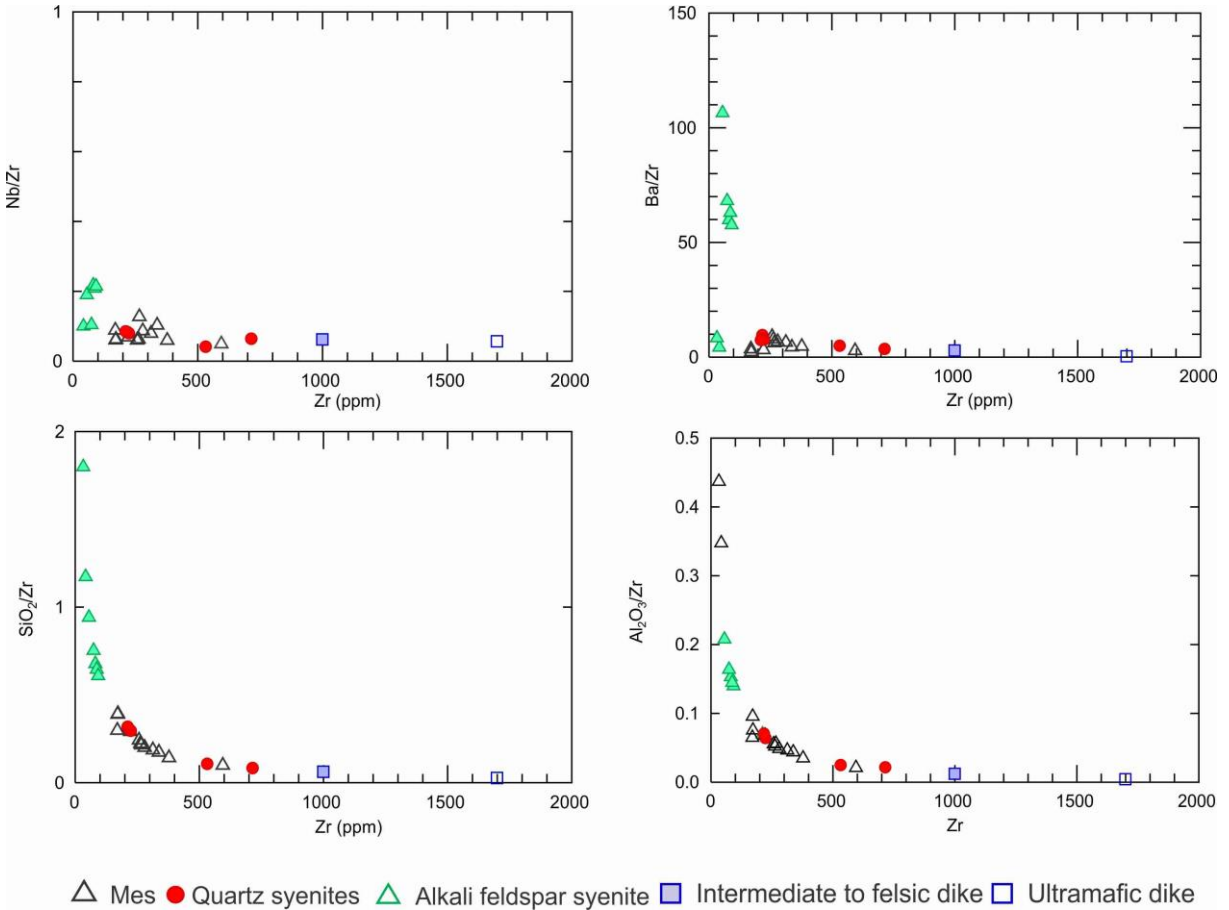


Figure 16 Selected trace element and major element oxide ratios vs Zr as an index of magma mixing (Prelevic et al., 2003).

2.5.4 Petrogenetic considerations

Potassic and ultrapotassic silica-saturated rocks are frequently associated with shoshonitic series in different tectonic settings as intraplate, island arc, active continental margin and post-collisional areas (Muller et al., 1992). Different authors (Foley & Wheller, 1990; Ringwood, 1990; Foley, 1992) suggest that potassic and ultrapotassic magmas are generated by partial melting of a metasomatic continental lithospheric mantle (MLCM). The metasomatism of the continental lithospheric mantle in collisional tectonic setting is related to the dehydration process of the subducted oceanic plate with participation of subducted sediments, a theory has been supported by several authors (Conceição 1993; Conceição et al. 1997, 2002; Cid et al., 2006; Rosa et al., 2011; Nardi et al., 2007, 2011; Janasi 2003; Hollanda et al., 2009; Pérez-Valera et al., 2013; Liu et al., 2014). The ascent of the fluids product of the dehydration the subducted slab through the overlying lithospheric plate would be responsible for the

LILE, LREE enrichment and for the “crustal” Sr-Nd isotopic signatures of the MCLM (Ringwood, 1990; Foley, 1992). This proposition has been verified experimentally on serpentines in previous studies by Tatsumi and Hamilton (1986). These authors have reported that the LILE are preferentially partitioned, relative to the HFSE, into the aqueous phase. Different authors propose (Menzies and Hawkesworth 1987; Conceição 1993; Conceição et al. 1997, 2002; Cid et al., 2006, 2011; Nardi et al., 2007; Hollanda et al., 2009; Pérez- Valera et al., 2013) that potassic and ultrapotassic magmas are generated in a heterogeneous anomalous phlogopite-apatite-clinopyroxene bearing veinlet lithospheric mantle. Different modal compositions of MCLM and the participation of different accessory minerals as garnet, spinel could explain the wide compositional range of potassic and ultrapotassic magmas.

The partial melting of the MLCM that generated the potassic and ultrapotassic rocks of the Uruana syenite may be explained by two different model: 1) the slab breakoff model (Secor and Sacks 1991, Davies and Blackenburg, 1995); in this model the subducted slab breaks during the continental collision and allowing the ascent of the hot asthenosphere up to the base of the lithosphere generating partial melting by thermal conduction; 2)The delamination model (Bird, 1979; Kay and Kay, 1993; Nelson,1991); in this model the crustal thickening related to continental collision generates metamorphic reactions in the lower continental crust as a consequence of continent-continent collision, that might lead to density increases with the appearance of garnet in the metamorphic assemblage (basalt – garnet – clinopyroxenite/eclogite). This may lead a density inversion at the base of the crust. The high density of eclogite may generate a gravitational instability and cause a lithospheric delamination process (Nelson et al 1991; Leech et al 2001; Moore et al 2004; Krystopowicz et al 2013). Consequently, the ascent of hot asthenospheric mantle may generate a thermal anomaly sufficient to trigger partial melting in the MLCM and in the lower crust. In both models the asthenospheric mantle may undergo partial melting by adiabatic decompression.

2.5.5 Petrogenesis of the Uruana syenite rocks

Geochemical and isotopic characteristics of the different lithotypes of the Uruana syenite suggest that related magmas were generated by partial melting of two different sources lithospheric, asthenospheric mantle and successively underwent mixing-mingling process in an upper crustal magma chamber.

The alkali feldspar syenite stocks with geochemical signatures of minette , the syn-magmatic dikes of lamproitic affinity and a group of Mes (samples Uru-19A and Uru-36), present strong enrichment in large ion lithophile elements (LILE) and light rare earth elements (LREE), as well as total REE contents and the negative anomalies of, Nb, Ta, P, Zr and Ti, indicate that these rocks possibly were produced by partial melting of an heterogeneous phlogopite-apatite bearing MCLM, as proposed by several authors for ultrapotassic rocks of post-collisional tectonic setting (Foley 1992; Wang et al., 2004; Williams et al., 2004; Nardi et al 2007; Condamine et al 2014; Prelevic et al., 2012).

The geochemical characteristics of the less enriched group of Mes and the similarity in the trace-element patterns with low-K and high-K calc-alkaline basalts suggests that related magma were generated by partial melting of the asthenospheric mantle. These magmas could have suffered a LILE enrichment during the ascent through the MCLM.

The 614 Ma age of the Uruana syenite is similar to the age of the metamorphic peak in the central part of the Brasilia Belt. This suggests that the partial melting occurred in the MCLM and the astenospheric mantle were generated in a syn- to post-collisional setting. In this context a lithopsheric delamination processes could have generated the ascent of the astenospheric mantle and triggered i) partial melting by adiabatic decompression of the astenospheric mantle, possibly the ancient mantle wedge related to the Goias magmatic arc ii) more extensive partial melting of an heterogeneous continental lithospheric mantle metasomatised during the Goiás magmatic arc activity (Figure 17).

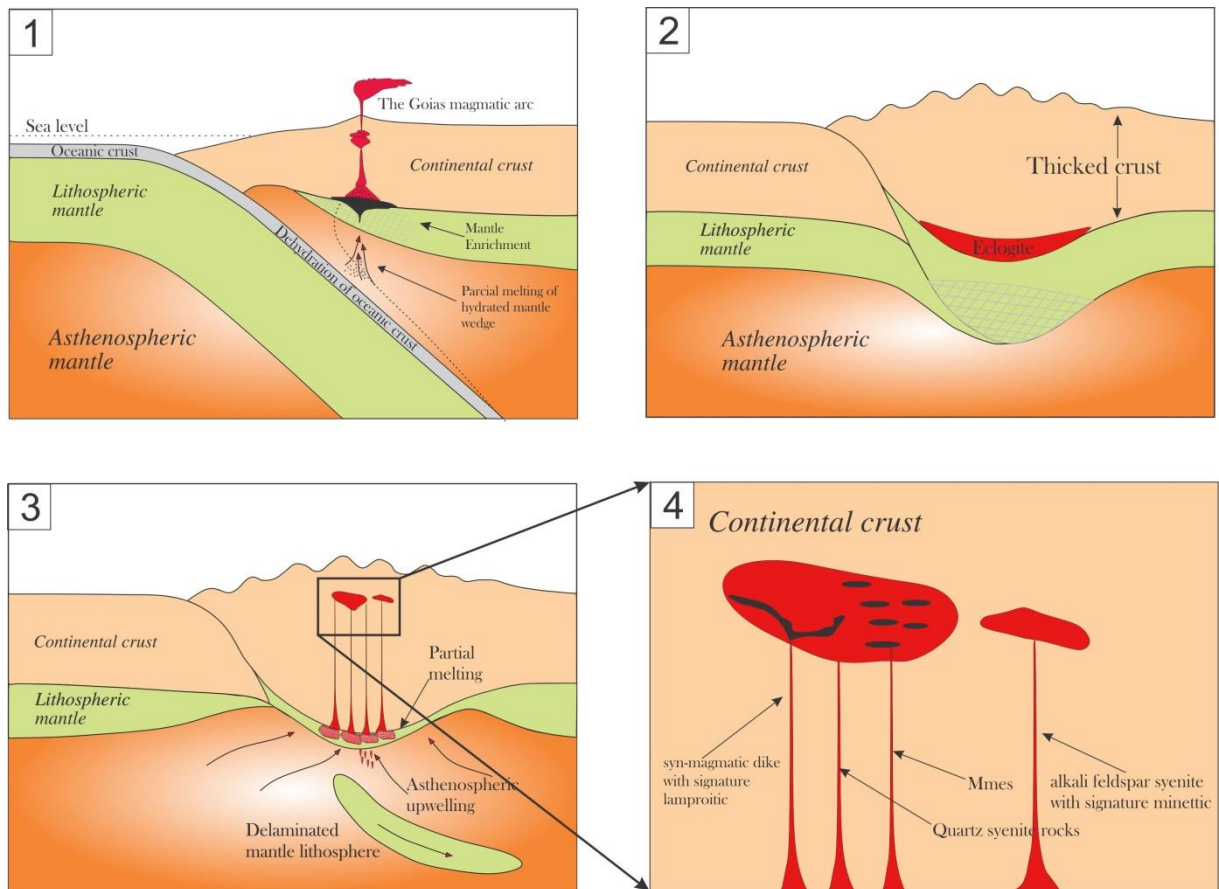


Figure 17. The following geological scheme is presented to show the evolution of rocks of the Uruana syenite summarizing the main stages. (1) 670-600 Ma, metasomatism of the continental lithospheric mantle produced by the dehydration of the oceanic slab of the Goiás magmatic arc (2) 630 Ma, thickening of the continental crust produced by the continental collision increasing the density of the lower crust. (3) 614 Ma, the continuous increase of thickening and the eclogitization of lower crust produced of the evolution of collision, creates a gravitational instability and eventually a lithospheric delamination which allowed the rise of the asthenospheric mantle inducing for one side increase isotherms that they would cause the melting of MCLM and lower crustal, for the other side a melting by adiabatic depressurization of the same asthenospheric mantle. (4) the melting of the MCLM generated potassic syenitic magmas that by field relationships and natural textures of mingling these would be the first to arise and stay in the crust, where subsequently these melts would be intruded by ultrapotassics magmas of transitional and lamproitic signature, at the same time the product of the partial melting of lithospheric mantle would generate another magmatic pulse surrounding of this body that would give

origin to the alkali feldspar syenite stocks with geochemical signatures of minette. The fusion of different portions of the lithospheric asthenosferic mantle and variations in mineralogy and chemistry of the lithospheric source would generate different magmatic melts and ultrapotassic rocks.

2.6 Conclusions

The principal conclusions of this study are as follows:

- 1) The Uruana Syenite is a complex intrusive composed by i) a main quartz syenite ellipsoidal body (20x7 km in size) elongate in the E-W direction characterized by the presence of microgranular enclaves (Mes) and syn-magmatic dykes, ultramafic to intermediate in composition and ii) minor (~1 km in diameter) peripheral subcircular alkali feldspar syenite stocks. All intrusive rock show a green schist metamorphic paragenesis constituted by actinolite+epidote+oligoclase+titanite and a proto-mylonitic to mylonitic deformation. Primary magmatic textures and minerals, such as hornblende and clinopyroxenes, are preserved.
- 2) The Quartz syenite is characterized by porphyritic texture with cm-size phenocrysts of microcline and microphenocrysts of hornblende in a faneritic matrix composed of edenite, phlogopite, k-feldspar, quartz and minor plagioclase. The Mes have granodioritic to quartz syenitic composition with paragenesis represented by microcline, edenite, pargasite, phlogopite, and minor diopside, the Mes composition vary with the relative abundance of mafic minerals, biotite and amphibole. Fine to medium-grained ultramafic dikes are composed of phlogopite, diopside, and minor microcline. The fine-grained intermediate dikes have paragenesis very similar to the host quartz syenite with abundant k-feldspar, amphibole, phlogopite and minor quartz and plagioclase. Alkali feldspar syenite represents the main lithology of the peripheral stocks, and show a porphyritic texture with cm-size phenocrysts of microcline, micro-phenocryst of diopside and augite immersed in a microfaneritic matrix of k-feldspar, biotite, and minor quartz and plagioclase. Titanite, epidote, apatite and zircon represent accessory minerals in all lithotypes.
- 3) Geochemical data indicate potassic-ultrapotassic affinity, whereas the quartz syenites have potassic signature, the ultramafic dike presents lamproitic signature, the alkali feldspar syenite has minettic signature and the felsic dike and the Mes are transitional ultrapotassic rocks.
- 4) Geochemical and isotopic characteristics of the different lithotypes of the Uruana syenite suggest that related magmas were derived by partial melting of a heterogeneous MCLM source and, in minor part, of a metasomatic asthenospheric mantle source. The metasomatic processes in both mantle reservoirs in the region could have been related to the subduction associated to the Neoproterozoic Goias magmatic arc. The mechanism responsible for the partial melting could be a lithospheric delamination. This process generated the ascent of the asthenospheric mantle and triggered i) partial melting by adiabatic decompression of the

- asthenospheric mantle, possibly the ancient mantle wedge related to the Goias magmatic arc
- ii) more extensive partial melting of an heterogeneous continental lithospheric mantle metasomatised during the Goias magmatic arc activity.
- 5) U-Pb zircon ages indicate that the Uruana syenite crystallized at ca. 614.7 ± 3.1 Ma. This age roughly contemporaneous or slightly younger than the metamorphic peak of the Brasiliano orogeny in the central part of the Brasilia Belt. This suggests that the partial melting occurred in the MCLM and the astenospheric mantle were generated in a syn- to post-collisional setting.

2.7 Acknowledgements

This study is part of the first author's (S.A.R. Sandoval) M.Sc. dissertation developed at the Instituto de Geociências (Universidade de Brasília). The authors are grateful to the Coordenação de Aperfeiçoamento de Pessoal de Nível Superior (CAPES) for continuous support for field and laboratory work through research grants.

2.8 References

- ALMEIDA, F.F.M.; et al. Brazilian structural provinces: an introduction. *Earth-Science Reviews*, v. 17, p. 1–29, 1981
- ALMEIDA. F.F.M. de. Observações sobre o Pré-Cambriano da região Central de Goiás. Curitiba. *B. Paranaense de Geodências*, v. 26, p. 19-22, 1967.
- ARAÚJO F.J.O. The Pireneus Syntaxis: An example of the intersection of two Brasiliano fold-thrust belts in central Brazil and its implications for the tectonic evolution of western Gondwana. *Rev. Bras. Geocienc.*, v. 30, n. 1, p. 144–148, 2000.
- BARBOSA O., et al. Geologia e inventário dos recursos minerais do Projeto Brasília. Rio de Janeiro, PROSPEC/DNPM, p.225, 1969.
- BIRD, P., TOKSOZ, M.N., AND SLEEP, N.H. Thermal and mechanical models of continentcontinent convergent zones: *Journal of Geophysical Research*, v. 80, p. 4405-4416, 1975.
- BLACK, L. P., et al. Improved $^{206}\text{Pb}^{238}\text{U}$ microprobe geochronology by the monitoring of trace element related matrix effect; SHRIMP, ID-TIMS, ELA-ICP-MS and oxygen isotope documentation for a series of zircon standards. *Chemical Geology*, v. 205, n. 1, p. 115-140, 2004.
- BRITO NEVES, B.B.; CORDANI, U.G. Tectonic evolution of South Amercia during the Late Proterozoic. *Precambrian Research*, v.53, n.1-2, p.23-40, 1991.
- CAMPOS NETO, M. C. Orogenic Systems from Southwestern Gondwana, an approach to Brasiliano-Pan African Cycle and Orogenic Collage in Southeastern Brazil. In: CORDANI, U. G. et al. Tectonic Evolution in South America. Rio de Janeiro: s.n., p. 335-365, 2000.
- CID, J. PLÁ; NARDI, L. V. S. Alkaline Ultrapotassic A-Type Granites Derived from Ultrapotassic Syenite Magmas Generated from Metasomatized Mantle. *International Geology Review*, v. 48, n. 10, p. 942-956, 2006.

COMPSTON W, et al. Zircon U-Pb ages for the early Cambrian timescale. *J Geol Soc Lond*, v.149, n. 2, p. 171-184, 1992.

CONCEIÇÃO H. Petrology of the syenites from Salvador-Curaça Mobile Belt (BahiaBrazil): geodynamic significance. *An. Acad. bras. Ci.*, v. 65, n. I, p. 17-32, 1993.

CONCEIÇÃO H., et al. Alkali-potassic magmas generated by partial melting of an enriched mantle source: example of the Lower Proterozoic plutonism from Bahia State (Brazil). *II ISGAM, Ext. Abstr*, p. 108- 109, 1997..

CONCEIÇÃO, H., et al. Zircon geochronology and petrology of alkaline-potassic syenites, southwestern Serrinha Nucleus, East São Francisco Craton, Brazil. *International Geology Review*, v. 44, n. 2, p. 117-136, 2002.

CONDAMINE, PIERRE, AND ETIENNE MÉDARD. "Experimental melting of phlogopite-bearing mantle at 1 GPa: Implications for potassic magmatism." *Earth and Planetary Science Letters*, v. 397, p. 80-92, 2014:

CONTICELLI, S., et al. Trace elements and Sr–Nd–Pb isotopes of K-rich, shoshonitic, and calc-alkaline magmatism of the Western Mediterranean Region: genesis of ultrapotasssic to calc-alkaline magmatic associations in a post-collisional geodynamic setting. *Lithos*, v. 107, n. 1, p. 68–92, 2009.

CRUMMY, J. M., et al. High-K Mafic Plinian Eruptions of Volcán de Colima, Mexico. *Journal of Petrology*, v. 55, n. 11, p. 2155-2192, 2014.

DARDENNE, M.A. The Brasília Fold Belt. In: U.G. Cordani, E.J. Milani, A. Thomaz Filho, D.A. Campos (eds). *Tectonic Evolution of South America*. 31st Int. Geol. Congr.; Rio de Janeiro, p. 231-263, 2000.

DAVIES, J. H., & VON BLANCKENBURG, F. Slab breakoff: a model of lithosphere detachment and its test in the magmatism and deformation of collisional orogens. *Earth and Planetary Science Letters*, v. 129, n. 1, p. 85-102, 1995.

DUGGEN, S., et al. Post-collisional transition from subduction- to intraplate-type magmatism in the Westernmost Mediterranean: evidence for continental-edge delamination of subcontinental lithosphere. *Journal of Petrology*, v. 46, p. 1155–1201, 2005.

FISCHEL, D. P.; PIMENTEL, M. M.; FUCK R. A. Idade do metamorfismo de alto grau no Complexo Anápolis-Itauçu, Goiás, determinada pelo método Sm-Nd. *Revista Brasileira de Geociências*, v. 28, n. 4, p. 543-544, 1998.

FOLEY SF & PECCERILLO A. Potassic and ultrapotasssic magmas and their origin. *Lithos* v. 28, p. 181-185, 1992.

FOLEY, S. F., & WHEELER, G. E. Parallels in the origin of the geochemical signatures of island arc volcanics and continental potassic igneous rocks: the role of residual titanates. *Chemical Geology*, v. 85, n. 1, p. 1-18, 1990.

FOLEY, S. Petrological characterization of the source components of potassic magmas: geochemical and experimental constraints: *Lithos*, v. 28, p. 187–204, 1992.

FOLEY, S.F., et al. The ultrapotasssic rocks: Characteristics, classification, and constraints for petrogenetic models: *Earth-Science Reviews*, v. 24, p. 81–134, 1987.

- FUCK, R.A. A Faixa Brasília e a compartimentação tectônica na Província Tocantins. In: SIMP. GEOL. CENTROOESTE, 4, Brasília, 1994. Anais... Brasília, SBG, p. 184-187, 1994.
- FUCK, R.A., et al. The Santa Terezinha Sequence, Goiás Magmatic Arc, Central Brazil: constraints from U-Pb and Sm-Nd data. In: South American Symposium on Isotope Geology, 5, Montevideo, Uruguay, p. 198–201, Short Papers, 2006.
- HOLLANDA, Maria Helena Bezerra Maia de et al. Geologia e caracterização química do magmatismo peralcalino ultrapotássico do enxame de diques Manaíra-Princesa Isabel, Província Borborema. Geologia USP. Série Científica, v. 9, n. 3, p. 13-46, 2009.
- IONOV, Dmitri A.; GRIFFIN, William L.; O'REILLY, Suzanne Y. Volatile-bearing minerals and lithophile trace elements in the upper mantle. *Chemical Geology*, v. 141, n. 3, p. 153-184, 1997.
- JUNGES, S.L., et al. New ID-TIMS U-Pb ages in the western portion of the Mara Rosa Arc: two hundred million years of arc building. In: SSAGI, IV, Salvador, Brazil, Short Papers, v. 1, p. 198–201, 2003.
- JUNGES, S.L., PIMENTEL, M.M., MORAES, R. Nd isotopic study of the Neoproterozoic Mara Rosa Arc, Central Brazil: implications for the evolution of the Brasília Belt. *Precamb. Res.*, v. 117, p. 101–118, 2002.
- KAY, ROBERT W.; KAY, S. MAHLBURG. Delamination and delamination magmatism. *Tectonophysics*, v. 219, n. 1-3, p. 177-189, 1993.
- KRYSTOPOWICZ, NEIL J.; CURRIE, CLAIRE A. Crustal eclogitization and lithosphere delamination in orogens. *Earth and Planetary Science Letters*, v. 361, p. 195-207, 2013.
- LACERDA FILHO, J. V.; OLIVEIRA, C. C. Geologia da Região Centro-Sul de Goiás. *Boletim de Geociências do Centro-Oeste*, v. 18, n. 1/2, p. 3-19, 1995.
- LAUX, J.H., et al. Two Neo- proterozoic crustal accretion events in the Brasília Belt, central Brazil. *J. South Am. Earth Sci.*, v. 18, p. 183–198, 2005.
- LEAKE, BERNARD E., et al. Report. Nomenclature of Amphiboles: Report of the Subcommittee on Amphiboles of the International Mineralogical Association Commission on New Minerals and Mineral Names. *Mineralogical Magazine*, v. 61, n. 2, p. 295-321, 1997.
- LEECH, M. L. Arrested orogenic development: Eclogitization, delamination, and tectonic collapse, *Earth Planet. Science Lett.*, v. 185, p. 149 – 159, 2001.
- LLOYD FE, ARIMA M, EDGAR AD. Partial melting of a phlogopite-clinopyroxenite nodule from southwest Uganda: an experimental study bearing on the origin of highly potassic continental rift volcanics. *Contrib Mineral Petrol*, v. 91, p. 321–329, 1985.
- LUDWIG, K.R. Isoplot/EX version 3.0, A geochronological toolkit for Microsoft Excel: Berkeley Geochronology Center Special Publication, 2003.
- MARINI, O.J.; FUCK, R.A. & DANNI, J.C. A evolução geotectônica da Faixa Brasília e seu embasamento. In: Simp. Sobre O Craton do São Francisco e suas Faixas Marginais. Salvador, 1981. Anais... Salvador, SBG/BA, p. 100-113, 1981.
- MENZIES, M.; et al. Metasomatic and enrichment processes in lithospheric peridotites, an effect of asthenosphere-lithosphere interaction. In: MENZIES, M. A., HAWKESWORTH, C. J . (Eds). *Mantle Metasomatism*. London: Academic Press, p. 313-361, 1987.

- MOORE, VERNON M.; WILTSCHKO, DAVID V. Syncollisional delamination and tectonic wedge development in convergent orogens. *Tectonics*, v. 23, n. 2, 2004.
- MORIMOTO, C.N. Nomenclature of pyroxenes. *Mineral. Mag.*, v. 52, p. 535–550, 1988.
- MULLER, D., ROCK, N. M. S., AND GROVES, D. I. Geochemical discrimination between shoshonitic and potassic volcanic rocks in different tectonic settings: A pilot study: *Mineral. Petrol.*, v. 46, p. 259-289, 1992.
- NARDI, L. V. S.; CID, J. P., & BITENCOURT, M. F. Minette mafic microgranular enclaves and their relationship to host syenites in systems formed at mantle pressures: major and trace element evidence from the Piquiri Syenite Massif, southernmost Brazil. *Mineralogy and Petrology*, v. 91, n.1-2, p. 101-116, 2007.
- NARDI, L. V. S.; CID, J. PLÁ; BITENCOURT, M. F. Minette mafic microgranular enclaves and their relationship to host syenites in systems formed at mantle pressures: major and trace element evidence from the Piquiri Syenite Massif, southernmost Brazil. *Mineralogy and Petrology*, v. 91, n. 1-2, p. 101-116, 2007.
- NARDI, L.V.S., et al. Geochemistry and petrogenesis of post-collisional ultrapotassic syenites and granites from southernmost Brazil: The Piquiri Syenite Massif: *Anais da Academia Brasileira de Ciencias*, v. 80, p. 353–371, 2008.
- OLIVEIRA,C.C. Folha SD.22-Z-C-VI, Itaguaru. Programa Levantamentos Geológicos Básicos do Brasil – PLGB. Brasilia, CPRM, p. 107,1997
- PECCERILLO A. Potassic and ultrapotassic rocks: compositional characteristics, petrogenesis, and geologic significance. *IUGS Episodes*, v. 15, p. 243-25, 1992.
- PENA, G.S. et al. Projeto Goiânia II. Relatório Final, Goiânia. DNPM/CPRM. v. 5. 1975.
- PÉREZ-VALERA, L. A., et al. Age distribution of lamproites along the Socovos Fault (southern Spain) and lithospheric scale tearing. *Lithos*, v. 180, p. 252-263, 2013.
- PIMENTEL M.M. & FUCK R.A. Neoproterozoic crustal accretion in central Brazil. *Geology*, v. 20, p. 375-379, 1992.
- PIMENTEL MM, et al. The basement of the Brasília Fold Belt and the Goiás Magmatic Arc. In: Cordani UG et al. (Eds); *Tectonic Evolution of South America*. Rio de Janeiro: 31st IGC, p. 190-229, 2000b.
- PIMENTEL, M. M., et al. The basement of the Brasília Fold Belt and the Goias Magmatic Arc. In:Cordani, U. G.; Milani, E. J.; Thomaz Filho, A. & Campos, D. A. (eds) *Tectonic Evolution of South America*. 31st International Geological Congress, Rio de Janeiro, p. 195–229, 2000.
- PIMENTEL, M.M., et al. Shrimp and conventional U-Pb age, Sm-Nd isotopic characteristics and tectonic significance of the K-rich Itapuranga suite in Goiás, central Brazil: *Anais da Academia Brasileira de Ciencias*, v. 75, p. 97–108, 2003.
- PIMENTEL, M.M., et al. The Mara Rosa arc in the Tocantins Province: Further evidence for Neoproterozoic crustal accretion in central Brazil. *Precambrian Research*, v. 81, p. 299–310, 1997.
- PIMENTEL, M.M.; FUCK, R. A.& BOTELHO, N.F. Granites and the geodynamic history of the Neoproterozoic Brasilia belt, Central Brazil: A review: *Lithos*, v. 46, p. 463–483, 1999.

PIUZANA D., et al. Neoproterozoic granulite fácies metamorphism and coeval granitic magmatism in the Brasília Belt, Central Brazil: regional implications of new SHRIMP U-Pb and Sm-Nd data. *Precambrian Research*, v. 125, p. 245-273, 2003.

PIUZANA, D. Geologia Isotópica U-Pb e Sm-Nd da Sequência Silvânia, Complexo Anápolis-Itauçu e Grupo Araxá na Região de Leopoldo de Bulhões, Goiás: Contribuições ao Estudo da Evolução da Faixa Brasília. 2002. 141p. Tese (Doutorado) – Instituto de Geociências, Universidade de Brasília - UnB, Brasília, 2002.

PIUZANA, D.; et al. SHRIMP U-Pb and Sm-Nd data for the Araxá Group and associated magmatic rocks: constraints for the age of sedimentation and geodynamic context of the southern Brasília Belt, central Brazil. *Precambrian Research*, v. 125, p. 139-160, 2003b.

PLÁ CID, JORGE et al. Petrology of Gameleira potassic lamprophyres, São Francisco Craton. *Anais da Academia Brasileira de Ciências*, v. 84, n. 2, p. 377-398, 2012.

PLÁ, CIDJ, et al. SIMS analysis on trace and rare earth elements in coexisting clinopyroxene and mica from minette mafic enclaves in potassic syenites crystallized under high pressures. *Contrib Mineral Petrol*, v. 148, p. 675-688, 2005.

PRELEVIC, D., et al. Ultrapotassic mafic rocks as geochemical proxies for post-collisional dynamics of orogenic lithospheric mantle: the case of Southwestern Anatolia, Turkey. *J. Petrol.* V. 53, p. 1019–1055, 2012.

PRELEVIĆ, D., et al. Mediterranean Tertiary lamproites derived from multiple source components in postcollisional geodynamics. *Geochimica et Cosmochimica Acta* v. 72, p. 2125–2156, 2008.

RICHARD P, SHIMIZU N & ALLÈGRE CJ. $^{143}\text{Nd}/^{146}\text{Nd}$ A Natural Tracer: An Application to Oceanic Basalts. *Earth Plan Sci Lett*, v. 31, p.269-278, 1976.

RIEDER, M., et al. Nomenclature of mica. *Can. Mineral*, v. 36, p. 905, 1998.

RINGWOOD, A.E. Slab-mantle interactions. 3. Petrogenesis of intraplate magmas and structure of the upper mantle. *Chem. Geol.* 82, p. 187–207, 1990.

ROCK NMS. The nature and origin of lamprophyres: an overview. In: FITTON JG AND UPTON BGJ (Eds), Alkaline igneous rocks. *Geol Soc Spec Publ* v. 30, p.191–226, 1987.

SA, ALBERTO MARTINS de. Projeto Mapas Metalogenéticos e de Previsão de Recursos Minerais; Carta Metalogenética; Carta de Previsão de Recursos Minerais; Carta de Previsão para Planejamento de Ações Governamentais. Folha SD.22-Z-C-Ceres, Brasília, DNPM/CPRM, 1987.

SACKS, P. E., AND D. T. SECOR. Delamination in collisional orogens, *Geology*, v. 18, n. 10, p. 999-1002, 1990.

SEER H.J. Evolução tectônica dos Grupos Araxá, Ibiá e Canastra na sinforma de Araxá, Araxá, Minas Gerais. Tese de Doutorado, UnB, p. 267, 1999.

SEER H.J., et al. O Grupo Ibiá na sinforma de Araxá: um terreno tectonoestratigráfico ligado a evolução de arcos magmáticos. *Revista Brasileira de Geociências*, v. 30, n. 4, p. 737- 744, 2000.

SIAL A.N., et al. The São Francisco Palaeocontinent. In: C. Gaucher, A.N. Sial, G.P. Halverson, H.E. Frimmel (eds) Neoproterozoic-Cambrian Tectonics, Global Change and Evolution: a focus on southwestern Gondwana. *Developments in Precambrian Geology*, 16, Elsevier, p. 31–69, 2009.

- SOUZA E.C., et al. Lithogeochemical panorama of the subalkaline (shoshonitic) Itapuranga Suite, SE Goiás State, central Brazil. In: WORKSHOP MAGMATISMO GRANÍTICO E MINERALIZAÇÕES ASSOCIADAS, 1.; Resumos Expandidos... Rio de Janeiro, Acad Bras Ciênc, p. 82, 1993.
- STACEY, J. S., KRAMERS, J. D. Approximation of terrestrial lead isotope evolution by a two-stage model. *Earth and Planetary Science Letters*, v. 26, n. 2, p. 207-221, 1975.
- STRIEDER, A.J.; SUITA, M.T.F. Neoproterozoic tectonic evolution of the Tocantins Structural Province, Central Brazil. *Journal of Geodynamics*, v. 28, p. 67–289, 1999.
- TAKAHASHI, T., et al. Primary magmas at the volcanic front of the NE Japan arc: coeval eruption of crustal low-K tholeiitic and mantle-derived medium-K calc-alkaline basalts at Azuma Volcano. *Journal of Petrology*, v. 54, n. 1, p. 103-148, 2013.
- TURNER, S.P., et al. Magmatism associated with orogenic collapse of the betic-Alboran Domain, SE Spain. *Journal of Petrology*, v. 40, p. 1011–1036, 1999.
- VALERIANO, C.M., et al. Tectonic evolution of the Brasilia Belt, Central Brazil, and early assembly of Gondwana: Geological Society, London, Special Publications, v. 294, p. 197–210, 2008.
- WANG, K.-L., et al. Geochemical constraints for the genesis of post-collisional magmatism and the geodynamic evolution of the Northern Taiwan region. *J. Petrol*, n. 45, p. 975–1011, 2004
- WILLIAMS, H.M., TURNER, S.P., PEARCE, J.A., KELLEY, S.P., HARRIS, N.B.W. Nature of the source regions for post-collisional, potassic magmatism in Southern and Northern Tibet from geochemical variations and inverse trace element modelling. *J. Petrol*, v. 45, n. 555–607. 2004.
- WILLIAMS, I. S. U-Th-Pb geochronology by ion microprobe. In: M. A. McKibben, I. Shanks, W. C. P. Ridley, W. I. Ridley (Eds.), *Application of Microanalytical Techniques to Understanding Mineralizing Process (1-35)*. Reviews in Economic Geology. Socorro, USA: Society Geologists, 1998.

3. CONCLUSÕES

- 1.) O Sienito Uruana é um complexo intrusivo composto principalmente por :(i) um corpo quartzo sienítico elipsoidal que mede 20x7 quilômetros e está alongado na direção E-W. Nele, há enclaves microgranulares (EM) e diques sin-magmáticos de composição ultramáfica a intermediária. (ii) stocks subordinados de composição álcali-feldspato sieníticas que afloram a norte do corpo principal e têm até 1 quilômetro de diâmetro. Todos os litotipos do sienito de Uruana apresentam deformação proto-milonítica a milonítica e uma paragênese metamórfica de Xisto Verde constituída por actinolita + epidoto + oligoclásio + titanita. Esses intrusivos preservam algumas texturas e minerais primários como hornblenda e clinopiroxênios.
- 2.) Os quartzo sienitos são caracterizados por apresentar uma textura porfirítica, que é caracterizada por fenocristais centimétricos de microclínio e microfenocristais de hornblenda, numa matriz fanerítica composta por edenita, flogopita, k-feldspato, quartzo e menor conteúdo de plagioclásio. Os enclaves microgranulares têm composições desde granodiorítica até quartzo sienítica e são representados por uma paragênese mineralógica de microclínio, edenita, pargasita, flogopita e menores quantidades de diopsídio plagioclásio e quartzo, o conteúdo dos minerais maficos biotita e anfibólio variam com a composição dos EM, titanita, epidoto, apatita e zircão representam as fases assessorias. Os diques ultramáficos são principalmente constituídos por flogopita, diopsídio e menores conteúdos de álcali feldspato, os diques sin-magmáticos intermediários de granulação fina apresentam uma paragênese mineralógica similar ao quartzo sienito hospedeiro que é representada por minerais essências de álcali feldspato, anfibólio, flogopita e menores quantidades de quartzo e plagioclásio. Os stocks subordinados são principalmente constituído por álcali-feldspato sienitos. Mostram uma textura porfirítica definida por fenocristais de tamanhos centimétricos de microclínio e em menor conteúdo microfenocristais de diopsídio e augita imersos numa matriz microfanerítica de k-feldspato, biotita e menores conteúdos de quartzo e plagioclásio. Titanita, epidoto, apatita e zircão estão presentes como fases Acessórias em todos os litotipos.
- 3.) Características geoquímicas indicam que as rochas do sienito de Uruana têm afinidade potássica a ultrapotásica. Os quartzo sienítos têm assinatura potássica, os diques ultramáficos têm assinatura lamproítica, enquanto que os álcali-feldspato sienito têm assinatura minettica e os diques e EM são rochas ultrapotássicas transicionais.
- 4.) Características geoquímicas e isotópicas dos diferentes litotipos do Sienito Uruana sugerem que os magmas geradores destas rochas, foram derivados da fusão parcial do manto litosférico heterógeno metassomatizado com pequenos aportes do manto astenosférico. O processo metassomático em ambos reservatórios mantélicos podem estar relacionados com subducção associada ao Arco Magmático neoproterozóico de Goiás. O mecanismo responsável pela fusão

parcial é associado a uma delaminação litosférica. Este processo pode ter gerado: (i) a ascensão do manto astenosférico que gerou a fusão parcial de pequenas porções do manto astenosférico, possivelmente a antiga cunha mantélica relacionado ao Arco Magmático de Goiás, (II) a fusão extensiva de um manto continental heterogêneo metassomatizado durante a atividade do Arco Magmático de Goiás.

- 5.) Idades de U-Pb em zircão indicam que o Sienito de Uruana se cristalizou em 614.7 ± 3.1 Ma, essa idade é contemporânea ou pouco mais jovem com o do pico metamórfico da orogenia Brasíliana na porção central da Faixa Brasília, sugerindo que a fusão parcial do manto continental litosférico metassomatizado e o manto astenosférico foi gerado num contexto sin a pós colisional.

4. ANEXOS

Tabela 8. Química mineral dos anfibólios estudados

Rocha Amostra	Enclaves Microgranulares								
	Uru-09								
SiO ₂	46.24	45.53	45.32	46.07	45.53	44.79	45.01	45.77	
TiO ₂	1.25	1.47	1.76	0.72	1.26	1.79	1.00	0.98	
Al ₂ O ₃	8.38	8.95	8.76	9.82	8.81	9.07	8.97	8.66	
FeO	15.49	15.94	15.50	15.87	14.97	15.51	16.34	15.37	
MnO	0.45	0.27	0.41	0.20	0.34	0.31	0.27	0.33	
MgO	12.19	12.11	12.31	11.82	11.99	12.28	11.97	12.60	
CaO	10.48	10.90	10.95	10.70	10.80	10.79	10.76	10.85	
Na ₂ O	2.02	2.27	1.98	2.14	2.25	2.29	2.19	2.05	
K ₂ O	1.20	1.24	1.25	1.34	1.29	1.24	1.28	1.20	
Cl	0.06	0.09	0.10	0.07	0.12	0.12	0.08	0.04	
V ₂ O ₃	0.00	0.04	0.04	0.08	0.07	0.08	0.06	0.02	
ZnO	0.00	0.04	0.02	0.06	0.00	0.10	0.06	0.01	
O=F,Cl	0.01	0.02	0.02	0.01	0.03	0.03	0.02	0.01	
TOTAL	97.73	98.84	98.37	98.87	97.39	98.34	97.98	97.86	
Si	6.8330	6.6990	6.6867	6.7441	6.7817	6.6223	6.6853	6.7593	
Al	1.1670	1.3010	1.3133	1.2559	1.2183	1.3777	1.3147	1.2407	
SUM T	8.0000	8.0000	8.0000	8.0000	8.0000	8.0000	8.0000	8.0000	
Al	0.2917	0.2502	0.2089	0.4372	0.3284	0.2023	0.2558	0.2667	
Ti	0.1390	0.1631	0.1948	0.0796	0.1409	0.1988	0.1121	0.1090	
Fe ³⁺	0.3020	0.2562	0.2839	0.2786	0.1658	0.2928	0.3363	0.3225	
V	0.0000	0.0051	0.0050	0.0094	0.0087	0.0095	0.0065	0.0020	
Mg	2.6858	2.6550	2.7078	2.5800	2.6627	2.7056	2.6514	2.7732	
Zn	0.0000	0.0045	0.0016	0.0059	0.0000	0.0105	0.0070	0.0010	
Fe ²⁺	1.5815	1.6660	1.5981	1.6092	1.6935	1.5804	1.6308	1.5256	
SUM C	5.0000	5.0000	5.0000	5.0000	5.0000	5.0000	5.0000	5.0000	
Mn	0.0563	0.0339	0.0511	0.0250	0.0425	0.0393	0.0335	0.0418	
Fe ²⁺	0.0302	0.0393	0.0301	0.0547	0.0047	0.0445	0.0630	0.0507	
Ca	1.6593	1.7180	1.7310	1.6776	1.7228	1.7090	1.7125	1.7172	
Sr	0.0000	0.0000	0.0000	0.0000	0.0000	0.0000	0.0000	0.0000	
Na	0.2542	0.2088	0.1877	0.2427	0.2300	0.2072	0.1911	0.1903	
SUM B	2.0000	2.0000	2.0000	2.0000	2.0000	2.0000	2.0000	2.0000	
Na	0.3231	0.4398	0.3789	0.3649	0.4191	0.4497	0.4402	0.3955	
K	0.2264	0.2323	0.2349	0.2493	0.2445	0.2329	0.2427	0.2263	
SUM A	0.5495	0.6721	0.6138	0.6142	0.6636	0.6826	0.6829	0.6218	
Si em fórmula	6.7879	6.6615	6.6452	6.7030	6.7571	6.5798	6.6361	6.7116	
NaB	0.3517	0.2916	0.2797	0.3326	0.2835	0.3020	0.3001	0.2949	
CaB	1.6483	1.7084	1.7203	1.6674	1.7165	1.6980	1.6999	1.7051	
Ti	0.1380	0.1622	0.1936	0.0791	0.1404	0.1976	0.1112	0.1082	
(Ca+Na)B	2.0000	2.0000	2.0000	2.0000	2.0000	2.0000	2.0000	2.0000	
(Na+K)A	0.4467	0.5844	0.5168	0.5190	0.6069	0.5821	0.5674	0.5115	
Mg/(Mg+Mn ²⁺)	0.9795	0.9874	0.9815	0.9904	0.9843	0.9857	0.9875	0.9852	

Formula estrutural baseada em 23 oxigênios

Tabela 8. Química mineral dos anfíbólios estudados (continuação).

Rocha	Enclaves Microgranulares							
Amostra	Uru-09							
SiO ₂	45.17	45.05	45.31	44.85	45.51	45.49	44.33	45.11
TiO ₂	1.36	1.36	1.62	1.01	1.17	1.34	1.16	0.75
Al ₂ O ₃	8.49	8.59	8.52	8.44	8.53	8.59	8.52	8.77
FeO	15.60	16.25	15.39	14.92	15.62	15.22	15.83	16.00
MnO	0.54	0.50	0.21	0.44	0.39	0.45	0.34	0.50
MgO	12.10	11.92	12.30	12.50	12.46	12.19	11.40	12.48
CaO	10.67	10.87	10.87	10.66	10.91	11.03	10.84	10.96
Na ₂ O	2.01	1.94	2.12	1.79	2.20	2.26	2.12	2.14
K ₂ O	1.28	1.18	1.13	1.17	1.22	1.17	1.20	1.22
Cl	0.06	0.08	0.06	0.11	0.07	0.09	0.12	0.14
V2O ₃	0.09	0.01	0.06	0.08	0.05	0.08	0.02	0.00
ZnO	0.09	0.11	0.03	0.08	0.00	0.01	0.00	0.05
O=F,Cl	0.01	0.02	0.01	0.02	0.02	0.28	0.30	0.26
TOTAL	97.47	97.84	97.60	96.01	98.10	98.25	96.22	98.40
Si	6.7286	6.7008	6.7286	6.7460	6.7324	6.7513	6.7476	6.6859
Al	1.2714	1.2992	1.2714	1.2540	1.2676	1.2487	1.2524	1.3141
SUM T	8.0000	8.0000	8.0000	8.0000	8.0000	8.0000	8.0000	8.0000
Al	0.2191	0.2063	0.2204	0.2420	0.2194	0.2542	0.2760	0.2180
Ti	0.1527	0.1522	0.1809	0.1138	0.1300	0.1494	0.1333	0.0836
Fe ³⁺	0.3223	0.3438	0.2551	0.3769	0.2950	0.1951	0.1995	0.3848
V	0.0112	0.0008	0.0070	0.0095	0.0058	0.0096	0.0022	0.0002
Mg	2.6867	2.6437	2.7236	2.8022	2.7483	2.6973	2.5861	2.7580
Zn	0.0102	0.0116	0.0029	0.0092	0.0000	0.0005	0.0000	0.0053
Fe ²⁺	1.5978	1.6416	1.6102	1.4463	1.6016	1.6934	1.8029	1.5502
SUM C	5.0000	5.0000	5.0000	5.0000	5.0000	5.0000	5.0000	5.0000
Mn	0.0686	0.0631	0.0265	0.0554	0.0484	0.0556	0.0440	0.0621
Fe ²⁺	0.0237	0.0355	0.0464	0.0529	0.0361	0.0000	0.0129	0.0485
Ca	1.7024	1.7317	1.7291	1.7179	1.7298	1.7535	1.7677	1.7397
Sr	0.0000	0.0000	0.0000	0.0000	0.0000	0.0000	0.0000	0.0000
Na	0.2053	0.1697	0.1980	0.1738	0.1858	0.1909	0.1754	0.1498
SUM B	2.0000	2.0000	2.0000	2.0000	2.0000	2.0000	2.0000	2.0000
Na	0.3760	0.3903	0.4109	0.3481	0.4440	0.4603	0.4503	0.4639
K	0.2426	0.2233	0.2143	0.2237	0.2293	0.2215	0.2332	0.2297
SUM A	0.6187	0.6136	0.6252	0.5718	0.6733	0.6818	0.6835	0.6936
Si em fórmula	6.6811	6.6504	6.6911	6.6902	6.6889	6.7226	6.7183	6.6295
NaB	0.3097	0.2813	0.2806	0.2963	0.2814	0.2539	0.2400	0.2750
CaB	1.6903	1.7187	1.7194	1.7037	1.7186	1.7461	1.7600	1.7250
Ti	0.1516	0.1510	0.1799	0.1129	0.1291	0.1487	0.1327	0.0829
(Ca+Na)B	2.0000	2.0000	2.0000	2.0000	2.0000	2.0000	2.0000	2.0000
(Na+K)A	0.5085	0.4960	0.5381	0.4432	0.5722	0.6150	0.6152	0.5613
Mg/(Mg+Mn ²⁺)	0.9751	0.9767	0.9903	0.9806	0.9827	0.9796	0.9833	0.9780

Formula estrutural baseada em 23 oxigênios.

Tabela 8. Química mineral dos anfíbolios estudados (continuação).

Rocha	Enclaves Microgranulares							
Amostra	Uru-09							
SiO ₂	44.74	44.82	45.26	44.15	46.09	44.39	44.68	44.99
TiO ₂	1.30	0.61	1.25	0.55	1.13	1.30	1.25	0.86
Al ₂ O ₃	9.04	9.30	8.64	9.17	8.05	9.33	9.01	9.40
FeO	16.14	16.51	16.31	16.32	15.39	16.44	16.27	16.44
MnO	0.36	0.47	0.34	0.36	0.38	0.45	0.56	0.44
MgO	11.94	11.52	11.91	11.61	12.77	11.74	11.63	11.57
CaO	11.14	11.10	11.24	11.15	11.34	10.99	10.84	11.05
Na ₂ O	2.13	2.15	2.22	2.17	2.13	2.22	2.24	2.26
K ₂ O	1.32	1.31	1.25	1.32	1.15	1.35	1.34	1.30
Cl	0.12	0.12	0.15	0.07	0.06	0.09	0.12	0.07
V ₂ O ₃	0.02	0.04	0.04	0.07	0.08	0.00	0.06	0.05
ZnO	0.00	0.06	0.03	0.11	0.06	0.13	0.02	0.07
O=F,Cl	0.30	0.34	0.30	0.32	0.27	0.28	0.31	0.25
TOTAL	98.59	98.42	98.95	97.45	98.97	98.76	98.37	98.80
Si	6.6490	6.6845	6.7102	6.6546	6.7855	6.5951	6.6629	6.6712
Al	1.3510	1.3155	1.2898	1.3454	1.2145	1.4049	1.3371	1.3288
SUM T	8.0000	8.0000	8.0000	8.0000	8.0000	8.0000	8.0000	8.0000
Al	0.2313	0.3197	0.2191	0.2836	0.1816	0.2285	0.2455	0.3138
Ti	0.1458	0.0685	0.1388	0.0621	0.1254	0.1456	0.1406	0.0963
Fe ³⁺	0.2644	0.2766	0.2176	0.2795	0.2368	0.3125	0.2781	0.2623
V	0.0020	0.0048	0.0049	0.0088	0.0090	0.0000	0.0074	0.0053
Mg	2.6456	2.5612	2.6322	2.6089	2.8032	2.6015	2.5847	2.5574
Zn	0.0000	0.0061	0.0030	0.0124	0.0062	0.0140	0.0017	0.0078
Fe ²⁺	1.7109	1.7632	1.7844	1.7447	1.6379	1.6978	1.7422	1.7571
SUM C	5.0000	5.0000	5.0000	5.0000	5.0000	5.0000	5.0000	5.0000
Mn	0.0456	0.0595	0.0424	0.0462	0.0479	0.0568	0.0706	0.0558
Fe ²⁺	0.0300	0.0196	0.0196	0.0337	0.0198	0.0328	0.0089	0.0192
Ca	1.7742	1.7740	1.7853	1.8005	1.7882	1.7496	1.7317	1.7553
Sr	0.0000	0.0000	0.0000	0.0000	0.0000	0.0000	0.0000	0.0000
Na	0.1503	0.1469	0.1526	0.1195	0.1441	0.1608	0.1888	0.1697
SUM B	2.0000	2.0000	2.0000	2.0000	2.0000	2.0000	2.0000	2.0000
Na	0.4622	0.4742	0.4860	0.5141	0.4644	0.4781	0.4582	0.4795
K	0.2498	0.2500	0.2372	0.2546	0.2162	0.2553	0.2557	0.2450
SUM A	0.7121	0.7242	0.7232	0.7687	0.6805	0.7334	0.7139	0.7244
Si em fórmula	6.6105	6.6441	6.6783	6.6140	6.7504	6.5500	6.6224	6.6330
NaB	0.2361	0.2367	0.2232	0.2105	0.2210	0.2623	0.2789	0.2548
CaB	1.7639	1.7633	1.7768	1.7895	1.7790	1.7377	1.7211	1.7452
Ti	0.1449	0.0681	0.1382	0.0618	0.1247	0.1446	0.1397	0.0957
(Ca+Na)B	2.0000	2.0000	2.0000	2.0000	2.0000	2.0000	2.0000	2.0000
(Na+K)A	0.6213	0.6291	0.6485	0.6723	0.5994	0.6258	0.6183	0.6342
Mg/(Mg+Mn ²⁺)	0.9831	0.9773	0.9841	0.9826	0.9832	0.9786	0.9734	0.9787

Formula estrutural baseada em 23 oxigênios.

Tabela 8. Química mineral dos anfibólios estudados (continuação).

Rocha	Enclaves Microgranulares						
Amostra	Uru-09						
SiO ₂	45.07	45.94	45.06	44.79	45.58	45.21	45.21
TiO ₂	0.58	0.40	1.21	0.49	0.27	1.23	1.26
Al ₂ O ₃	9.16	8.88	9.23	9.59	9.31	8.82	8.54
FeO	16.52	15.86	15.48	16.66	15.57	16.14	15.44
MnO	0.30	0.38	0.27	0.38	0.34	0.36	0.44
MgO	11.70	12.13	12.23	11.54	11.90	12.00	12.52
CaO	11.12	10.91	11.16	11.09	11.12	11.07	11.20
Na ₂ O	2.08	2.03	2.29	2.03	1.98	1.95	2.09
K ₂ O	1.28	1.25	1.25	1.41	1.27	1.21	1.14
Cl	0.11	0.11	0.04	0.09	0.03	0.10	0.13
V ₂ O ₃	0.09	0.05	0.11	0.01	0.01	0.07	0.04
ZnO	0.00	0.00	0.00	0.10	0.11	0.00	0.00
O=F,Cl	0.34	0.31	0.30	0.26	0.29	0.35	0.29
TOTAL	98.42	98.30	98.72	98.48	97.86	98.60	98.33
Si	6.7080	6.7999	6.6643	6.6628	6.7791	6.7011	6.7042
Al	1.2920	1.2001	1.3357	1.3372	1.2209	1.2989	1.2958
SUM T	8.0000	8.0000	8.0000	8.0000	8.0000	8.0000	8.0000
Al	0.3152	0.3481	0.2726	0.3434	0.4105	0.2420	0.1965
Ti	0.0644	0.0448	0.1348	0.0545	0.0301	0.1366	0.1408
Fe ³⁺	0.2837	0.3035	0.2248	0.3148	0.2522	0.2982	0.2782
V	0.0110	0.0063	0.0128	0.0010	0.0008	0.0082	0.0051
Mg	2.5958	2.6776	2.6957	2.5593	2.6380	2.6521	2.7675
Zn	0.0000	0.0000	0.0000	0.0108	0.0124	0.0000	0.0000
Fe ²⁺	1.7299	1.6198	1.6593	1.7163	1.6561	1.6629	1.6119
SUM C	5.0000	5.0000	5.0000	5.0000	5.0000	5.0000	5.0000
Mn	0.0383	0.0470	0.0336	0.0483	0.0432	0.0453	0.0546
Fe ²⁺	0.0429	0.0399	0.0306	0.0419	0.0288	0.0401	0.0249
Ca	1.7732	1.7300	1.7673	1.7673	1.7712	1.7584	1.7789
Sr	0.0000	0.0000	0.0000	0.0000	0.0000	0.0000	0.0000
Na	0.1456	0.1830	0.1685	0.1425	0.1567	0.1562	0.1415
SUM B	2.0000	2.0000	2.0000	2.0000	2.0000	2.0000	2.0000
Na	0.4552	0.3990	0.4883	0.4438	0.4128	0.4054	0.4597
K	0.2438	0.2368	0.2360	0.2678	0.2411	0.2280	0.2162
SUM A	0.6990	0.6357	0.7243	0.7116	0.6539	0.6334	0.6759
Si em fórmula	6.6663	6.7547	6.6316	6.6169	6.7418	6.6574	6.6634
NaB	0.2378	0.2815	0.2413	0.2449	0.2385	0.2530	0.2319
CaB	1.7622	1.7185	1.7587	1.7551	1.7615	1.7470	1.7681
Ti	0.0640	0.0445	0.1342	0.0541	0.0299	0.1357	0.1399
(Ca+Na)B	2.0000	2.0000	2.0000	2.0000	2.0000	2.0000	2.0000
(Na+K)A	0.6015	0.5319	0.6471	0.6033	0.5676	0.5314	0.5805
Mg/(Mg+Mn ²⁺)	0.9855	0.9827	0.9877	0.9815	0.9839	0.9832	0.9806

Formula estrutural baseada em 23 oxigênios.

Tabela 8. Química mineral dos anfibólios estudados (continuação).

Rocha Amostra		Enclaves Microgranulares Uru-19			
SiO ₂	46.17	46.37	46.07	47.88	48.92
TiO ₂	0.37	0.78	0.89	0.55	0.21
Al ₂ O ₃	8.74	7.65	8.26	7.28	6.68
FeO	15.47	14.10	14.86	13.78	13.04
MnO	0.33	0.47	0.36	0.44	0.53
MgO	12.70	13.37	13.01	13.80	14.66
CaO	10.88	11.28	11.34	11.13	11.48
Na ₂ O	2.20	2.06	2.14	1.95	1.80
K ₂ O	1.22	1.19	1.08	0.96	0.82
Cl	0.05	0.13	0.09	0.03	0.04
V ₂ O ₃	0.02	0.07	0.10	0.10	0.00
ZnO	0.08	0.00	0.05	0.00	0.00
O=F,Cl	0.35	0.31	0.29	0.36	0.29
TOTAL	98.76	97.85	98.63	98.46	98.60
Si	6.7945	6.8705	6.8111	7.3286	6.8452
Al	1.2055	1.1295	1.1889	0.6714	1.1548
SUM T	8.0000	8.0000	8.0000	8.0000	8.0000
Al	0.3101	0.2064	0.1760	0.0843	0.1494
Ti	0.0408	0.0871	0.1070	0.0213	0.1568
Fe ³⁺	0.3247	0.2145	0.2367	0.0637	0.3843
V	0.0025	0.0084	0.0115	0.0118	0.0000
Mg	2.7863	2.9527	2.8670	3.1489	3.0575
Zn	0.0088	0.0002	0.0059	0.0000	0.0000
Fe ²⁺	1.5268	1.5307	1.5959	1.6358	1.2520
SUM C	5.0000	5.0000	5.0000	5.0000	5.0000
Mn	0.0409	0.0587	0.0511	0.0181	0.0502
Fe ²⁺	0.0522	0.0025	0.0165	0.0000	0.0602
Ca	1.7152	1.7902	1.7959	1.8248	1.7208
Sr	0.0073	0.0027	0.0028	0.0090	0.0045
Na	0.1843	0.1459	0.1337	0.1482	0.1642
SUM B	2.0000	2.0000	2.0000	2.0000	2.0000
Na	0.4424	0.4470	0.4800	0.4290	0.3251
K	0.2284	0.2249	0.2044	0.1882	0.1465
SUM A	0.6709	0.6719	0.6844	0.6173	0.4717
Si em fórmula	6.7462	6.8383	6.7759	7.3184	6.7875
NaB	0.2897	0.2155	0.2106	0.1688	0.2892
CaB	1.7030	1.7818	1.7866	1.8223	1.7063
Ti	0.0406	0.0866	0.1064	0.0213	0.1555
(Ca+Na)B	1.9927	1.9973	1.9972	1.9910	1.9955
(Na+K)A	0.5595	0.5985	0.6033	0.5956	0.3414
Mg/(Mg+Mn ²⁺)	0.9855	0.9805	0.9825	0.9836	0.9838

Formula estrutural baseada em 23 oxigênios.

Tabela 8. Química mineral dos anfíbólios estudados (continuação).

Rocha Amostra	Enclaves Microgranulares							
	Uru-23							
SiO ₂	45.29	46.60	44.87	45.98	43.88	43.56	44.81	42.60
TiO ₂	0.86	0.90	1.15	1.42	0.70	1.44	1.19	0.42
Al ₂ O ₃	8.48	7.94	8.87	8.45	9.54	9.50	8.55	10.54
FeO	15.78	15.80	16.76	16.84	17.52	17.23	16.75	18.00
MnO	0.40	0.31	0.20	0.22	0.39	0.32	0.44	0.39
MgO	12.08	12.47	11.64	11.86	11.12	10.86	11.68	10.55
CaO	10.99	11.07	11.02	10.45	10.97	10.85	11.08	10.98
Na ₂ O	2.12	2.15	2.10	2.12	2.20	2.10	1.92	2.36
K ₂ O	1.25	1.15	1.30	1.23	1.46	1.45	1.20	1.63
F	0.75	0.65	0.71	0.44	0.77	0.64	0.66	0.65
Cl	0.06	0.06	0.05	0.06	0.04	0.09	0.09	0.04
V ₂ O ₃	0.06	0.07	0.03	0.05	0.04	0.05	0.03	0.06
ZnO	0.01	0.01	0.12	0.00	0.07	0.08	0.08	0.00
SrO	0.00	0.02	0.00	0.16	0.00	0.00	0.12	0.07
O=F,Cl	0.33	0.29	0.31	0.20	0.33	0.29	0.30	0.28
TOTAL	97.80	98.90	98.50	99.07	98.37	97.87	98.29	98.01
Si	6.7647	6.8607	6.6819	6.7663	6.5830	6.5648	6.6915	6.4483
Al	1.2353	1.1393	1.3181	1.2337	1.4170	1.4352	1.3085	1.5517
SUM T	8.0000	8.0000	8.0000	8.0000	8.0000	8.0000	8.0000	8.0000
Al	0.2576	0.2385	0.2393	0.2314	0.2705	0.2527	0.1962	0.3282
Ti	0.0967	0.0993	0.1283	0.1566	0.0793	0.1630	0.1339	0.0476
Fe ³⁺	0.2595	0.2349	0.2846	0.3331	0.3424	0.2899	0.3114	0.3531
V	0.0073	0.0080	0.0038	0.0060	0.0049	0.0060	0.0038	0.0078
Mg	2.6898	2.7364	2.5851	2.6025	2.4881	2.4397	2.5998	2.3815
Zn	0.0011	0.0013	0.0130	0.0000	0.0079	0.0091	0.0084	0.0000
Fe ²⁺	1.6879	1.6815	1.7459	1.6703	1.8069	1.8395	1.7466	1.8819
SUM C	5.0000	5.0000	5.0000	5.0000	5.0000	5.0000	5.0000	5.0000
Mn	0.0509	0.0382	0.0247	0.0268	0.0497	0.0411	0.0557	0.0495
Fe ²⁺	0.0233	0.0289	0.0567	0.0687	0.0485	0.0419	0.0336	0.0437
Ca	1.7582	1.7462	1.7586	1.6482	1.7631	1.7516	1.7724	1.7809
Sr	0.0000	0.0017	0.0000	0.0133	0.0000	0.0000	0.0104	0.0064
Na	0.1677	0.1850	0.1599	0.2430	0.1387	0.1654	0.1280	0.1195
SUM B	2.0000	2.0000	2.0000	2.0000	2.0000	2.0000	2.0000	2.0000
Na	0.4468	0.4290	0.4473	0.3616	0.5006	0.4470	0.4291	0.5716
K	0.2382	0.2152	0.2464	0.2313	0.2787	0.2790	0.2282	0.3153
SUM A	0.6850	0.6442	0.6937	0.5929	0.7792	0.7260	0.6573	0.8869
Si em fórmula	6.7263	6.8255	6.6404	6.7169	6.5336	6.5232	6.6459	6.4024
NaB	0.2518	0.2610	0.2523	0.3506	0.2502	0.2595	0.2293	0.2254
CaB	1.7482	1.7373	1.7477	1.6362	1.7498	1.7405	1.7603	1.7683
Ti	0.0962	0.0988	0.1275	0.1555	0.0787	0.1620	0.1330	0.0473
(Ca+Na)B	2.0000	1.9983	2.0000	1.9868	2.0000	2.0000	1.9897	1.9936
(Na+K)A	0.5960	0.5639	0.5960	0.4791	0.6609	0.6262	0.5506	0.7739
Mg/(Mg+Mn ²⁺)	0.6499	0.6500	0.6306	0.6500	0.6226	0.6058	0.6397	0.5988

Formula estrutural baseada em 23 oxigênios.

Tabela 8. Química mineral dos anfibólios estudados (continuação).

Rocha	Enclaves Microgranulares							
Amostra	Uru-23							
SiO ₂	42.65	43.85	45.44	44.63	43.54	44.64	43.38	45.94
TiO ₂	0.65	1.86	1.62	1.04	0.93	1.61	0.50	0.49
Al ₂ O ₃	10.62	8.87	8.75	9.08	9.70	8.69	10.29	8.66
FeO	18.03	17.52	16.06	16.93	17.26	17.11	17.57	16.38
MnO	0.50	0.28	0.46	0.44	0.52	0.36	0.30	0.35
MgO	10.39	10.88	11.91	11.49	11.13	11.35	10.97	12.09
CaO	11.05	11.05	10.89	10.77	10.81	10.91	10.88	11.07
Na ₂ O	2.17	2.08	2.20	2.17	2.24	1.93	2.19	2.10
K ₂ O	1.63	1.24	1.22	1.34	1.45	1.36	1.54	1.28
F	0.67	0.62	0.64	0.68	0.62	0.65	0.76	0.73
Cl	0.10	0.09	0.08	0.05	0.05	0.08	0.05	0.03
V ₂ O ₃	0.06	0.05	0.10	0.06	0.05	0.10	0.08	0.02
ZnO	0.01	0.09	0.07	0.11	0.02	0.18	0.00	0.00
SrO	0.03	0.00	0.00	0.00	0.00	0.03	0.13	0.07
O=F,Cl	0.30	0.28	0.29	0.30	0.27	0.29	0.33	0.32
TOTAL	98.26	98.19	99.13	98.48	98.04	98.69	98.31	98.91
Si	6.4426	6.5956	6.7008	6.6515	6.5443	6.6526	6.5148	6.7864
Al	1.5574	1.4044	1.2992	1.3485	1.4557	1.3474	1.4852	1.2136
SUM T	8.0000	8.0000	8.0000	8.0000	8.0000	8.0000	8.0000	8.0000
Al	0.3340	0.1686	0.2211	0.2458	0.2620	0.1783	0.3358	0.2940
Ti	0.0742	0.2100	0.1794	0.1167	0.1049	0.1804	0.0563	0.0548
Fe ³⁺	0.3411	0.2570	0.2611	0.3443	0.3599	0.3119	0.3637	0.2847
V	0.0076	0.0058	0.0112	0.0066	0.0059	0.0119	0.0101	0.0026
Mg	2.3397	2.4396	2.6177	2.5529	2.4934	2.5219	2.4564	2.6634
Zn	0.0011	0.0101	0.0073	0.0116	0.0021	0.0193	0.0000	0.0000
Fe ²⁺	1.9023	1.9090	1.7021	1.7221	1.7718	1.7763	1.7777	1.7005
SUM C	5.0000	5.0000	5.0000	5.0000	5.0000	5.0000	5.0000	5.0000
Mn	0.0635	0.0354	0.0578	0.0550	0.0656	0.0454	0.0387	0.0432
Fe ²⁺	0.0344	0.0380	0.0168	0.0438	0.0378	0.0439	0.0658	0.0383
Ca	1.7875	1.7805	1.7200	1.7190	1.7407	1.7417	1.7503	1.7522
Sr	0.0026	0.0000	0.0000	0.0000	0.0000	0.0029	0.0109	0.0063
Na	0.1120	0.1460	0.2054	0.1822	0.1560	0.1661	0.1344	0.1600
SUM B	2.0000	2.0000	2.0000	2.0000	2.0000	2.0000	2.0000	2.0000
Na	0.5238	0.4605	0.4227	0.4456	0.4953	0.3927	0.5018	0.4417
K	0.3145	0.2385	0.2297	0.2549	0.2788	0.2578	0.2956	0.2412
SUM A	0.8383	0.6991	0.6524	0.7006	0.7740	0.6505	0.7974	0.6829
Si em fórmula	6.3945	6.5586	6.6625	6.6014	6.4927	6.6072	6.4629	6.7441
NaB	0.2233	0.2295	0.2898	0.2940	0.2730	0.2674	0.2529	0.2525
CaB	1.7741	1.7705	1.7102	1.7060	1.7270	1.7298	1.7363	1.7413
Ti	0.0736	0.2088	0.1783	0.1158	0.1041	0.1792	0.0558	0.0544
(Ca+Na)B	1.9974	2.0000	2.0000	2.0000	2.0000	1.9972	1.9892	1.9938
(Na+K)A	0.7199	0.6109	0.5630	0.5822	0.6497	0.5437	0.6715	0.5852
Mg/(Mg+Mn ²⁺)	0.5953	0.5912	0.6428	0.6432	0.6333	0.6264	0.6250	0.6474

Formula estrutural baseada em 23 oxigênios.

Tabela 8. Química mineral dos anfibólios estudados (continuação).

Rocha	Enclaves Microgranulares						
Amostra	Uru-33						
SiO ₂	45.44	45.26	43.76	45.06	44.78	45.23	45.10
TiO ₂	0.56	0.41	0.66	1.35	1.17	0.45	0.84
Al ₂ O ₃	8.79	8.89	8.85	9.64	8.96	9.04	9.17
FeO	16.65	17.04	17.36	17.28	16.23	16.74	17.36
MnO	0.29	0.43	0.32	0.41	0.35	0.49	0.51
MgO	11.91	11.57	11.51	11.25	12.28	11.57	11.67
CaO	10.64	10.67	10.78	10.79	10.84	10.96	11.05
Na ₂ O	2.16	2.46	2.30	2.24	2.46	2.24	2.05
K ₂ O	1.27	1.22	1.29	1.38	1.15	1.32	1.36
F	0.69	0.63	0.62	0.61	0.57	0.61	0.57
Cl	0.02	0.12	0.04	0.09	0.09	0.06	0.05
V ₂ O ₃	0.06	0.07	0.04	0.01	0.01	0.05	0.00
ZnO	0.14	0.09	0.22	0.14	0.02	0.16	0.05
SrO	0.01	0.08	0.00	0.01	0.00	0.14	0.07
O=F,Cl	0.29	0.29	0.27	0.28	0.26	0.27	0.25
TOTAL	98.32	98.64	97.47	99.96	98.62	98.79	99.60
Si	6.7458	6.7327	6.6107	6.6197	6.6346	6.7211	6.6474
Al	1.2542	1.2673	1.3893	1.3803	1.3654	1.2789	1.3526
SUM T	8.0000	8.0000	8.0000	8.0000	8.0000	8.0000	8.0000
Al	0.2834	0.2907	0.1866	0.2889	0.1985	0.3044	0.2396
Ti	0.0626	0.0460	0.0745	0.1493	0.1304	0.0505	0.0932
Fe ³⁺	0.3759	0.3301	0.4047	0.3169	0.3440	0.2916	0.3714
V	0.0067	0.0081	0.0048	0.0008	0.0008	0.0056	0.0005
Mg	2.6366	2.5665	2.5926	2.4629	2.7128	2.5630	2.5639
Zn	0.0153	0.0102	0.0241	0.0149	0.0022	0.0179	0.0058
Fe ²⁺	1.6195	1.7484	1.7127	1.7663	1.6113	1.7670	1.7256
SUM C	5.0000	5.0000	5.0000	5.0000	5.0000	5.0000	5.0000
Mn	0.0365	0.0537	0.0406	0.0509	0.0435	0.0613	0.0639
Fe ²⁺	0.0715	0.0410	0.0759	0.0399	0.0551	0.0222	0.0428
Ca	1.6924	1.7009	1.7454	1.6984	1.7207	1.7450	1.7445
Sr	0.0004	0.0066	0.0000	0.0005	0.0000	0.0121	0.0060
Na	0.1992	0.1978	0.1382	0.2103	0.1806	0.1595	0.1428
SUM B	2.0000	2.0000	2.0000	2.0000	2.0000	2.0000	2.0000
Na	0.4216	0.5128	0.5346	0.4269	0.5254	0.4853	0.4421
K	0.2405	0.2313	0.2476	0.2584	0.2164	0.2504	0.2553
SUM A	0.6621	0.7442	0.7822	0.6853	0.7419	0.7357	0.6974
Si em fórmula	6.6903	6.6841	6.5521	6.5738	6.5846	6.6782	6.5933
NaB	0.3211	0.3048	0.2701	0.3129	0.2923	0.2541	0.2637
CaB	1.6785	1.6886	1.7299	1.6866	1.7077	1.7339	1.7303
Ti	0.0621	0.0457	0.0739	0.1483	0.1294	0.0502	0.0925
(Ca+Na)B	1.9996	1.9934	2.0000	1.9995	2.0000	1.9880	1.9941
(Na+K)A	0.5331	0.6304	0.6421	0.5765	0.6233	0.6353	0.5696
Mg/(Mg+Mn ²⁺)	0.6683	0.6383	0.6532	0.6239	0.6731	0.6318	0.6483

Formula estrutural baseada em 23 oxigênios.

Tabela 8. Química mineral dos anfibólios estudados (continuação).

Rocha	Quartzo sienito		
Amostra	Uru-49	Uru-25	
SiO ₂	55.27	54.88	56.07
TiO ₂	0.06	0.36	0.00
Al ₂ O ₃	1.34	1.63	1.16
FeO	11.05	10.00	10.57
MnO	0.43	0.36	0.38
MgO	16.88	17.09	17.71
CaO	11.31	11.43	11.43
Na ₂ O	0.93	1.28	0.78
K ₂ O	0.17	0.30	0.18
F	0.00	0.00	0.00
Cl	0.01	0.01	0.00
ZnO	0.06	0.00	0.10
SrO	0.10	0.00	0.10
O=F,Cl	0.00	0.00	0.00
TOTAL	97.79	97.41	98.47
Si	7.8599	7.8262	7.8901
Al	0.1401	0.1738	0.1099
Ti	0.0000	0.0000	0.0000
SUM T	8.0000	8.0000	8.0000
Al	0.0846	0.1006	0.0818
Ti	0.0066	0.0390	0.0000
Fe ³⁺	0.1478	0.0561	0.1270
Mg	3.5791	3.6326	3.7156
Zn	0.0059	0.0000	0.0099
Fe ²⁺	1.1546	1.1368	1.0657
SUM C	5.0000	5.0000	5.0000
Mn	0.0517	0.0159	0.0452
Fe ²⁺	0.0113	0.0000	0.0509
Ca	1.7225	1.7461	1.7233
Na	0.2065	0.2380	0.1723
SUM B	2.0000	2.0000	2.0000
Na	0.0485	0.1158	0.0416
K	0.0310	0.0542	0.0318
SUM A	0.0795	0.1700	0.0734
Si em fórmula	7.8345	7.8166	7.8682
NaB	0.2542	0.2561	0.2133
CaB	1.7170	1.7439	1.7185
Ti	0.0066	0.0390	0.0000
(Ca+Na)B	1.9711	2.0000	1.9318
(Na+K)A	0.0309	0.1515	0.0317
Mg/(Mg+Fe ²⁺)	0.7787	0.7707	0.7898
			0.8011

Tabela 9. Química mineral dos clinopiroxênios estudados (continuação).

Rocha	Álcali-feldspato sienito				
Amostra	Uru-47		Uru-49		
	Centro Cpx				Centro Cpx
SiO ₂	54.06	53.28	53.35	54.05	53.61
TiO ₂	0.08	0.04	0.25	0.19	0.24
Al ₂ O ₃	1.18	0.96	0.94	1.18	0.99
FeO	9.99	9.66	11.00	9.81	9.13
MnO	0.50	0.46	0.40	0.35	0.43
MgO	13.35	12.92	11.38	12.30	13.16
CaO	18.68	20.19	19.15	19.57	19.67
Na ₂ O	1.98	1.82	2.53	2.47	1.85
Total	99.82	99.33	99.00	99.92	99.08
Ti	0.0023	0.0011	0.0071	0.0054	0.0066
Al	0.0515	0.0280	0.0417	0.0500	0.0431
Fe ³⁺	0.0828	0.1153	0.1235	0.1179	0.0778
Fe ²⁺	0.2027	0.1760	0.2130	0.1776	0.1923
Mg	0.6591	0.6796	0.6122	0.6492	0.6801
Sum M1	1.00	1.00	1.00	1.00	1.00
ideal	1.00	1.00	1.00	1.00	1.00
Fe ²⁺	0.0238	0.0099	0.0086	0.0079	0.0146
Mn	0.0157	0.0146	0.0127	0.0109	0.0137
Mg	0.0775	0.0382	0.0246	0.0289	0.0516
Ca	0.7410	0.8061	0.7699	0.7753	0.7863
Na	0.1420	0.1313	0.1843	0.1770	0.1339
Sum M2	1.00	1.00	1.00	1.00	1.00
ideal	1.00	1.00	1.00	1.00	1.00
Si	2.0016	1.9858	2.0024	1.9984	1.9996
Al	0.0000	0.0142	0.0000	0.0016	0.0004
Sum T	2.00	2.00	2.00	2.00	2.00
ideal	2.00	2.00	2.00	2.00	2.00
Wo	41.46	44.17	43.95	44.13	43.62
En	41.22	39.33	36.35	38.60	40.59
Fs	17.31	16.50	19.70	17.27	15.79

Fórmula estrutural calculada na base de 11 oxigênios.

Tabela 10. Química mineral das flogopitas estudadas (continuação).

Rock Sample	Enclaves Microgranulares Uru-33					Enclaves Microgranulares Uru-42				
	SiO ₂	38.49	38.61	39.02	38.68	38.52	38.85	38.49	38.61	39.33
TiO ₂	1.46	1.16	1.72	1.40	0.82	1.43	1.73	1.38	1.16	
Al ₂ O ₃	13.80	14.02	13.45	14.18	14.41	14.13	13.80	14.48	14.22	
FeO	16.55	16.79	16.11	16.74	16.97	16.02	16.95	16.97	16.41	
MnO	0.37	0.29	0.21	0.37	0.31	0.43	0.19	0.31	0.28	
MgO	14.80	14.64	15.30	14.28	14.61	14.79	15.04	14.00	14.82	
CaO	0.07	0.08	0.05	0.06	0.04	0.05	0.05	0.02	0.00	
Na ₂ O	0.19	0.14	0.07	0.13	0.09	0.03	0.10	0.09	0.05	
K ₂ O	9.75	9.89	9.71	9.79	9.96	10.03	9.89	9.71	9.70	
SrO	0.00	0.00	0.02	0.00	0.00	0.00	0.00	0.00	0.03	
ZnO	0.08	0.07	0.06	0.08	0.00	0.18	0.04	0.18	0.06	
Cl	0.07	0.07	0.08	0.11	0.08	0.14	0.11	0.09	0.15	
Li ₂ O*	1.50	1.53	1.65	1.55	1.50	1.60	1.49	1.53	1.74	
H ₂ O*	4.05	4.06	4.08	4.05	4.05	4.06	4.07	4.06	4.09	
O=F,Cl	0.02	0.02	0.02	0.03	0.02	0.03	0.02	0.02	0.03	
Total	101.14	101.32	101.50	101.41	101.34	101.70	101.93	101.40	101.99	
Si	5.67	5.68	5.70	5.68	5.67	5.68	5.64	5.67	5.72	
Al ^{IV}	2.33	2.32	2.30	2.32	2.33	2.32	2.36	2.33	2.28	
Al ^{VI}	0.07	0.11	0.02	0.14	0.17	0.12	0.02	0.18	0.15	
Ti	0.16	0.13	0.19	0.15	0.09	0.16	0.19	0.15	0.13	
Fe	2.04	2.07	1.97	2.06	2.09	1.96	2.08	2.09	1.99	
Mn	0.05	0.04	0.03	0.05	0.04	0.05	0.02	0.04	0.03	
Mg	3.25	3.21	3.33	3.13	3.20	3.22	3.28	3.07	3.21	
Zn	0.01	0.01	0.01	0.01	0.00	0.02	0.00	0.02	0.01	
Li*	0.89	0.90	0.97	0.92	0.89	0.94	0.88	0.90	1.02	
Ca	0.01	0.01	0.01	0.01	0.01	0.01	0.01	0.00	0.00	
Na	0.05	0.04	0.02	0.04	0.02	0.01	0.03	0.03	0.01	
K	1.83	1.86	1.81	1.84	1.87	1.87	1.85	1.82	1.80	
Al total	2.40	2.43	2.32	2.45	2.50	2.43	2.38	2.51	2.44	
Fe/Fe+Mg	0.39	0.39	0.37	0.40	0.39	0.38	0.39	0.40	0.38	

Fórmula estrutural calculada na base de 11 oxigênios.

Tabela 10. Química mineral das flogopitas estudadas (continuação).

Rock Sample	Enclaves Microgranulares Uru-42								Enclaves Microgranulares Uru-09					
SiO ₂	40.50	38.85	38.91	39.02	38.91	38.91	39.18	39.03	38.83	38.95	38.50	38.97	38.77	38.84
TiO ₂	1.40	1.49	1.07	1.78	1.04	1.11	1.13	1.35	1.51	1.27	1.15	1.11	1.30	1.26
Al ₂ O ₃	14.90	14.14	14.63	14.33	14.25	14.13	14.21	13.95	14.06	14.29	14.51	14.90	14.39	14.22
FeO	15.30	16.74	15.87	16.44	16.24	15.99	16.20	15.56	16.52	16.06	16.09	16.00	15.95	16.18
MnO	0.39	0.40	0.29	0.27	0.17	0.80	0.24	0.15	0.27	0.33	0.41	0.30	0.19	0.25
MgO	14.33	14.79	14.78	13.69	14.99	14.80	14.86	15.32	14.51	14.96	14.80	14.47	15.17	14.72
CaO	0.20	0.02	0.00	0.05	0.11	0.10	0.04	0.04	0.00	0.01	0.02	0.01	0.00	0.00
Na ₂ O	0.22	0.07	0.11	0.06	0.25	0.46	0.08	0.11	0.02	0.15	0.06	0.11	0.09	0.10
K ₂ O	8.63	9.77	10.12	9.94	9.67	9.52	9.88	9.73	9.88	9.79	9.77	9.69	9.75	10.04
SrO	0.01	0.08	0.00	0.00	0.00	0.00	0.00	0.01	0.06	0.04	0.04	0.01	0.01	0.00
ZnO	0.08	0.05	0.00	0.00	0.14	0.26	0.09	0.06	0.14	0.06	0.00	0.08	0.12	0.00
Cl	0.15	0.15	0.09	0.10	0.19	0.22	0.06	0.13	0.11	0.11	0.09	0.09	0.09	0.09
Li ₂ O*	2.07	1.60	1.62	1.65	1.61	1.62	1.69	1.65	1.59	1.63	1.50	1.63	1.58	1.60
H ₂ O*	4.16	4.08	4.08	4.07	4.05	4.05	4.10	4.07	4.06	4.08	4.05	4.09	4.08	4.07
O=F,Cl	0.03	0.03	0.02	0.02	0.04	0.05	0.01	0.03	0.02	0.02	0.02	0.02	0.02	0.02
Total	102.31	102.18	101.55	101.37	101.58	101.91	101.75	101.11	101.54	101.70	100.98	101.45	101.46	101.34
Si	5.78	5.66	5.68	5.72	5.69	5.68	5.71	5.71	5.69	5.68	5.66	5.69	5.66	5.69
Al ^{iv}	2.22	2.34	2.32	2.28	2.31	2.32	2.29	2.29	2.31	2.32	2.34	2.31	2.34	2.31
Al ^{vi}	0.29	0.09	0.20	0.19	0.14	0.11	0.15	0.11	0.12	0.14	0.18	0.25	0.14	0.15
Ti	0.15	0.16	0.12	0.20	0.11	0.12	0.12	0.15	0.17	0.14	0.13	0.12	0.14	0.14
Fe	1.83	2.04	1.94	2.01	1.99	1.95	1.97	1.90	2.02	1.96	1.98	1.95	1.95	1.98
Mn	0.05	0.05	0.04	0.03	0.02	0.10	0.03	0.02	0.03	0.04	0.05	0.04	0.02	0.03
Mg	3.05	3.21	3.22	2.99	3.27	3.22	3.23	3.34	3.17	3.25	3.25	3.15	3.30	3.22
Zn	0.01	0.01	0.00	0.00	0.02	0.03	0.01	0.01	0.02	0.01	0.00	0.01	0.01	0.00
Li*	1.19	0.94	0.95	0.97	0.95	0.95	0.99	0.97	0.94	0.95	0.88	0.96	0.93	0.94
Ca	0.03	0.00	0.00	0.01	0.02	0.02	0.01	0.01	0.00	0.00	0.00	0.00	0.00	0.00
Na	0.06	0.02	0.03	0.02	0.07	0.13	0.02	0.03	0.01	0.04	0.02	0.03	0.03	0.03
K	1.57	1.82	1.88	1.86	1.80	1.77	1.84	1.81	1.85	1.82	1.83	1.80	1.82	1.88
Al total	2.51	2.43	2.52	2.47	2.46	2.43	2.44	2.41	2.43	2.46	2.51	2.56	2.48	2.46
Fe/Fe+Mg	0.37	0.39	0.38	0.40	0.38	0.38	0.38	0.36	0.39	0.38	0.38	0.37	0.37	0.38

Fórmula estrutural calculada na base de 11 oxigênios.

Tabela 10. Química mineral das flogopitas estudadas (continuação).

Rock Sample	Enclaves Microgranulares							
	Uru-09							
SiO ₂	38.70	38.96	39.43	39.58	39.47	39.12	39.06	38.55
TiO ₂	1.18	1.05	1.03	0.92	1.29	0.99	1.03	1.77
Al ₂ O ₃	14.55	14.43	14.13	14.14	14.49	14.08	14.10	13.77
FeO	15.43	15.89	16.13	15.26	14.89	15.40	15.56	16.05
MnO	0.24	0.21	0.20	0.36	0.27	0.16	0.23	0.33
MgO	15.02	14.85	15.13	15.62	15.40	15.17	15.36	14.80
CaO	0.06	0.04	0.00	0.05	0.04	0.06	0.00	0.02
Na ₂ O	0.11	0.11	0.09	0.21	0.14	0.08	0.06	0.07
K ₂ O	9.84	9.89	9.76	9.81	9.78	9.86	9.70	10.11
SrO	0.07	0.03	0.00	0.00	0.00	0.02	0.04	0.00
ZnO	0.03	0.00	0.09	0.02	0.07	0.00	0.01	0.17
Cl	0.09	0.11	0.10	0.12	0.10	0.11	0.11	0.12
Li ₂ O*	1.56	1.63	1.76	1.81	1.77	1.68	1.66	1.51
H ₂ O*	4.07	4.07	4.10	4.11	4.12	4.06	4.07	4.05
O=F,Cl	0.02	0.02	0.02	0.03	0.02	0.03	0.02	0.03
Total	100.91	101.22	101.95	101.98	101.82	100.76	100.95	101.29
Si	5.68	5.70	5.72	5.73	5.71	5.74	5.72	5.67
Al iv	2.32	2.30	2.28	2.27	2.29	2.26	2.28	2.33
Al vi	0.19	0.19	0.14	0.14	0.18	0.17	0.15	0.06
Ti	0.13	0.12	0.11	0.10	0.14	0.11	0.11	0.20
Fe	1.89	1.94	1.96	1.85	1.80	1.89	1.90	1.97
Mn	0.03	0.03	0.02	0.04	0.03	0.02	0.03	0.04
Mg	3.28	3.24	3.27	3.37	3.32	3.31	3.35	3.24
Zn	0.00	0.00	0.01	0.00	0.01	0.00	0.00	0.02
Li*	0.92	0.96	1.03	1.05	1.03	0.99	0.98	0.89
Ca	0.01	0.01	0.00	0.01	0.01	0.01	0.00	0.00
Na	0.03	0.03	0.03	0.06	0.04	0.02	0.02	0.02
K	1.84	1.85	1.81	1.81	1.80	1.84	1.81	1.90
Al total	2.52	2.49	2.42	2.41	2.47	2.43	2.43	2.39
Fe/Fe+Mg	0.37	0.38	0.37	0.35	0.35	0.36	0.36	0.38

Fórmula estrutural calculada na base de 11 oxigênios.

Tabela 10. Química mineral das flogopitas estudadas (continuação).

Rock Sample	Quartzo sienito Uru-37											
SiO ₂	38.39	39.34	39.08	38.80	39.24	38.62	38.43	38.37	39.55	38.97	39.18	38.55
TiO ₂	1.04	0.85	1.22	1.34	1.22	1.00	1.38	1.58	1.03	0.92	1.55	1.53
Al ₂ O ₃	14.23	13.63	14.01	14.04	13.99	13.80	14.30	14.39	13.79	13.97	13.90	14.00
FeO	16.91	16.48	16.69	16.69	15.87	16.45	16.76	16.95	16.34	16.29	16.53	15.62
MnO	0.32	0.21	0.31	0.42	0.30	0.33	0.30	0.25	0.31	0.29	0.32	0.27
MgO	13.94	14.70	14.44	14.66	14.77	14.52	14.38	14.24	14.77	14.40	14.45	14.71
CaO	0.00	0.07	0.02	0.08	0.05	0.06	0.04	0.10	0.02	0.06	0.00	0.00
Na ₂ O	0.13	0.12	0.07	0.25	0.11	0.24	0.09	0.12	0.21	0.18	0.11	0.06
K ₂ O	9.82	9.88	9.95	9.60	10.06	9.78	9.68	9.99	9.94	9.38	9.78	9.80
SrO	0.00	0.00	0.05	0.00	0.00	0.05	0.00	0.09	0.00	0.04	0.08	0.04
ZnO	0.23	0.00	0.11	0.09	0.13	0.08	0.04	0.00	0.00	0.16	0.09	0.09
Cl	0.06	0.16	0.11	0.14	0.08	0.23	0.11	0.09	0.17	0.12	0.10	0.09
Li ₂ O*	1.47	1.74	1.66	1.58	1.71	1.53	1.48	1.46	1.80	1.63	1.69	1.51
H ₂ O*	4.02	4.05	4.07	4.06	4.09	3.99	4.04	4.06	4.08	4.03	4.08	4.03
O=F,Cl	0.01	0.03	0.03	0.03	0.02	0.05	0.02	0.02	0.04	0.03	0.02	0.02
Total	100.54	101.20	101.75	101.72	101.60	100.63	100.99	101.65	101.95	100.40	101.83	100.30
Si	5.70	5.77	5.72	5.68	5.73	5.72	5.67	5.64	5.76	5.75	5.72	5.70
Al ^{IV}	2.30	2.23	2.28	2.32	2.27	2.28	2.33	2.36	2.24	2.25	2.28	2.30
Al ^{VI}	0.19	0.13	0.13	0.10	0.14	0.13	0.15	0.13	0.12	0.19	0.11	0.14
Ti	0.12	0.09	0.13	0.15	0.13	0.11	0.15	0.17	0.11	0.10	0.17	0.17
Fe	2.10	2.02	2.04	2.04	1.94	2.04	2.07	2.08	1.99	2.01	2.02	1.93
Mn	0.04	0.03	0.04	0.05	0.04	0.04	0.04	0.03	0.04	0.04	0.04	0.03
Mg	3.08	3.22	3.15	3.20	3.21	3.21	3.16	3.12	3.20	3.17	3.14	3.24
Zn	0.03	0.00	0.01	0.01	0.01	0.01	0.00	0.00	0.00	0.02	0.01	0.01
Li*	0.88	1.03	0.98	0.93	1.00	0.91	0.88	0.86	1.05	0.97	0.99	0.90
Ca	0.00	0.01	0.00	0.01	0.01	0.01	0.01	0.01	0.00	0.01	0.00	0.00
Na	0.04	0.03	0.02	0.07	0.03	0.07	0.03	0.03	0.06	0.05	0.03	0.02
K	1.86	1.85	1.86	1.79	1.87	1.85	1.82	1.87	1.85	1.77	1.82	1.85
Al total	2.49	2.36	2.41	2.42	2.41	2.41	2.48	2.49	2.37	2.43	2.39	2.44
Fe/Fe+Mg	0.40	0.39	0.39	0.39	0.38	0.39	0.40	0.40	0.38	0.39	0.39	0.37

Fórmula estrutural calculada na base de 11 oxigênios.

Tabela 10. Química mineral das flogopitas estudadas (continuação).

Rock Sample	Enclaves Microgranulares Uru-23									
	SiO ₂	39.03	39.23	39.17	38.94	39.29	38.65	38.90	38.98	38.45
TiO ₂	1.16	1.18	1.11	1.70	0.98	0.98	1.26	1.36	1.86	
Al ₂ O ₃	14.51	14.24	14.24	14.29	14.32	14.19	14.15	13.70	14.06	
FeO	15.57	15.43	15.39	15.88	16.18	16.58	16.53	17.21	15.50	
MnO	0.17	0.24	0.33	0.31	0.24	0.27	0.24	0.25	0.23	
MgO	14.63	15.50	15.07	14.26	14.29	14.91	14.41	13.56	14.49	
CaO	0.05	0.12	0.05	0.16	0.16	0.03	0.02	0.04	0.04	
Na ₂ O	0.09	0.08	0.00	0.21	0.10	0.14	0.09	0.08	0.11	
K ₂ O	9.63	9.48	9.89	8.19	9.13	9.93	10.04	9.85	9.76	
SrO	0.08	0.07	0.04	0.00	0.00	0.00	0.05	0.00	0.05	
ZnO	0.11	0.10	0.02	0.02	0.16	0.17	0.12	0.15	0.03	
Cl	0.10	0.14	0.11	0.14	0.13	0.11	0.11	0.21	0.14	
Li ₂ O*	1.65	1.71	1.69	1.62	1.72	1.54	1.61	1.64	1.48	
H ₂ O*	4.07	4.09	4.08	4.04	4.06	4.06	4.06	4.00	4.02	
O=F,Cl	0.02	0.03	0.03	0.03	0.03	0.02	0.02	0.05	0.03	
Total	100.81	101.56	101.16	99.72	100.73	101.54	101.56	100.97	100.17	
Si	5.72	5.70	5.72	5.73	5.76	5.67	5.70	5.76	5.69	
Al ^{IV}	2.28	2.30	2.28	2.27	2.24	2.33	2.30	2.24	2.31	
Al ^{VI}	0.22	0.14	0.17	0.22	0.23	0.13	0.15	0.15	0.14	
Ti	0.13	0.13	0.12	0.19	0.11	0.11	0.14	0.15	0.21	
Fe	1.91	1.88	1.88	1.96	1.98	2.03	2.03	2.13	1.92	
Mn	0.02	0.03	0.04	0.04	0.03	0.03	0.03	0.03	0.03	
Mg	3.19	3.36	3.28	3.13	3.12	3.26	3.15	2.99	3.20	
Zn	0.01	0.01	0.00	0.00	0.02	0.02	0.01	0.02	0.00	
Li*	0.97	1.00	0.99	0.96	1.02	0.91	0.95	0.97	0.88	
Ca	0.01	0.02	0.01	0.03	0.03	0.01	0.00	0.01	0.01	
Na	0.02	0.02	0.00	0.06	0.03	0.04	0.03	0.02	0.03	
K	1.80	1.76	1.84	1.54	1.71	1.86	1.88	1.86	1.84	
Al total	2.51	2.44	2.45	2.48	2.47	2.45	2.44	2.39	2.45	
Fe/Fe+Mg	0.37	0.36	0.36	0.38	0.39	0.38	0.39	0.42	0.38	

Fórmula estrutural calculada na base de 11 oxigênios.

Tabela 10. Química mineral das flogopitas estudadas (continuação).

Rock Sample	Enclaves Microgranulares Uru-23										
	SiO ₂	38.62	38.14	39.46	38.87	38.56	39.26	39.15	38.95	39.14	38.47
TiO ₂	1.16	0.77	1.41	1.45	1.23	0.75	1.22	1.55	0.90	1.31	
Al ₂ O ₃	14.48	14.18	14.25	14.39	14.37	14.16	13.95	14.43	14.21	14.57	
FeO	15.31	16.70	16.03	16.81	16.66	15.72	15.31	16.18	16.03	16.18	
MnO	0.34	0.26	0.22	0.24	0.30	0.34	0.07	0.13	0.15	0.32	
MgO	15.47	14.51	14.44	14.05	14.73	15.61	14.59	14.65	14.77	14.98	
CaO	0.03	0.07	0.00	0.01	0.00	0.05	0.03	0.05	0.00	0.04	
Na ₂ O	0.08	0.29	0.05	0.09	0.06	0.10	0.04	0.09	0.07	0.09	
K ₂ O	10.14	9.59	9.91	10.00	10.14	9.99	9.94	9.79	10.14	10.02	
SrO	0.05	0.00	0.07	0.00	0.00	0.00	0.05	0.00	0.02	0.11	
ZnO	0.05	0.00	0.04	0.03	0.03	0.00	0.00	0.15	0.05	0.05	
Cl	0.10	0.14	0.13	0.14	0.15	0.11	0.12	0.10	0.12	0.07	
Li ₂ O*	1.53	1.39	1.77	1.60	1.52	1.71	1.68	1.63	1.68	1.49	
H ₂ O*	4.07	3.99	4.09	4.06	4.05	4.10	4.04	4.09	4.07	4.08	
O=F,Cl	0.02	0.03	0.03	0.03	0.03	0.02	0.03	0.02	0.03	0.01	
Total	101.39	100.01	101.84	101.71	101.77	101.87	100.17	101.75	101.31	101.76	
Si	5.65	5.68	5.74	5.69	5.65	5.71	5.77	5.68	5.73	5.63	
Al ^{IV}	2.35	2.32	2.26	2.31	2.35	2.29	2.23	2.32	2.27	2.37	
Al ^{VI}	0.14	0.18	0.18	0.17	0.13	0.13	0.19	0.15	0.18	0.14	
Ti	0.13	0.09	0.15	0.16	0.14	0.08	0.14	0.17	0.10	0.14	
Fe	1.87	2.08	1.95	2.06	2.04	1.91	1.89	1.97	1.96	1.98	
Mn	0.04	0.03	0.03	0.03	0.04	0.04	0.01	0.02	0.02	0.04	
Mg	3.37	3.22	3.13	3.07	3.22	3.38	3.21	3.18	3.22	3.27	
Zn	0.01	0.00	0.00	0.00	0.00	0.00	0.00	0.02	0.01	0.01	
Li*	0.90	0.84	1.04	0.94	0.89	1.00	1.00	0.95	0.99	0.88	
Ca	0.00	0.01	0.00	0.00	0.00	0.01	0.00	0.01	0.00	0.01	
Na	0.02	0.08	0.01	0.03	0.02	0.03	0.01	0.02	0.02	0.02	
K	1.89	1.82	1.84	1.87	1.90	1.85	1.87	1.82	1.89	1.87	
Al total	2.50	2.49	2.44	2.48	2.48	2.43	2.42	2.48	2.45	2.51	
Fe/Fe+Mg	0.36	0.39	0.38	0.40	0.39	0.36	0.37	0.38	0.38	0.38	

Fórmula estrutural calculada na base de 11 oxigênios.

Tabela 10. Química mineral das flogopitas estudadas (continuação).

Rock Sample	Enclaves Microgranulares										
	Uru-36										
SiO ₂	38.79	38.62	38.88	38.56	38.43	39.23	39.17	39.35	38.61	38.45	
TiO ₂	1.60	1.04	1.10	2.03	1.69	1.74	1.24	1.48	1.38	1.50	
Al ₂ O ₃	14.09	14.56	14.56	14.29	13.81	13.97	14.32	14.40	14.42	14.59	
FeO	16.16	15.34	16.34	16.42	15.91	15.97	15.70	15.32	16.21	16.43	
MnO	0.14	0.18	0.20	0.21	0.17	0.28	0.38	0.17	0.47	0.32	
MgO	15.04	15.37	15.09	14.51	14.44	14.88	14.51	14.88	14.80	14.64	
CaO	0.03	0.02	0.02	0.00	0.06	0.06	0.08	0.06	0.03	0.05	
Na ₂ O	0.11	0.03	0.07	0.11	0.13	0.11	0.06	0.06	0.15	0.08	
K ₂ O	9.71	10.09	9.90	9.92	9.61	9.86	9.55	10.03	9.84	10.01	
SrO	0.00	0.00	0.00	0.00	0.00	0.00	0.01	0.00	0.00	0.00	
ZnO	0.00	0.01	0.00	0.09	0.08	0.00	0.07	0.11	0.01	0.00	
Cl	0.08	0.04	0.07	0.05	0.09	0.06	0.05	0.04	0.06	0.08	
Li ₂ O*	1.58	1.53	1.61	1.51	1.48	1.71	1.69	1.74	1.53	1.48	
H ₂ O*	4.08	4.08	4.10	4.09	4.01	4.11	4.08	4.12	4.08	4.08	
O=F,Cl	0.02	0.01	0.02	0.01	0.02	0.01	0.01	0.01	0.01	0.02	
Total	101.38	100.90	101.92	101.79	99.89	101.96	100.90	101.74	101.56	101.68	
Si	5.67	5.66	5.66	5.64	5.71	5.70	5.73	5.71	5.65	5.63	
Al ^{IV}	2.33	2.34	2.34	2.36	2.29	2.30	2.27	2.29	2.35	2.37	
Al ^{VI}	0.10	0.18	0.16	0.10	0.12	0.09	0.20	0.17	0.14	0.15	
Ti	0.18	0.11	0.12	0.22	0.19	0.19	0.14	0.16	0.15	0.17	
Fe	1.98	1.88	1.99	2.01	1.98	1.94	1.92	1.86	1.98	2.01	
Mn	0.02	0.02	0.03	0.03	0.02	0.03	0.05	0.02	0.06	0.04	
Mg	3.28	3.36	3.28	3.16	3.20	3.22	3.17	3.22	3.23	3.20	
Zn	0.00	0.00	0.00	0.01	0.01	0.00	0.01	0.01	0.00	0.00	
Li*	0.93	0.90	0.94	0.89	0.88	1.00	1.00	1.02	0.90	0.87	
Ca	0.00	0.00	0.00	0.00	0.01	0.01	0.01	0.01	0.00	0.01	
Na	0.03	0.01	0.02	0.03	0.04	0.03	0.02	0.02	0.04	0.02	
K	1.81	1.89	1.84	1.85	1.82	1.83	1.78	1.86	1.84	1.87	
Al total	2.43	2.52	2.50	2.46	2.42	2.39	2.47	2.46	2.49	2.52	
Fe/Fe+Mg	0.38	0.36	0.38	0.39	0.38	0.38	0.38	0.37	0.38	0.39	

Fórmula estrutural calculada na base de 11 oxigênios.

Tabela 10. Química mineral das flogopitas estudadas (continuação).

Rock Sample	Quartzo sienito									
	Uru-25									
SiO ₂	39.34	39.28	40.07	39.45	39.28	39.26	39.33	39.65	39.13	
TiO ₂	1.01	1.04	0.79	0.74	0.94	1.18	1.07	0.99	1.44	
Al ₂ O ₃	12.07	11.92	11.88	12.29	12.02	12.25	11.81	11.93	12.15	
FeO	17.85	18.36	16.37	17.55	17.87	17.66	17.78	17.92	18.45	
MnO	0.30	0.14	0.22	0.29	0.09	0.15	0.43	0.20	0.30	
MgO	15.08	14.82	15.97	15.18	15.30	15.25	15.25	15.20	14.95	
CaO	0.00	0.03	0.04	0.00	0.02	0.00	0.02	0.09	0.01	
Na ₂ O	0.00	0.15	0.08	0.06	0.06	0.10	0.08	0.08	0.09	
K ₂ O	9.98	9.75	9.78	9.88	9.62	9.87	9.81	9.41	9.70	
SrO	0.04	0.03	0.00	0.01	0.00	0.00	0.00	0.00	0.06	
ZnO	0.12	0.00	0.08	0.00	0.05	0.00	0.05	0.00	0.11	
Cl	0.32	0.32	0.29	0.32	0.25	0.33	0.20	0.32	0.25	
Li ₂ O*	1.74	1.72	1.95	1.77	1.72	1.72	1.74	1.83	1.68	
H ₂ O*	3.98	3.97	4.02	3.99	3.99	3.99	4.01	3.99	4.01	
O=F,Cl	0.07	0.07	0.07	0.07	0.06	0.07	0.04	0.07	0.06	
Total	101.75	101.46	101.47	101.46	101.13	101.67	101.54	101.54	102.27	
Si	5.80	5.81	5.86	5.82	5.81	5.78	5.81	5.83	5.75	
Al ^{IV}	2.10	2.08	2.05	2.14	2.10	2.13	2.06	2.07	2.11	
Al ^{VI}	0.00	0.00	0.00	0.00	0.00	0.00	0.00	0.00	0.00	
Ti	0.11	0.12	0.09	0.08	0.10	0.13	0.12	0.11	0.16	
Fe	2.20	2.27	2.00	2.16	2.21	2.18	2.20	2.20	2.27	
Mn	0.04	0.02	0.03	0.04	0.01	0.02	0.05	0.03	0.04	
Mg	3.32	3.27	3.48	3.34	3.37	3.35	3.36	3.33	3.28	
Zn	0.01	0.00	0.01	0.00	0.01	0.00	0.01	0.00	0.01	
Li*	1.03	1.02	1.15	1.05	1.02	1.02	1.03	1.08	0.99	
Ca	0.00	0.01	0.01	0.00	0.00	0.00	0.00	0.01	0.00	
Na	0.00	0.04	0.02	0.02	0.02	0.03	0.02	0.02	0.02	
K	1.88	1.84	1.83	1.86	1.81	1.85	1.85	1.77	1.82	
Al total	2.10	2.08	2.05	2.14	2.10	2.13	2.06	2.07	2.11	
Fe/Fe+Mg	0.40	0.41	0.37	0.39	0.40	0.39	0.40	0.40	0.41	

Fórmula estrutural calculada na base de 11 oxigênios.

Tabela 10. Química mineral das flogopitas estudadas (continuação).

Rock Sample	Dique sin-magmático ultramáfico					Quartzo sienito				
	Uru-27					Uru-6				
SiO ₂	38.72	39.25	38.75	37.83	38.21	37.64	38.11	38.46	38.21	
TiO ₂	1.04	0.87	0.52	1.71	1.39	1.61	1.01	0.85	1.60	
Al ₂ O ₃	11.28	11.87	11.20	13.71	13.86	13.75	13.76	13.76	13.50	
FeO	17.12	17.37	17.65	17.54	17.71	17.10	17.91	17.16	16.67	
MnO	0.36	0.19	0.13	0.39	0.27	0.35	0.36	0.28	0.24	
MgO	15.47	16.23	15.47	13.55	13.80	13.83	13.45	14.61	14.16	
CaO	0.01	0.05	0.05	0.03	0.00	0.00	0.07	0.01	0.01	
Na ₂ O	0.10	0.05	0.09	0.09	0.03	0.05	0.02	0.01	0.03	
K ₂ O	9.90	9.85	9.45	9.58	9.71	9.70	9.47	9.82	9.77	
SrO	0.00	0.00	0.00	0.00	0.00	0.00	0.00	0.00	0.00	
ZnO	0.00	0.00	0.00	0.00	0.00	0.00	0.00	0.00	0.00	
Cl	0.14	0.14	0.16	0.14	0.12	0.11	0.14	0.12	0.14	
Li ₂ O*	1.56	1.71	1.57	1.31	1.41	1.25	1.39	1.48	1.41	
H ₂ O*	3.06	3.18	3.43	3.52	3.50	3.44	3.46	3.51	3.44	
O=F,Cl	0.82	0.80	0.48	0.42	0.46	0.48	0.47	0.47	0.51	
Total	99.81	101.78	99.79	100.01	100.47	99.31	99.75	100.64	99.71	
Si	5.83	5.78	5.87	5.68	5.69	5.67	5.73	5.71	5.72	
Al ^{IV}	2.00	2.06	2.00	2.32	2.31	2.33	2.27	2.29	2.28	
Al ^{VI}	0.00	0.00	0.00	0.11	0.13	0.11	0.17	0.12	0.10	
Ti	0.12	0.10	0.06	0.19	0.16	0.18	0.11	0.09	0.18	
Fe	2.16	2.14	2.23	2.20	2.21	2.16	2.25	2.13	2.09	
Mn	0.05	0.02	0.02	0.05	0.03	0.05	0.05	0.04	0.03	
Mg	3.47	3.56	3.49	3.03	3.06	3.11	3.01	3.23	3.16	
Zn	0.00	0.00	0.00	0.00	0.00	0.00	0.00	0.00	0.00	
Li*	0.94	1.01	0.96	0.79	0.85	0.76	0.84	0.89	0.85	
Ca	0.00	0.01	0.01	0.00	0.00	0.00	0.01	0.00	0.00	
Na	0.03	0.01	0.03	0.03	0.01	0.01	0.01	0.00	0.01	
K	1.90	1.85	1.82	1.83	1.85	1.86	1.82	1.86	1.87	
Al total	2.00	2.06	2.00	2.43	2.43	2.44	2.44	2.41	2.38	
Fe/Fe+Mg	0.38	0.38	0.39	0.42	0.42	0.41	0.43	0.40	0.40	

Fórmula estrutural calculada na base de 11 oxigênios.

Tabela 10. Química mineral das flogopitas estudadas (continuação).

Rock Sample	Quartzo sienito							
	Uru-6							
SiO ₂	38.72	38.40	38.07	37.89	38.21	38.24	38.10	37.70
TiO ₂	1.71	1.13	1.70	1.56	1.35	1.19	1.24	1.55
Al ₂ O ₃	13.66	13.74	13.30	13.40	13.96	13.52	13.90	13.63
FeO	16.28	16.76	17.01	16.78	16.89	17.44	17.19	16.38
MnO	0.34	0.20	0.24	0.29	0.28	0.42	0.36	0.19
MgO	15.02	14.55	14.55	14.46	14.17	14.18	13.99	13.81
CaO	0.01	0.00	0.04	0.00	0.00	0.00	0.00	0.00
Na ₂ O	0.00	0.11	0.04	0.08	0.08	0.06	0.07	0.06
K ₂ O	9.63	9.89	9.88	9.55	9.78	9.97	9.71	9.78
SrO	0.00	0.00	0.00	0.00	0.00	0.00	0.00	0.00
ZnO	0.00	0.00	0.00	0.00	0.00	0.00	0.00	0.00
Cl	0.12	0.17	0.15	0.13	0.14	0.12	0.13	0.16
Li ₂ O*	1.56	1.47	1.37	1.32	1.41	1.42	1.38	1.27
H ₂ O*	3.59	3.49	3.49	3.57	3.53	3.48	3.45	3.92
O=F,Cl	0.44	0.48	0.47	0.38	0.44	0.48	0.50	0.04
Total	101.33	100.41	100.41	99.67	100.49	100.77	100.11	99.51
Si	5.69	5.71	5.68	5.69	5.69	5.70	5.69	5.72
Al ^{IV}	2.31	2.29	2.32	2.31	2.31	2.30	2.31	2.28
Al ^{VI}	0.05	0.11	0.02	0.06	0.14	0.08	0.14	0.15
Ti	0.19	0.13	0.19	0.18	0.15	0.13	0.14	0.18
Fe	2.00	2.08	2.12	2.11	2.10	2.18	2.15	2.08
Mn	0.04	0.02	0.03	0.04	0.04	0.05	0.05	0.02
Mg	3.29	3.22	3.23	3.24	3.14	3.15	3.12	3.12
Zn	0.00	0.00	0.00	0.00	0.00	0.00	0.00	0.00
Li*	0.92	0.88	0.82	0.80	0.85	0.85	0.83	0.77
Ca	0.00	0.00	0.01	0.00	0.00	0.00	0.00	0.00
Na	0.00	0.03	0.01	0.02	0.02	0.02	0.02	0.02
K	1.80	1.87	1.88	1.83	1.86	1.90	1.85	1.89
Al total	2.37	2.41	2.34	2.37	2.45	2.38	2.45	2.44
Fe/Fe+Mg	0.38	0.39	0.40	0.39	0.40	0.41	0.41	0.40

Fórmula estrutural calculada na base de 11 oxigênios.

Tabela 10. Química mineral das flogopitas estudadas (continuação).

Rock Sample	Dique sin-magmático félsico Uru- 26							
	SiO ₂	39.58	38.96	39.13	39.17	38.97	39.47	39.24
TiO ₂	0.82	0.52	0.69	0.84	0.68	1.12	0.96	0.89
Al ₂ O ₃	11.23	11.38	10.87	11.15	10.87	11.06	11.33	10.98
FeO	17.56	16.93	16.72	17.30	17.11	16.80	16.87	16.76
MnO	0.21	0.21	0.37	0.20	0.24	0.26	0.25	0.33
MgO	16.47	15.72	15.61	15.57	15.94	15.46	15.45	15.76
CaO	0.00	0.04	0.03	0.06	0.00	0.02	0.01	0.00
Na ₂ O	0.07	0.06	0.06	0.07	0.03	0.08	0.07	0.16
K ₂ O	9.64	9.70	9.77	9.64	9.49	9.30	9.74	9.35
SrO	0.00	0.00	0.00	0.00	0.00	0.00	0.00	0.00
ZnO	0.00	0.00	0.00	0.00	0.00	0.00	0.00	0.00
Cl	0.15	0.17	0.19	0.18	0.18	0.18	0.18	0.18
Li ₂ O*	1.81	1.63	1.68	1.69	1.63	1.78	1.71	1.53
H ₂ O*	3.06	3.04	3.04	3.06	3.03	3.06	3.06	3.91
O=F,Cl	0.90	0.84	0.83	0.83	0.84	0.84	0.84	0.04
Total	101.87	99.24	99.28	99.97	99.23	99.63	99.92	100.34
Si	5.82	5.86	5.91	5.87	5.88	5.90	5.87	5.86
Al ^{IV}	1.95	2.02	1.93	1.97	1.93	1.95	2.00	1.96
Al ^{VI}	0.00	0.00	0.00	0.00	0.00	0.00	0.00	0.00
Ti	0.09	0.06	0.08	0.09	0.08	0.13	0.11	0.10
Fe	2.16	2.13	2.11	2.17	2.16	2.10	2.11	2.13
Mn	0.03	0.03	0.05	0.03	0.03	0.03	0.03	0.04
Mg	3.61	3.53	3.51	3.48	3.58	3.45	3.45	3.56
Zn	0.00	0.00	0.00	0.00	0.00	0.00	0.00	0.00
Li*	1.07	0.99	1.02	1.02	0.99	1.07	1.03	0.94
Ca	0.00	0.01	0.00	0.01	0.00	0.00	0.00	0.00
Na	0.02	0.02	0.02	0.02	0.01	0.02	0.02	0.05
K	1.81	1.86	1.88	1.84	1.83	1.77	1.86	1.81
Al total	1.95	2.02	1.93	1.97	1.93	1.95	2.00	1.96
Fe/Fe+Mg	0.37	0.38	0.38	0.38	0.38	0.38	0.38	0.37

Fórmula estrutural calculada na base de 11 oxigênios.